[redacted]

NASA TECHNICAL MEMORANDUM

UB
NASA TM X-1668

UB
NASA TM X-1668

Declassified by authority of NASA
Classification Change Notices No. CNR-216
Dated ** 12-15-70

# PREDICTED LAUNCH CHARACTERISTICS OF THE HL-10 MANNED LIFTING ENTRY VEHICLE LAUNCHED FROM THE B-52 AIRPLANE

[redacted]

*by Linwood W. McKinney and Richmond P. Boyden*

*Langley Research Center*
*Langley Station, Hampton, Va.*

NATIONAL AERONAUTICS AND SPACE ADMINISTRATION • WASHINGTON, D. C. • NOVEMBER 1968

[redacted]

[redacted]

NASA TM X-1668

DECLASSIFIED

# PREDICTED LAUNCH CHARACTERISTICS OF THE HL-10 MANNED LIFTING ENTRY VEHICLE LAUNCHED FROM THE B-52 AIRPLANE

By Linwood W. McKinney and Richmond P. Boyden

Langley Research Center
Langley Station, Hampton, Va.

[redacted]

NATIONAL AERONAUTICS AND SPACE ADMINISTRATION

[redacted]

[redacted]

# PREDICTED LAUNCH CHARACTERISTICS OF THE HL-10 MANNED LIFTING ENTRY VEHICLE LAUNCHED FROM THE B-52 AIRPLANE*

By Linwood W. McKinney and Richmond P. Boyden
Langley Research Center

## SUMMARY

An investigation has been made to assess the effects of the aerodynamic interference of the B-52 flow field on the launch characteristics of both the subsonic and transonic HL-10 configurations using six-degrees-of-freedom motion calculations. The static aerodynamic data used as inputs in the investigation were obtained from high-speed wind-tunnel tests of 0.025-scale models of the HL-10/B-52 combination in the Langley high-speed 7- by 10-foot tunnel.

The launch motion studies of the subsonic HL-10 configuration indicate that launches without contact should be expected at a B-52 angle of attack of $4^{\circ}$ at a Mach number of 0.60, and at a B-52 angle of attack of $2^{\circ}$ at a Mach number of 0.65, both with and without the rate damper system operating. However, the launches at a Mach number of 0.60 indicate larger safety margins (that is, more clearance between the center fin and pylons) than those at a Mach number of 0.65. For the transonic configuration, changes in B-52 angle of attack with the accompanying changes in dynamic pressure had only minor effects on the safety margins. The margins were not significantly affected by the rate damper system for any of the launch conditions. The computed launch characteristics for all launch conditions simulated in the investigation indicate safe launches of the HL-10 from the B-52 should be expected.

It is felt that the effect of Reynolds number on the interference data are not well understood, and that although there seems to be no apparent serious effect of Reynolds number on the free-air data in the trimmed condition, no such statement may be made with certainty regarding the interference forces and moments.

## INTRODUCTION

The Flight Research Center of the National Aeronautics and Space Administration is currently engaged in a flight research program to investigate the subsonic handling

*Title, Unclassified.

[redacted]

qualities and landing characteristics of a number of proposed lifting-body entry vehicles, one of which is the HL-10 (horizontal lander 10). The HL-10 will be carried to an altitude of between 40 000 and 50 000 feet (12 192 and 15 240 meters) and launched at high subsonic speeds, through the asymmetrical flow field beneath the right wing of a B-52 carrier. Prior to making the first aerial launch, it is necessary, from a flight-safety standpoint, to investigate the probability of contact between the HL-10 vehicle and those parts of the B-52 airplane in close proximity to the HL-10 vehicle at launch.

Investigations were therefore undertaken by the Langley Research Center to determine the static aerodynamic interference effects from high-speed wind-tunnel tests of a 0.025-scale model of the HL-10 in proximity to a 0.025-scale B-52 model and to assess the effects of the aerodynamic interference on the HL-10 motions immediately after launch by use of six-degrees-of-freedom motion studies.

This paper presents the results of this analysis of the calculated launch motions to permit assessment of the safety margins and to indicate the effect of various launch parameters on the safety margin at launch.

## SYMBOLS

The longitudinal force and moment coefficients are referred to the stability axes and the lateral data are referred to the body axes. The angles and normal acceleration presented in the form of time histories are with reference to the principal-axis system as shown in figure 1. The units herein were taken in the U.S. Customary System and where practical are listed also in the International System (SI).

$a_z$ normal acceleration along principal axes of HL-10, g units

b reference span

$C_L$ lift coefficient, $\frac{\text{Lift}}{\bar{q}S}$

$C_l$ rolling-moment coefficient, $\frac{\text{Rolling moment}}{\bar{q}Sb}$

$C_{l_p}$ rolling-moment coefficient due to rolling velocity, $\frac{\partial C_l}{\partial \frac{pb}{2V}}$, per radian

$C_{l_r}$ rolling-moment coefficient due to yawing velocity, $\frac{\partial C_l}{\partial \frac{rb}{2V}}$, per radian

$C_{l_\beta}$ effective-dihedral parameter (measured between $\beta = 5^o$ and $\beta = -5^o$), per degree

[redacted]

$C_m$ pitching-moment coefficient, $\frac{\text{Pitching moment}}{\bar{q}Sl}$

[redacted]

$C_{m_q}$ pitching-moment coefficient due to pitching velocity, $\frac{\partial C_m}{\partial \frac{ql}{2V}}$, per radian

$C_n$ yawing-moment coefficient, $\frac{\text{Yawing moment}}{\bar{q}Sb}$

$C_{n_p}$ yawing-moment coefficient due to rolling velocity, $\frac{\partial C_n}{\partial \frac{pb}{2V}}$, per radian

$C_{n_r}$ yawing-moment coefficient due to yawing velocity, $\frac{\partial C_n}{\partial \frac{rb}{2V}}$, per radian

$C_{n_\beta}$ directional-stability parameter (measured between $\beta = 5^o$ and $\beta = -5^o$), per degree

$C_{Y_\beta}$ side-force coefficient per degree of sideslip angle (measured between $\beta = 5^o$ and $\beta = -5^o$)

g acceleration due to gravity

h altitude, feet (meters)

$I_X, I_Y, I_Z$ moments of inertia about X, Y, and Z, slug-feet$^2$ (kilogram-meters$^2$)

$I_{XZ}$ product of inertia, slug-feet$^2$ (kilogram-meters$^2$)

$K_p$ roll damper gain, $\delta_a/p$, seconds

$K_q$ pitch damper gain, $\delta_e/q$, seconds

$K_r$ yaw damper gain, $\delta_r/r$, seconds

L/D lift-drag ratio

$l$ model length

M Mach number

[redacted]

[redacted]

| | |
|---|---|
| p | rolling velocity, radians per second or degrees per second |
| q | pitching velocity, radians per second or degrees per second |
| $\bar{q}$ | free-stream dynamic pressure, $\frac{1}{2}\rho V^2$, pounds/foot$^2$ (newtons/meter$^2$) |
| R | Reynolds number |
| r | yawing velocity, radians per second or degrees per second |
| S | reference area, feet$^2$ (meters$^2$) |
| t | time, seconds |
| V | free-stream velocity, feet/second (meters/second) |
| W | weight, pounds (newtons) |
| X,Y,Z | Euler axes |
| z | distances along Z-axis, feet (meters) |
| $\alpha$ | angle of attack, degrees |
| $\Delta\alpha$ | incidence angle of HL-10 reference line relative to B-52 reference line, degrees |
| $\beta$ | angle of sideslip of HL-10 center line, degrees |
| $\delta_a$ | differential deflection of elevons when used as ailerons, $\delta_{e,R} - \delta_{e,L}$, degrees |
| $\delta_e$ | elevon deflection measured from local body surface, positive when trailing edge is down, degrees |
| $\delta_r$ | rudder deflection, positive when trailing edge is deflected to left, degrees |
| $\delta_{of}$ | deflection of outboard flap |
| $\delta_{ef}$ | deflection of elevon flap |



[redacted]

$\delta_{if}$ deflection of inboard flap

$\gamma_T$ angle of tangent to center fin path computed between t = 0 and t = 0.1 second, degrees

$\gamma_C$ clearance angle allowed by pylon support structure, degrees

$\epsilon$ inclination of HL-10 principal axes from angle-of-attack reference axes, positive when principal axes are inclined nose down with respect to reference axes, degrees

$\theta$ Euler pitch angle, degrees

$\rho$ mass density of air, slugs/feet$^3$ (kilograms/meters$^3$)

$\phi$ Euler roll angle, degrees

$\psi$ Euler yaw angle, degrees

Subscripts:

d effect of dampers

p principal HL-10 axes

L left

R right

HL-10 pertains to HL-10 vehicle

B-52 pertains to B-52 airplane

max maximum

ref reference

trim value at trim condition

A dot over a symbol indicates the first derivative with respect to time.

[redacted]

## HL-10 FLIGHT VEHICLE

Design concepts of the basic HL-10 lifting-body vehicle are presented in reference 1. Basic geometric characteristics of the HL-10 launch vehicle are given in figure 2. In order to obtain improved stability characteristics in the transonic speed range and an increased lift-drag ratio on the landing approach, the HL-10 employs two-position flaps on the tip fins and on the upper surface of the elevons and a split rudder on the center fin. Details of these flaps are given in figure 2(b). In the landing-approach configuration, hereafter referred to as the subsonic configuration, the movable surfaces are retracted to provide maximum boattailing on the aft section of the vehicle. Photographs showing the highly boattailed subsonic configuration are presented in figures 3(a) and 3(b). In the high subsonic and transonic speed range where the flow on the upper surface of the vehicle becomes sonic, the movable flaps are deflected to minimize flow separation in the region of the control surfaces. The HL-10 in this mode is hereafter referred to as the transonic configuration. Photographs showing the flaps in the transonic configuration are presented in figures 3(c) and 3(d). The captive flight location of the HL-10 beneath the right wing of the B-52 airplane is shown in figure 4.

## LAUNCH MOTION CALCULATIONS

To assess the launch safety of the HL-10/B-52 combination, the forces and moments acting on the HL-10 in the B-52 interference flow field were required as a function of HL-10 angle of attack, sideslip angle, and separation distance. These aerodynamic data were obtained from static wind-tunnel tests of a 0.025-scale model of the HL-10 in proximity to a comparable scaled B-52 model in the Langley high-speed 7- by 10-foot tunnel.

Time histories of the HL-10 motions were computed by solving a system of six-degrees-of-freedom rigid-body equations of motion programed to allow nonlinear variations of the aerodynamic coefficients as a function of $\alpha_{HL-10}$, $\beta_{HL-10}$, and z. The equations were solved by performing a Runge-Kutta variable-step size integration procedure. The cross-plotted wind-tunnel static interference data were stored in the computer as a function of $\alpha_{HL-10}$, $\beta_{HL-10}$, and separation distance for a constant B-52 angle of attack and Mach number. Appropriate values of the aerodynamic coefficients as functions of $\alpha_{HL-10}$, $\beta_{HL-10}$, and z were determined from tabular values by using linear interpolation. The computer program is designated D-1085 and is available from the Analytical Computing Division of the Langley Research Center. Values of HL-10 physical characteristics and aerodynamic damping used in the launch studies are given in tables I to III.



[redacted]

[redacted]

TABLE I.- PHYSICAL AND DAMPER CHARACTERISTICS OF THE HL-10 CONFIGURATION

| Measurement | Transonic configuration | | Subsonic configuration |
|---|---|---|---|
| | Lightweight HL-10 | Heavyweight HL-10 | |
| Weight of HL-10, $W_{HL-10}$, lb (N) | 5308 (23 611) | 7968 (35 443) | 5460 (24 287) |
| Moment of inertia about X reference axis, $I_{X_{ref}}$, slug-ft$^2$ (kg-m$^2$) | 897.8 ( 1217) | 1321 ( 1791) | 1187 ( 1609) |
| Moment of inertia about Y reference axis, $I_{Y_{ref}}$, slug-ft$^2$ (kg-m$^2$) | 3792.1 ( 5141) | 5129 ( 6953) | 4724 ( 6404) |
| Moment of inertia about Z reference axis, $I_{Z_{ref}}$, slug-ft$^2$ (kg-m$^2$) | 4184.6 ( 5673) | 5903 ( 8003) | 5377 ( 7290) |
| Product of inertia, $I_{XZ}$, slug-ft$^2$ (kg-m$^2$) | 392.1 ( 531.6) | 422 ( 572) | 396 ( 537) |
| Axis inclination, $\epsilon$, deg | 6.72 | 5.2 | 5.37 |
| Pitch damper gain, $K_q$, sec | 0.50 | 0.50 | 0.50 |
| Roll damper gain, $K_p$, sec | -0.50 | -0.50 | -0.50 |
| Yaw damper gain, $K_r$, sec | 0.50 | 0.50 | 0.50 |

TABLE II.- DAMPER LIMITS FOR THE HL-10

| | |
|---|---|
| Damper authority limits: | |
| $\delta_{a,d}$, deg | ±20 |
| $\delta_{e,d}$, deg | ±5 |
| $\delta_{r,d}$, deg | ±10 |
| Damper rate limits: | |
| $\dot{\delta}_{a,d}$, deg/sec | ±50 |
| $\dot{\delta}_{e,d}$, deg/sec | ±25 |
| $\dot{\delta}_{r,d}$, deg/sec | ±25 |

TABLE III.- DAMPING DERIVATIVES OF THE HL-10
USED IN THE LAUNCH STUDY

| Derivative | Mach number | | | |
|---|---|---|---|---|
| | 0.60 | 0.65 | 0.70 | 0.80 |
| $C_{m_q}$, per rad | -0.4 | -0.4 | -0.45 | -0.5 |
| $C_{l_p}$, per rad | -.15 | -.15 | -.15 | -.15 |
| $C_{n_p}$, per rad | .1 | .1 | .1 | .1 |
| $C_{l_r}$, per rad | .2 | .2 | .2 | .2 |
| $C_{n_r}$, per rad | -.6 | -.6 | -.7 | -.8 |

[redacted]

[redacted]

The results of the computed launch motions are presented in the form of locus plots of the tip of the HL-10 outboard fins, center fin, and center of gravity in the Y,Z reference plane and time histories of the quantities z, $a_z$, $q$, $\theta$, $\phi$, $\beta$, and $\psi$. A sketch of the HL-10 showing points for which loci were computed is shown in figure 5. A cross section showing the initial relationship between the HL-10 fins and the X-15 pylon (as seen when looking through the HL-10 center of gravity in the direction of flight) is included on each of the loci plots for reference.

To assess the effect of stability augmentation on the drop motions, a rate damper system about all axes was included in the equations of the system. Limits for damper-imposed control deflection rates and magnitudes are given in table II.

The B-52 flight conditions for which HL-10 launches were computed are given in table IV.

TABLE IV.- B-52 FLIGHT CONDITIONS

| M | $\alpha_{B-52}$, deg | $W_{B-52}$ | | Altitude | | $W_{HL-10}$ | | $\delta_e$, deg |
|---|---|---|---|---|---|---|---|---|
| | | pounds | newtons | feet | meters | pounds | newtons | |
| Subsonic configuration | | | | | | | | |
| 0.60 | 4 | 240 000 | 1 067 568 | 45 500 | 13 868 | 5460 | 24 287 | -10.5, -13.0, -15.5 |
| .65 | 2 | ↓ | ↓ | 44 200 | 13 472 | ↓ | ↓ | -7.5, -10.0, -12.5 |
| Transonic configuration | | | | | | | | |
| 0.60 | 4 | 250 000 | 1 112 050 | 44 600 | 13 594 | 5308 | 23 611 | 0, 5, 10 |
| | 2 | | | 40 000 | 12 192 | | | |
| | -1 | | | 30 000 | 9 144 | | | |
| .70 | 2 | | | 47 300 | 14 417 | | | |
| | 0 | | | 41 500 | 12 649 | | | |
| .80 | 0 | | | 49 000 | 14 935 | | | |
| | -2 | | | 39 700 | 12 100 | ↓ | ↓ | ↓ |
| .60 | 4 | | | 44 600 | 13 594 | 7968 | 35 443 | 0 |
| .70 | 2 | ↓ | ↓ | 47 300 | 14 417 | ↓ | ↓ | ↓ |

## DISCUSSION OF RESULTS

### HL-10 Free-Air Characteristics

An investigation of the effects of Reynolds number on the longitudinal aerodynamic characteristics of the subsonic HL-10 configuration is reported in reference 2. However,



[redacted]

[redacted]

the results of that investigation indicate pronounced effects of Reynolds number on the longitudinal characteristics over the range of Reynolds numbers from $R = 2.66 \times 10^6$ to $R = 19.6 \times 10^6$. In view of the Reynolds number effects noted in reference 2 and the small scale of the models used in the present investigation of the interference forces and moments in the B-52 flow field, a discussion of the free-air characteristics is presented here for both the subsonic and transonic HL-10 configuration.

Free-air characteristics of the subsonic HL-10 configuration are presented in figures 6 to 8. Figure 6 shows curves of model trimmed lift-drag ratio and $\delta_e$ required for trim as a function of angle of attack at $R = 4.0 \times 10^6$. Pitch control settings between $\delta_e = -12^o$ and $-15^o$ give values of trimmed lift-drag ratio near $(L/D)_{max}$. Figure 7(a) shows curves of lift and pitching-moment coefficient as a function of angle of attack from reference 2. These data (fig. 7(a)) were obtained on a 0.063-scale model at a Mach number of approximately 0.3 over a Reynolds number range from $R = 2.66 \times 10^6$ to $R = 18.0 \times 10^6$ based on model length. For the out-of-trim pitch control setting, $\delta_e = 0$, the data of figure 7(a) indicate an abrupt unstable break in the pitching-moment variation with angle of attack at $\alpha = 6^o$ for a Reynolds number of $2.66 \times 10^6$. This unstable break in the pitching-moment curves apparently results from flow separation in the region of the highly boattailed elevons. When the elevons are deflected trailing edge up $15^o$ $(\delta_e = -15^o)$ as is required for trim near $(L/D)_{max}$, the high slopes on the elevons are reduced and no effects of Reynolds number are indicated in the data. (See fig. 7(b).)

The free-air characteristics of the 0.025-scale HL-10 model (model used for the investigation in the B-52 flow field) are compared with data from a 0.063-scale HL-10 model in figures 7(c) and 7(d). The data shown are for a Mach number of 0.60 and Reynolds numbers of $1.6 \times 10^6$ and $4.0 \times 10^6$ based on model lengths. Trends with varying Reynolds number, as a result of varying model size at $M = 0.60$, similar to those shown in figure 7(a) at $M \approx 0.3$ are seen in figure 7(c) for the out-of-trim pitch control setting $(\delta_e = 0)$; whereas for the control setting near trim (see fig. 7(d)), reasonable agreement is noted for the two models. The comparison of the lateral-directional characteristics presented in figure 8 show similar trends with angle of attack for the two models. The difference in level of $C_{l_\beta}$ and $C_{n_\beta}$ may be due in part to model construction differences.

Free-air characteristics for the HL-10 transonic configuration are shown in figures 9 to 11. Curves of lift-drag ratio for trim flight and $\delta_e$ required for trim are presented as a function of angle of attack in figure 9 for the transonic HL-10 configuration. Curves of lift and pitching-moment coefficients as a function of angle of attack are compared in figure 10(a) for $R = 2.45 \times 10^6$ and $R = 19.3 \times 10^6$ at $M = 0.282$ and $M = 0.208$, respectively. These data, which are for a near trim control setting, $\delta_e = 0$, do not indicate the existence of flow separation due to low Reynolds number. The free-air characteristics of the 0.025-scale model, used for the investigation in the B-52 flow

[redacted]

field, are compared with results from a 0.063-scale HL-10 model (transonic configuration) in figures 10(b) to 11 at $M = 0.6$ and $M = 0.8$. In general, the agreement between the two models (shown in fig. 11) is acceptable. The differences shown would appear to be associated more with model differences than with Reynolds number effects.

The free-air characteristics presented in the preceding figures 6 to 11 for the subsonic and transonic HL-10 configuration show in general that for control settings near trim, the aerodynamic characteristics are not significantly affected by variations in Reynolds number over the range covered. It is felt, however, that the effects of Reynolds number on the interference data are not well understood, and that although there seems to be no apparent serious effect of Reynolds number on the free-air data in the trimmed condition, no such statement may be made with certainty regarding the interference forces and moments. Since the flow-field interference data were obtained at control settings near the free-air trim setting, $\delta_e = -12.9^\circ$ and $\delta_e = 0^\circ$ for the subsonic and transonic HL-10 configurations, respectively, it is assumed that the data used in the launch calculations are not affected by Reynolds number, and their use will therefore predict the launch motions correctly.

A typical variation of the HL-10 aerodynamic characteristics with separation distance between the HL-10 and B-52 is shown in figure 12 for a B-52 angle of attack of $4^\circ$ at $M = 0.6$. In this figure, the HL-10 angle of attack is $9^\circ$ over the z-range. An interesting point to note is the change in sign of the rolling moment and yawing moment at $z \approx 2$ feet; this change is responsible for an initial lateral oscillation in all the calculated launches.

## Launch Characteristics

Subsonic configuration.- The computed launch motions for the subsonic HL-10 configuration at $M = 0.6$ and $h = 45\,500$ feet (13 868 meters) are shown in figures 13 and 14 for dampers off and for dampers on, respectively. This launch condition corresponds to a B-52 angle of attack of $4^\circ$ (based on a gross weight of 240 000 pounds (1 067 568 newtons)). The values of HL-10 longitudinal trim setting used in the calculations were $\delta_e = -15.5^\circ$, $-13^\circ$, and $-10.5^\circ$ which correspond to trim near $(L/D)_{max}$. (See fig. 6.) The plots showing the paths of the center fin indicate launches without contact should be expected without dampers operating and are slightly improved with the addition of the dampers. The variation of the motion variables with time (figs. 13(b) and 14(b)) show maximum roll angles of approximately $40^\circ$ at the end of 2 seconds with the dampers off. However, significant reductions in the maximum roll angle are shown with the dampers operating. Launches for the HL-10 subsonic configuration at $M = 0.65$ at an altitude of 44 200 feet (13 472 meters) were computed with $\delta_e$ settings of $-12.5^\circ$, $-10^\circ$, and $-7.5^\circ$, and are shown in figures 15 and 16 for dampers off and on, respectively.

[redacted]

The B-52 angle of attack for this case was 2°. In general, higher rates of roll are indicated at M = 0.65; these higher roll rates are shown in the motion plots, and their effect on the path of the fin tips is also shown.

Transonic configuration.- The variation of altitude with Mach number for trimmed flight of the HL-10 transonic configuration at $\delta_e = 0^\circ$ and $\delta_e = 5^\circ$ is shown in figure 17 for both the lightweight and heavyweight HL-10. These lines give the envelope for flight at or near $(L/D)_{max}$. The B-52 flight conditions for which launches were computed are shown in the figure as solid symbols. The B-52 angles of attack corresponding to the launch points were based on a gross weight of 250 000 pounds (1 112 050 newtons) and are as follows:

| M | $\alpha_{B-52}$, deg |
|---|---|
| 0.60 | 4 |
| | 2 |
| | -1 |
| 0.70 | 2 |
| | 0 |
| 0.80 | 0 |
| | -2 |

The results of the computed launches of the HL-10 transonic configuration at a launch weight of 5 308 pounds (23 611 newtons) are presented in figures 18 to 31 for M = 0.60, 0.70, and 0.80. Launches were computed at $\delta_e$ settings of 0°, 5°, and 10°. The plots showing the paths of the HL-10 fin tips indicate launches without contact should be expected for all launch conditions investigated. The angular motions that develop over the first 2 seconds after launch are fairly well behaved without stability augmentation with the exception of the roll angle. High rates of roll resulting from the high local sideslip angle in the B-52 flow field are indicated at $t \approx 1.0$ second which in some cases results in roll angles on the order of 80° at the end of 2 seconds. (For example, see fig. 18.) The addition of the simulated rate dampers provided significant reduction in the angular excursions, and the maximum roll angles computed over the 2-second time interval of the calculation were less than 20°.

The launch characteristics for an HL-10 launch weight of 7968 pounds (35 443 newtons) are presented in figures 32 and 33 for $\alpha_{B-52} = 4^\circ$ at M = 0.60 and $\alpha_{B-52} = 2^\circ$ at M = 0.70, respectively. The path of the center fin for the heavy HL-10 is essentially the same as that for the light HL-10 at equal Mach number and angle of attack of the B-52. This result may be explained by comparing the effects of moment of inertia and mass on the launch motions. The angular accelerations about all axes are reduced for the heavy HL-10 because of the higher inertias, and since the initial pitch acceleration is positive

[redacted]

and tends to rotate the center fin out of the region of probable contact with the pylon support structure, a reduction in pitch acceleration is in a direction to cancel the benefits obtained from the reduced rolling and yawing accelerations. The initial acceleration along the Z-axis is negative for both weight conditions because of the attitude of the HL-10 in captive flight. Therefore the initial acceleration along the Z-axis is also reduced for the heavy HL-10. As a result the center fin is in proximity to the pylon support structure for a longer period of time, this condition tends to cancel the beneficial effect of the reduced rolling and yawing accelerations further.

The increases in moment of inertia about the X-axis is reflected in the time history of the roll angles for the dampers-off conditions; however, with the rate dampers simulated, no appreciable difference between the lightweight and heavyweight condition is noted.

Since this study was designed primarily to ascertain whether the HL-10 launch vehicle will contact the B-52 carrier airplane at launch, a summary of the HL-10 center fin paths is presented in figures 34 and 35. The parameter plotted as the ordinates in these figures is the angle of the tangent of the fin path computed between $t = 0$ and $t = 0.1$ second expressed in a ratio to the maximum clearance angle allowed by the pylon support structure. (See sketch in figs. 34 and 35.) Values of $\gamma_T/\gamma_C$ near zero are desirable for safe launches since when $\gamma_T/\gamma_C = 1$ the HL-10 center fin would contact the pylon support structure. Larger margins of fin clearance (that is, lower values of $\gamma_T/\gamma_C$) are shown for the most negative $\delta_e$ setting for all Mach numbers on both the subsonic and transonic configurations. This condition results from the large positive initial pitch rotation associated with these trim settings. Larger clearance margins are indicated for the subsonic configuration at $M = 0.60$ than at $M = 0.65$. (See fig. 34.) This result is probably associated with the higher Mach number flow-separation effects on the subsonic configuration at $M = 0.65$.

For the launches of the transonic configuration, changes in B-52 angle of attack with the resulting change in dynamic pressure have only small effects on the values of $\gamma_T/\gamma_C$ at all Mach numbers. The rate damper system simulated, shown by the solid symbols, made only small improvements on the launch clearance margins.

The results presented here indicate launches without contact between the HL-10 launch vehicle and the B-52 carrier airplane should be expected for all conditions covered in the investigation.

## CONCLUDING REMARKS

An investigation has been made to assess the effects of the aerodynamic interference of the B-52 flow field on the launch characteristics of both the subsonic and

[redacted]

transonic HL-10 configurations by use of six-degrees-of-freedom motion calculations. The static aerodynamic data used as inputs in the investigation were obtained from high-speed wind-tunnel tests of 0.025-scale models of the HL-10/B-52 combination in the Langley high-speed 7- by 10-foot tunnel.

The launch motion studies of the subsonic HL-10 configuration indicate that launches without contact should be expected at a B-52 angle of attack of $4^{\circ}$ at a Mach number of 0.60, and at a B-52 angle of attack of $2^{\circ}$ at a Mach number of 0.65, both with and without the rate damper system operating. However, the launches at a Mach number of 0.60 indicate larger safety margins (that is, more clearance between the center fin and pylons) than those at a Mach number of 0.65. For the transonic configuration, changes in B-52 angle of attack with the accompanying changes in dynamic pressure had only minor effects on the safety margins. The margins were not significantly affected by the rate damper system for any of the launch conditions. The computed launch characteristics for all launch conditions simulated in the investigation indicate safe launches of the HL-10 from the B-52 should be expected.

It is felt, however, that the effect of Reynolds number on the interference data are not well understood, and that although there seems to be no apparent serious effect of Reynolds number on the free-air data in the trimmed condition, no such statement may be made with certainty regarding the interference forces and moments.

Langley Research Center,
National Aeronautics and Space Administration,
Langley Station, Hampton, Va., April 18, 1968,
124-07-02-71-23.

## REFERENCES

1. Rainey, Robert W.: Summary of an Advanced Manned Lifting Entry Vehicle Study. NASA TM X-1159, 1965.

2. Spencer, Bernard, Jr.: Effects of Elevon Planform on Low-Speed Aerodynamic Characteristics of the HL-10 Manned Lifting Entry Vehicle. NASA TM X-1409, 1967.

[redacted]

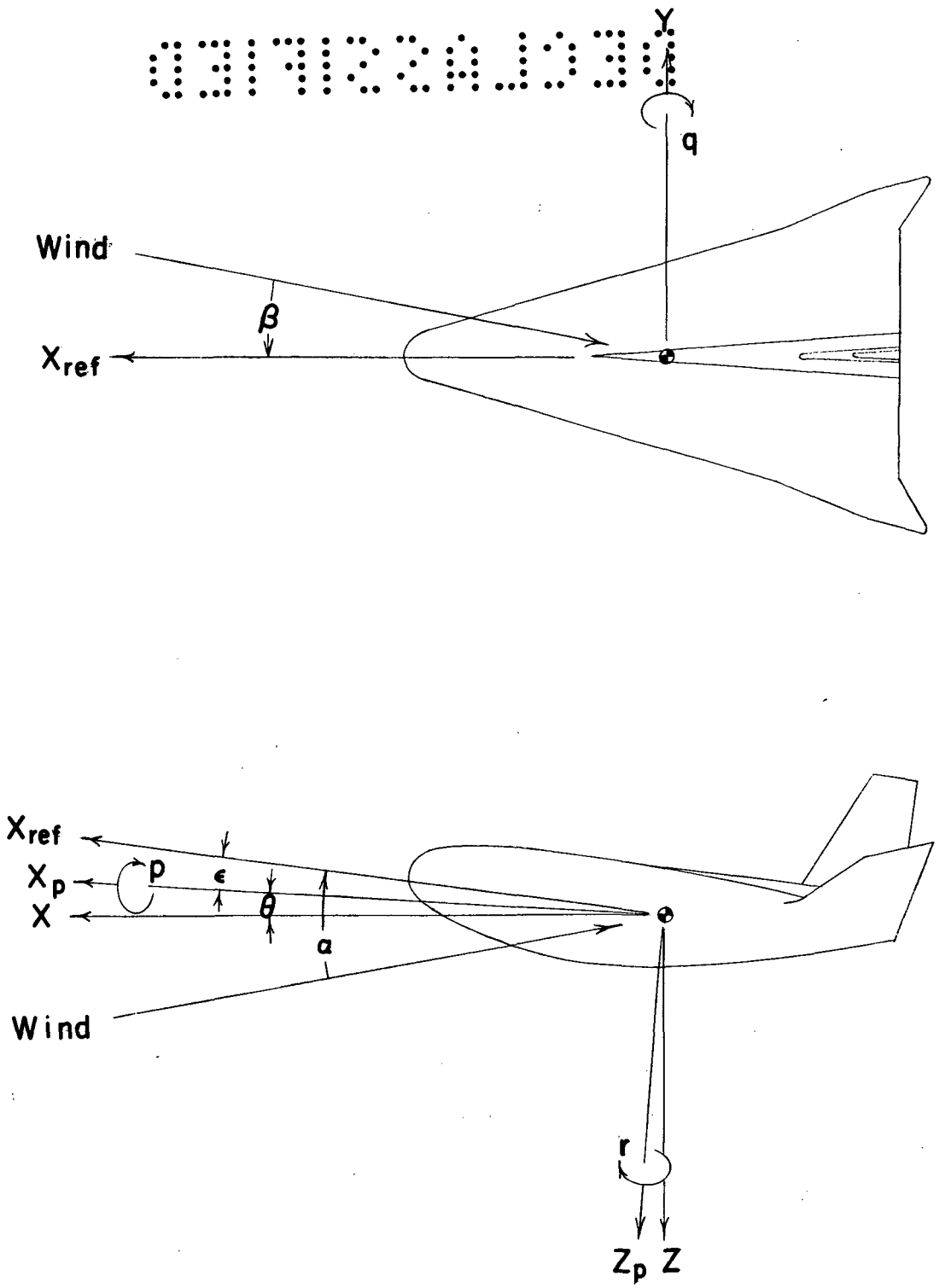


Figure 1.- Axes system used in motion calculations.

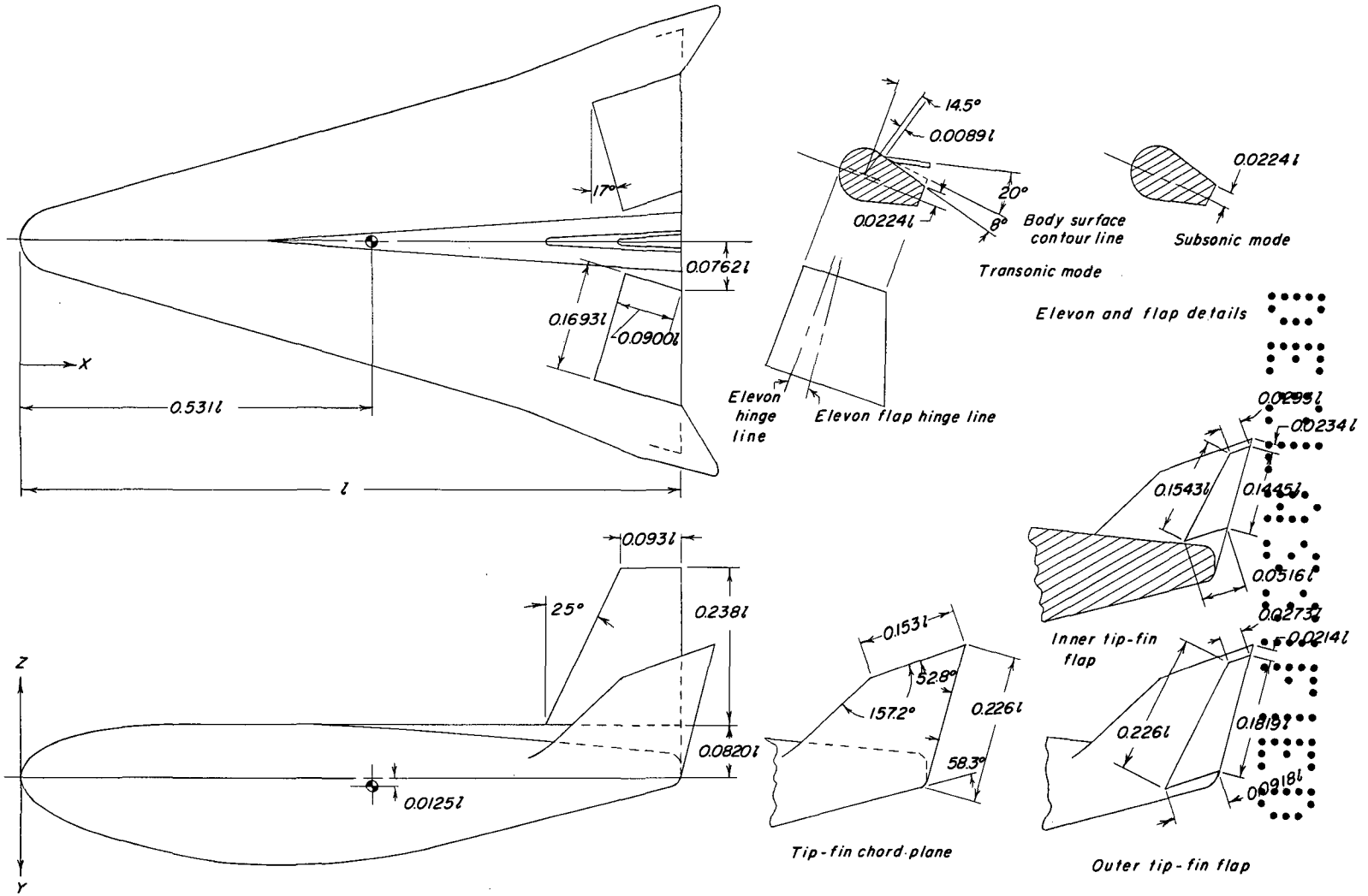


(a) Basic dimensions.

Figure 2.- Geometric characteristics of HL-10.

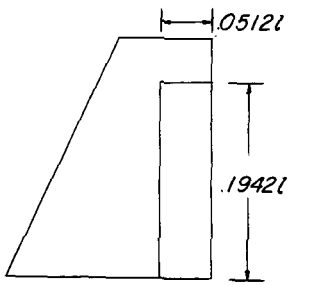


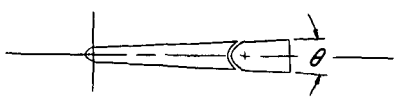


Rudder detail

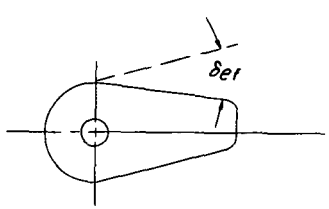


Elevon flap detail

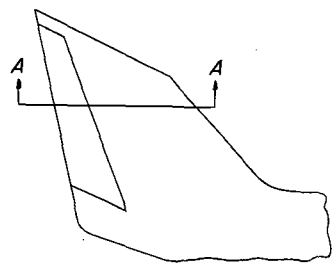


Tip-fin outer surface detail

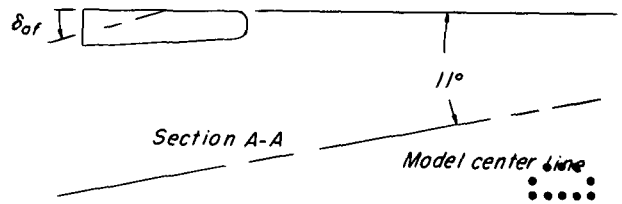


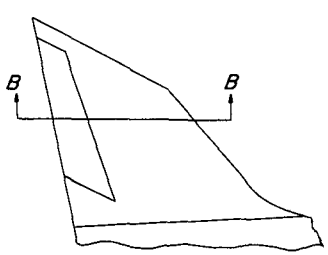


Tip-fin inner surface detail

Section B-B

Flap details

(b) Details of flap hinge lines.

Figure 2.- Concluded.

CONFIDENTIAL

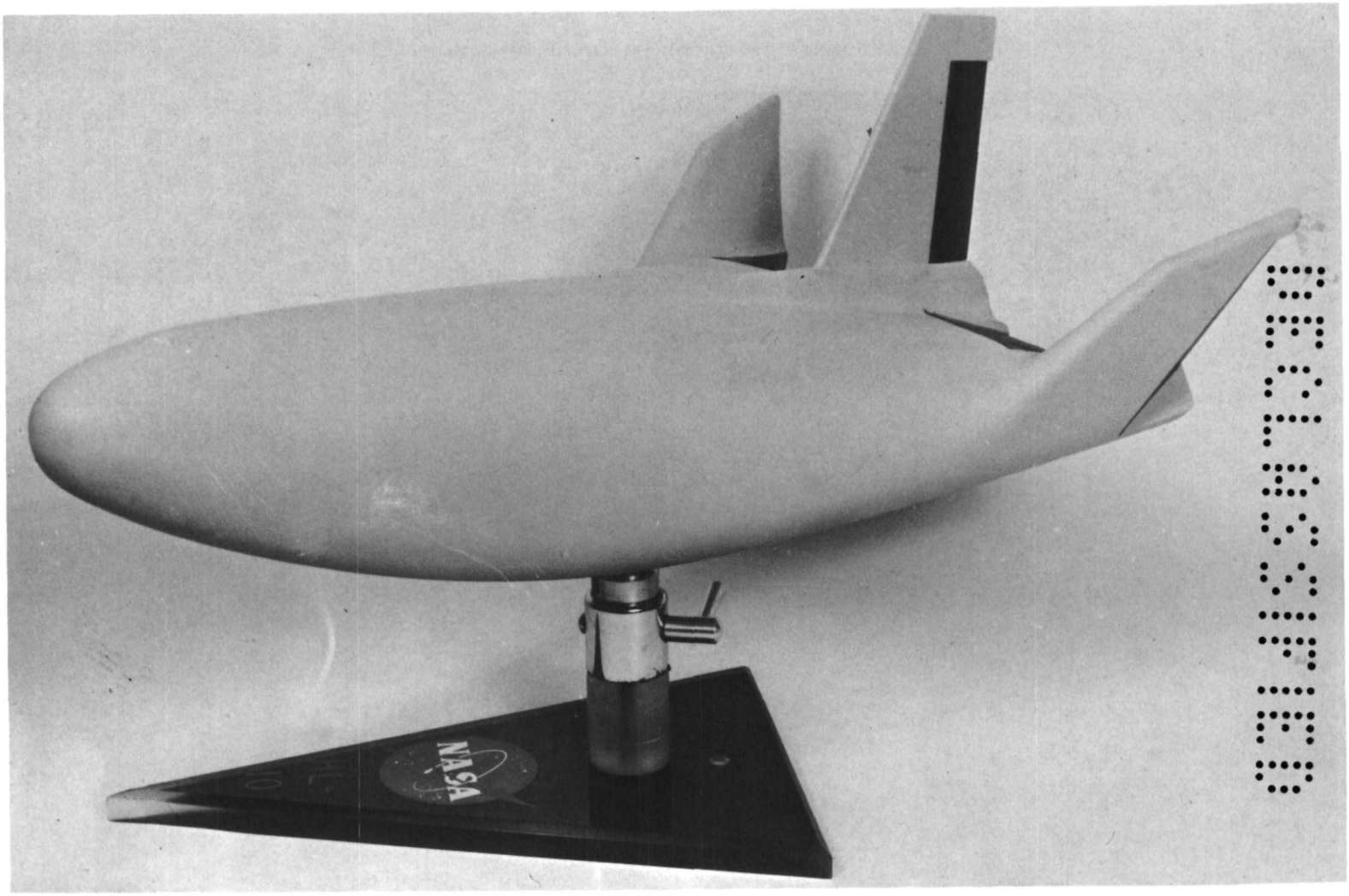


CONFIDENTIAL

(a) One-quarter front view (subsonic configuration). L-65-6177

Figure 3.- Photographs of HL-10 configuration.

CONFIDENTIAL

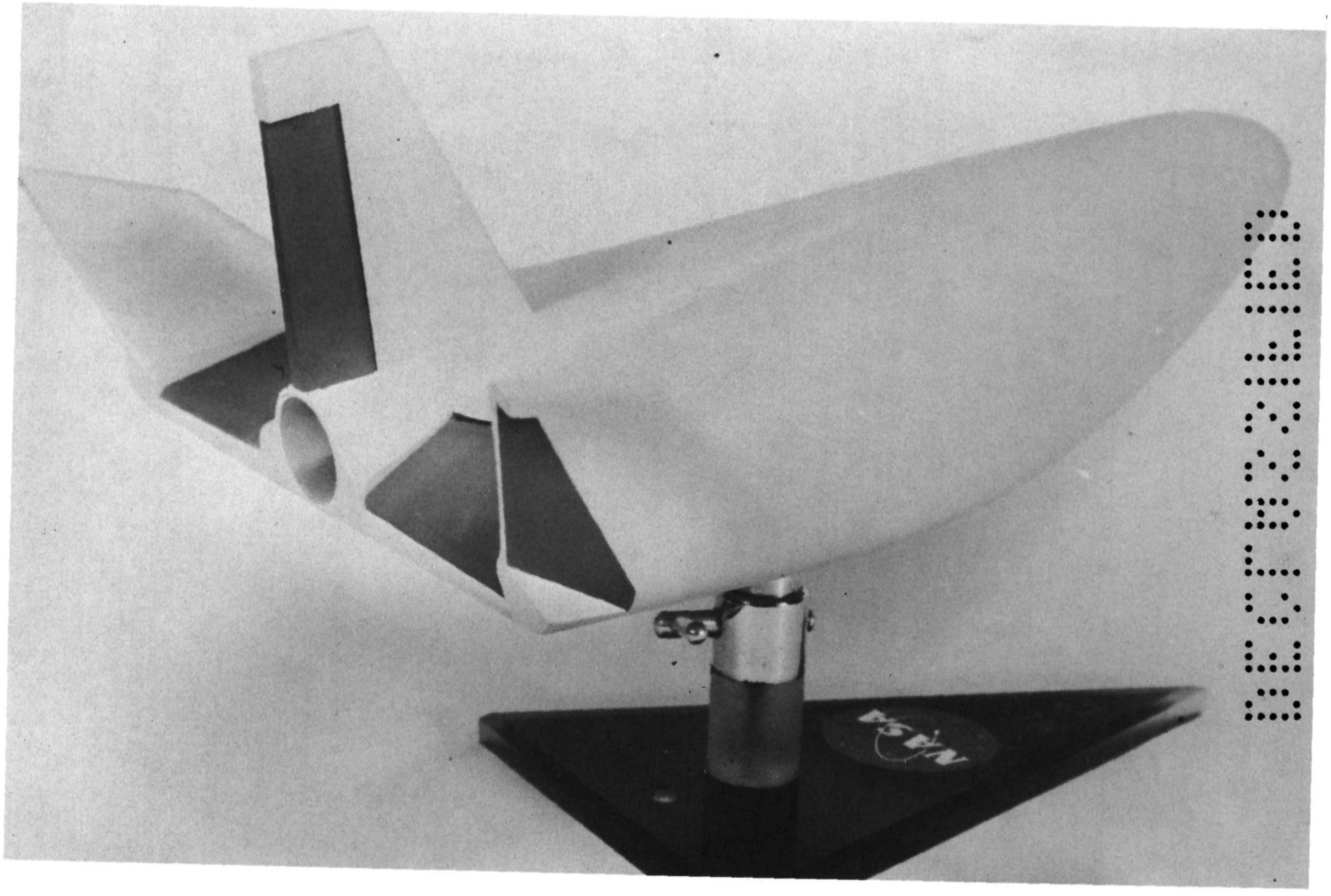

CONFIDENTIAL

(b) Three-quarter rear view (subsonic configuration). L-65-6178

Figure 3.- Continued.

CONFIDENTIAL

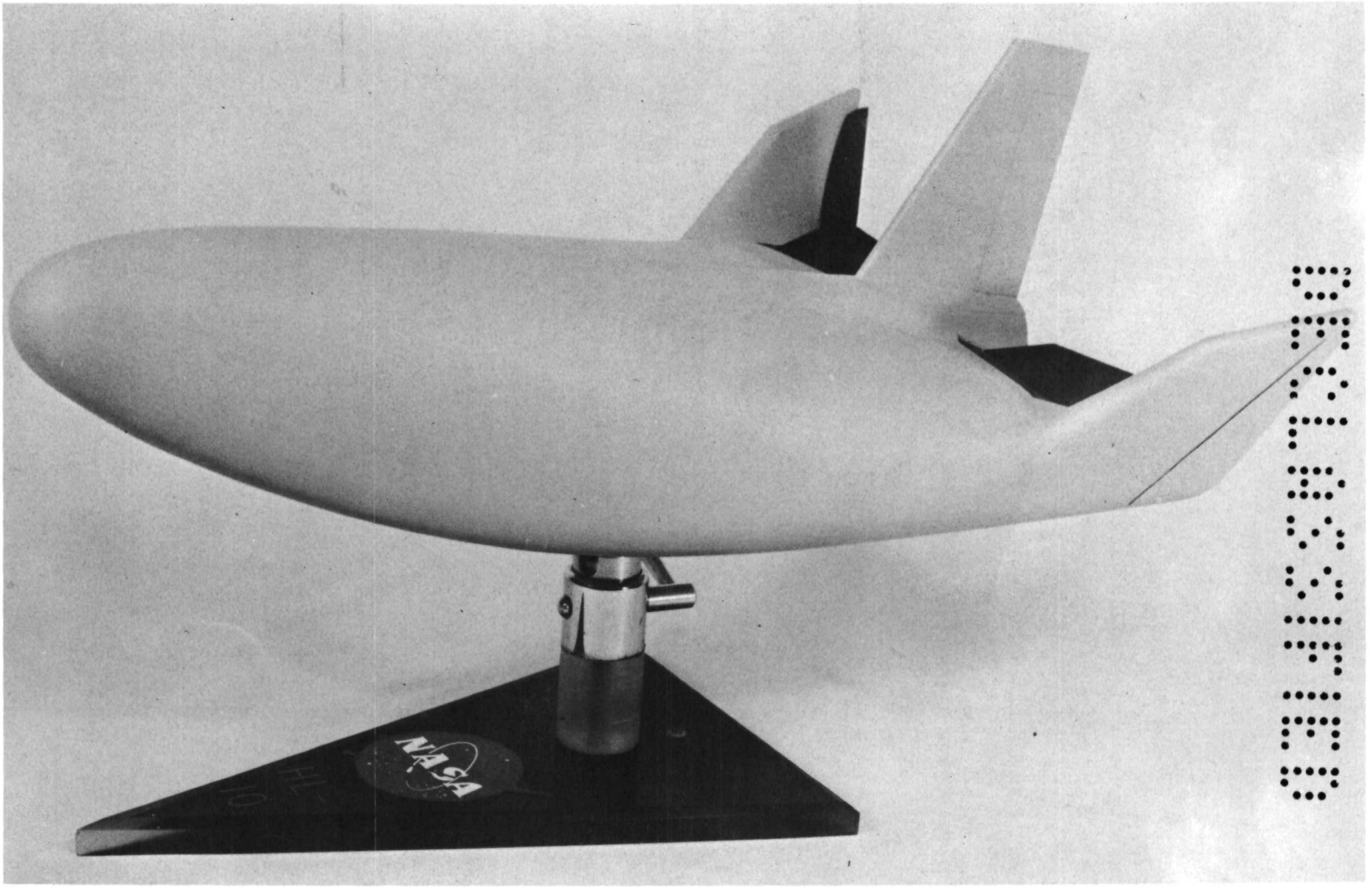


CONFIDENTIAL

(c) One-quarter front view (transonic configuration). L-65-6175

Figure 3.- Continued.

CONFIDENTIAL

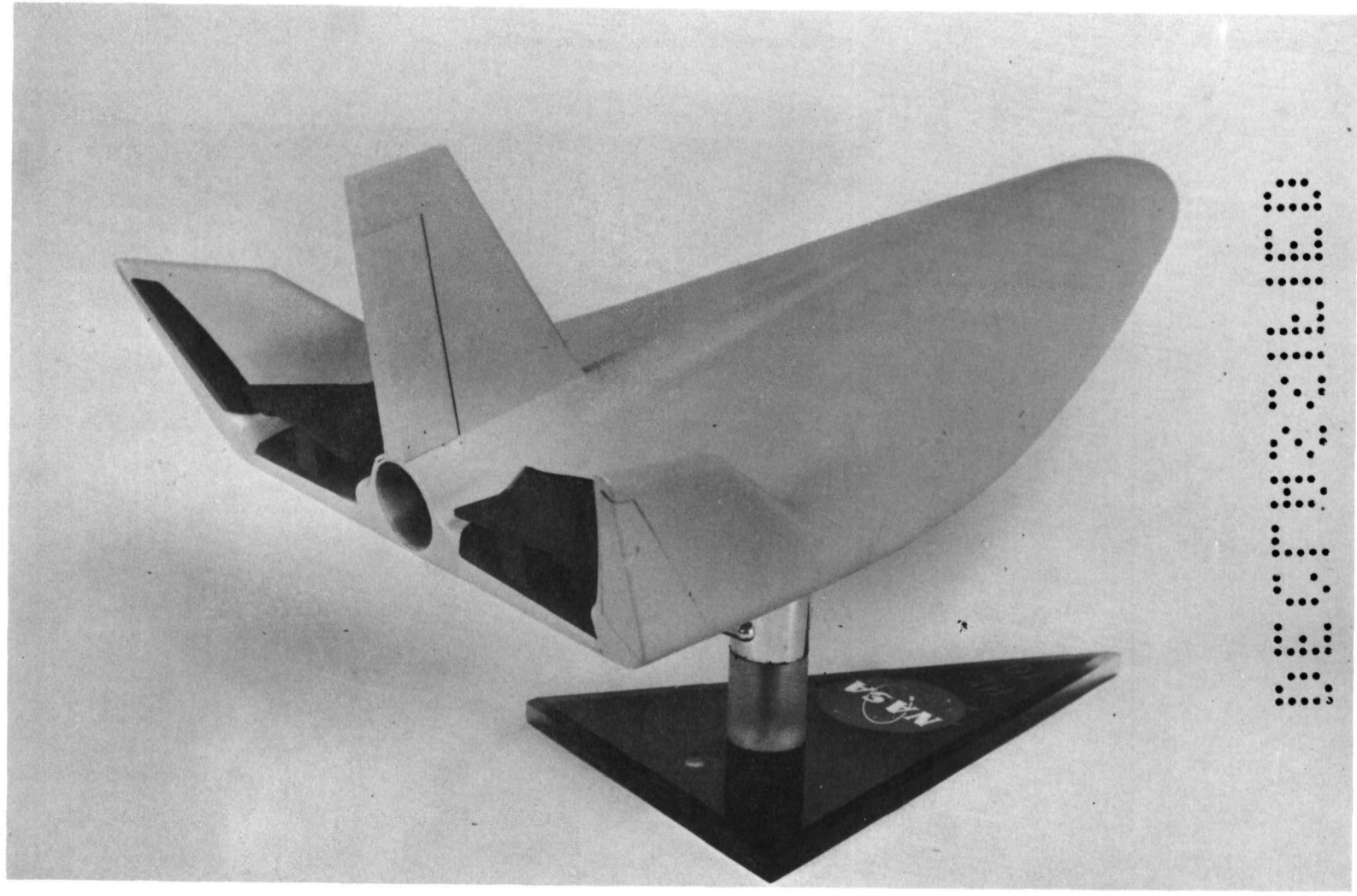

CONFIDENTIAL

(d) Three-quarter rear view (transonic configuration). L-65-6176

Figure 3.- Concluded.

[redacted]
DECLASSIFIED

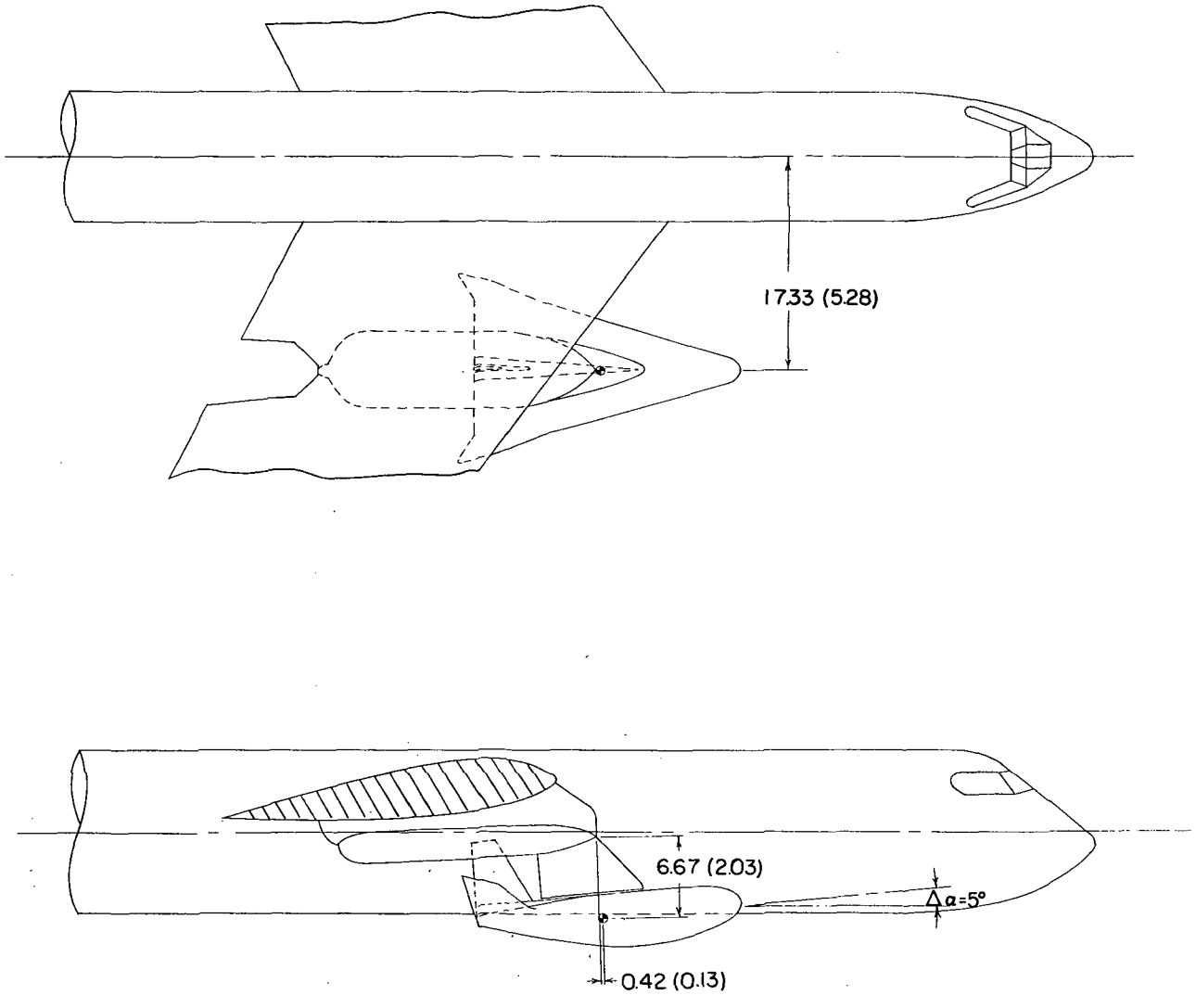


Figure 4.- Location of HL-10 on B-52. All dimensions are full scale and are shown in feet (meters).

[redacted]

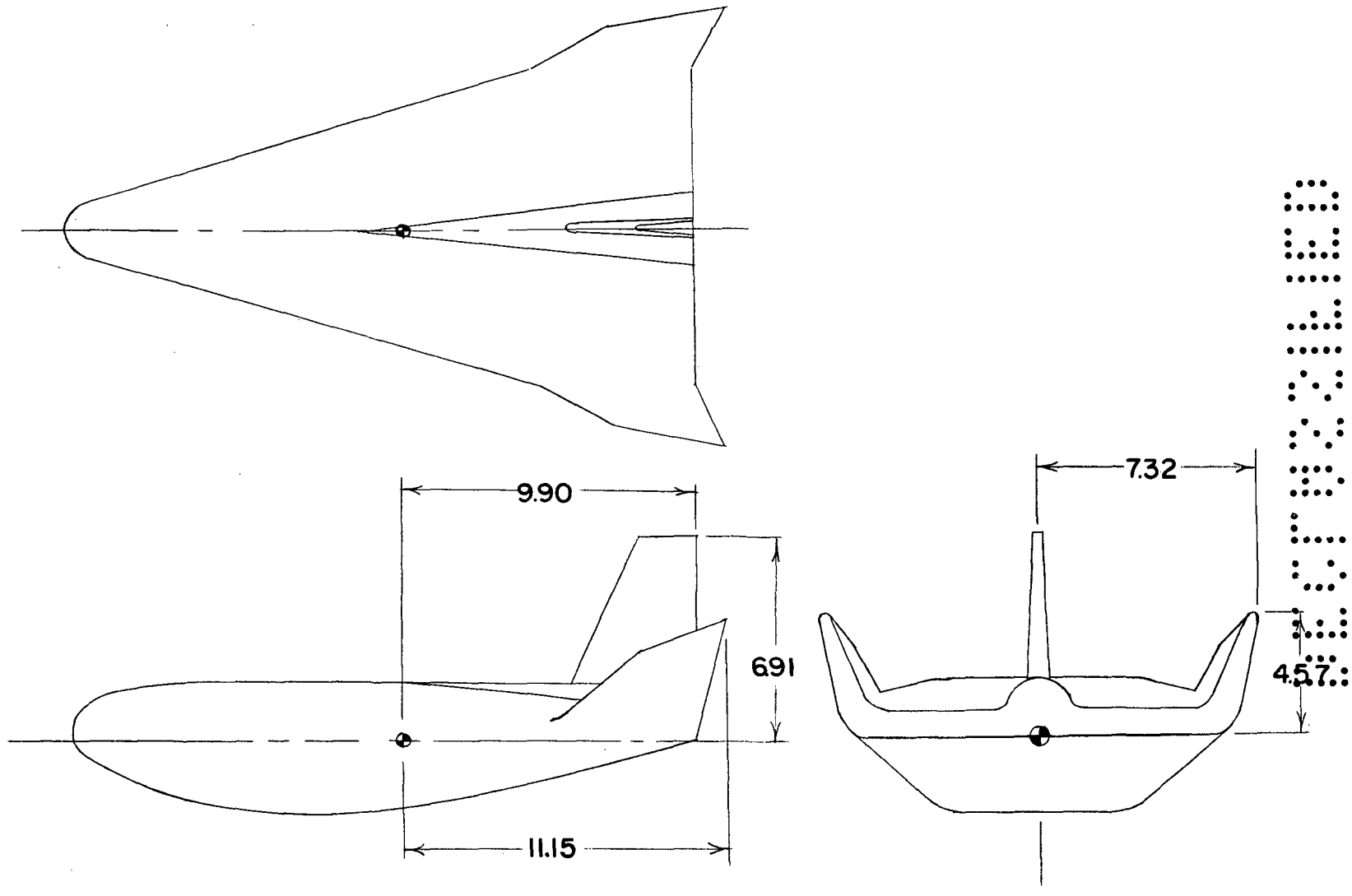


Figure 5.- Sketch of HL-10 showing points for which loci were computed. Dimensions are shown full scale in feet (1 foot = 0.3048 meter).

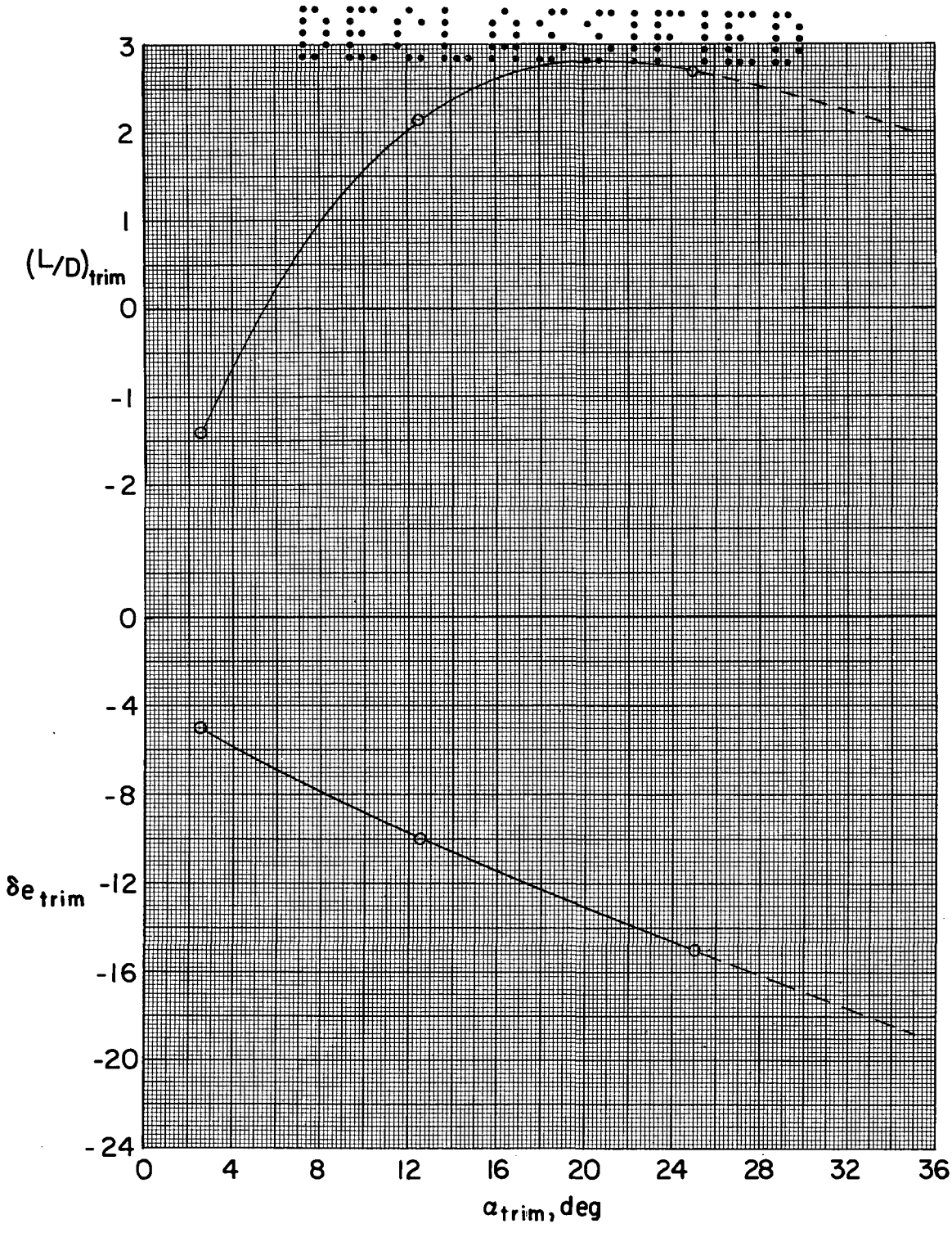


Figure 6.- Trim characteristics of the HL-10 subsonic configuration in free air. M = 0.60; 0.063-scale model. R = $4 \times 10^6$.

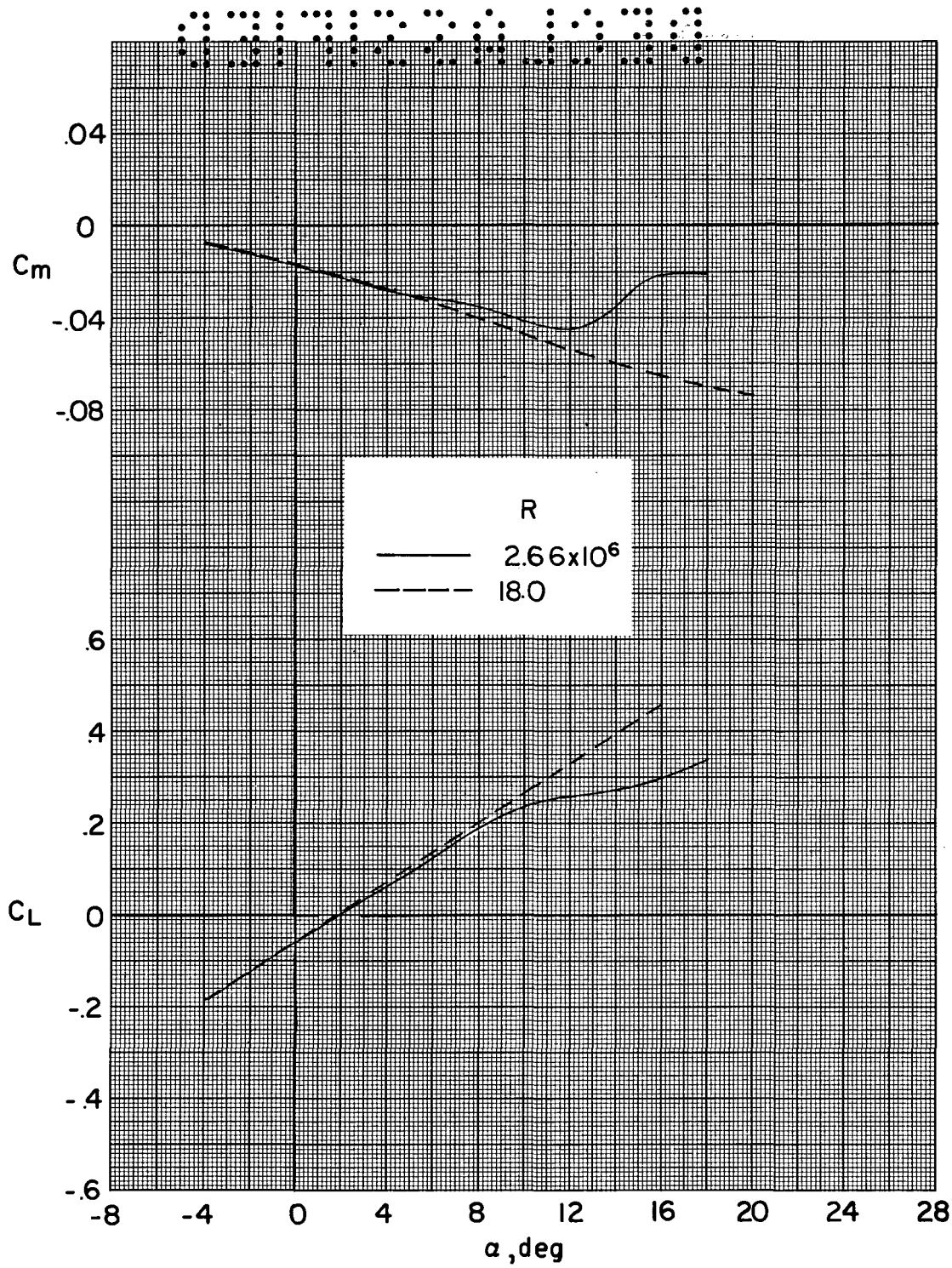


(a) $M \approx 0.3$; $\delta_e = 0$; 0.063-scale model.

Figure 7.- Effect of Reynolds number on the longitudinal characteristics of the HL-10 subsonic configuration in free air.

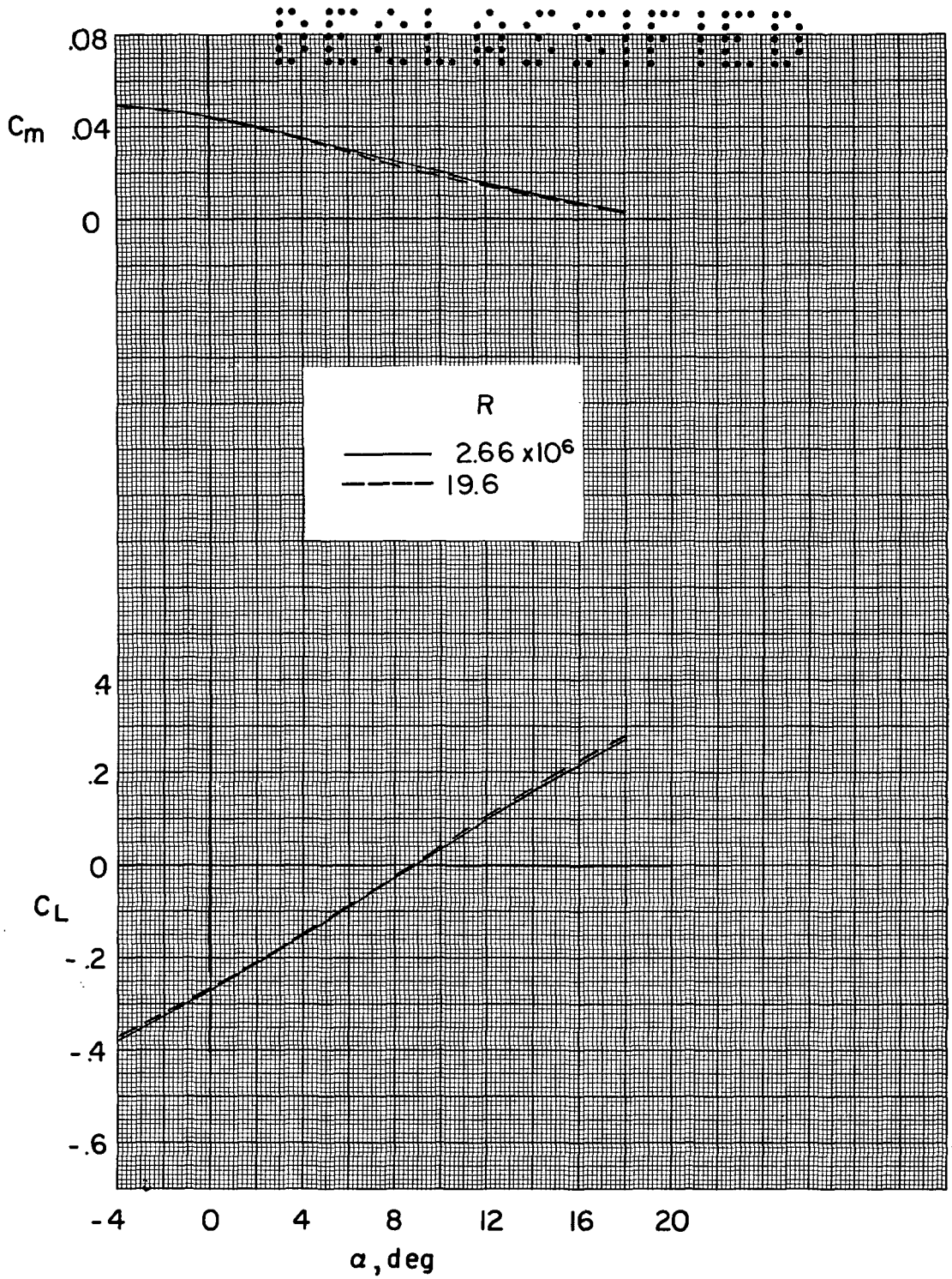


(b) $M \approx 0.3$; $\delta_e = -15^0$; 0.063-scale model.

Figure 7.- Continued.

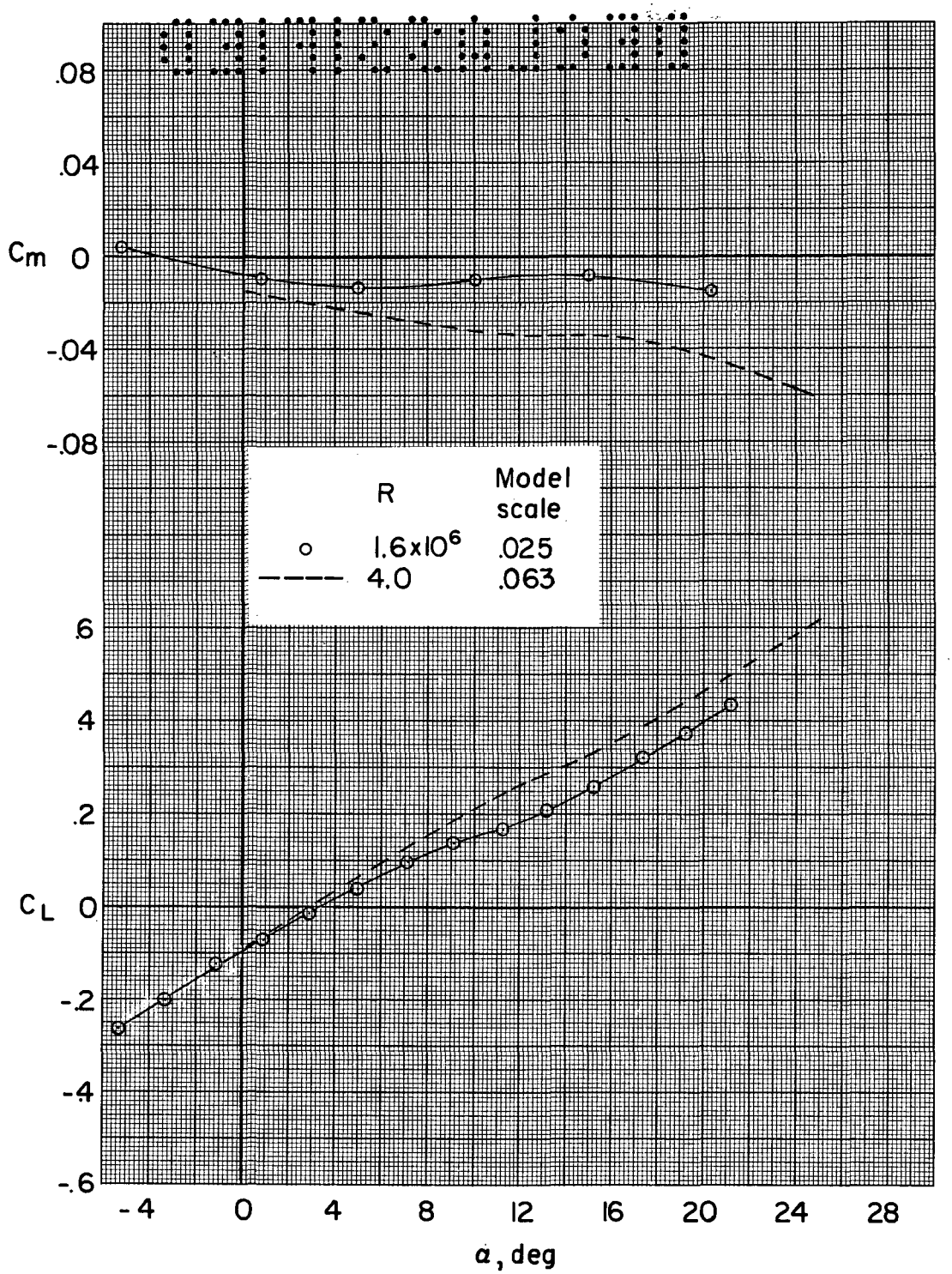


(c) M = 0.60; $\delta_e$ = 0.

Figure 7.- Continued.

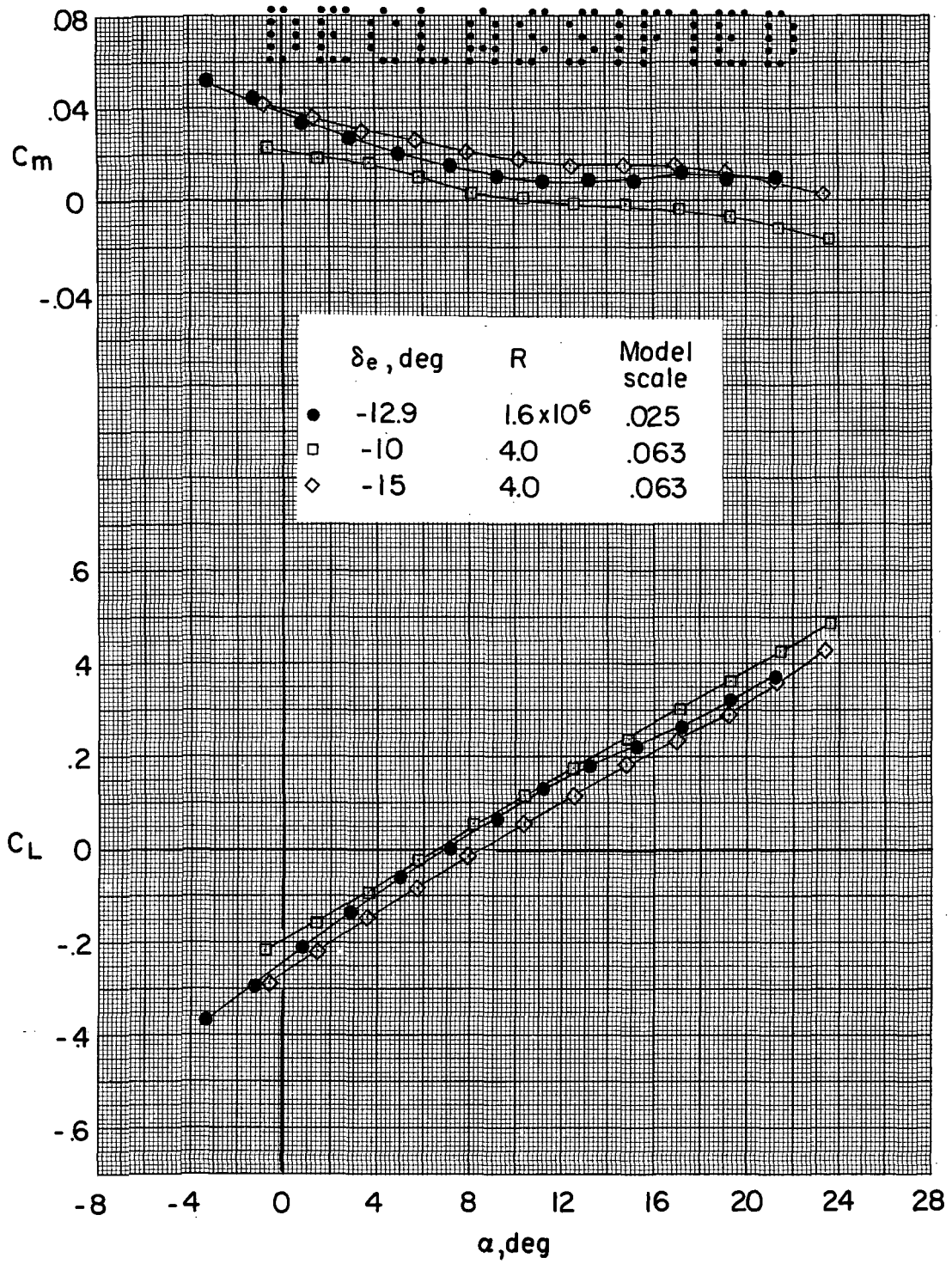


(d) M = 0.60; $\delta_e$ near trim.

Figure 7.- Concluded.

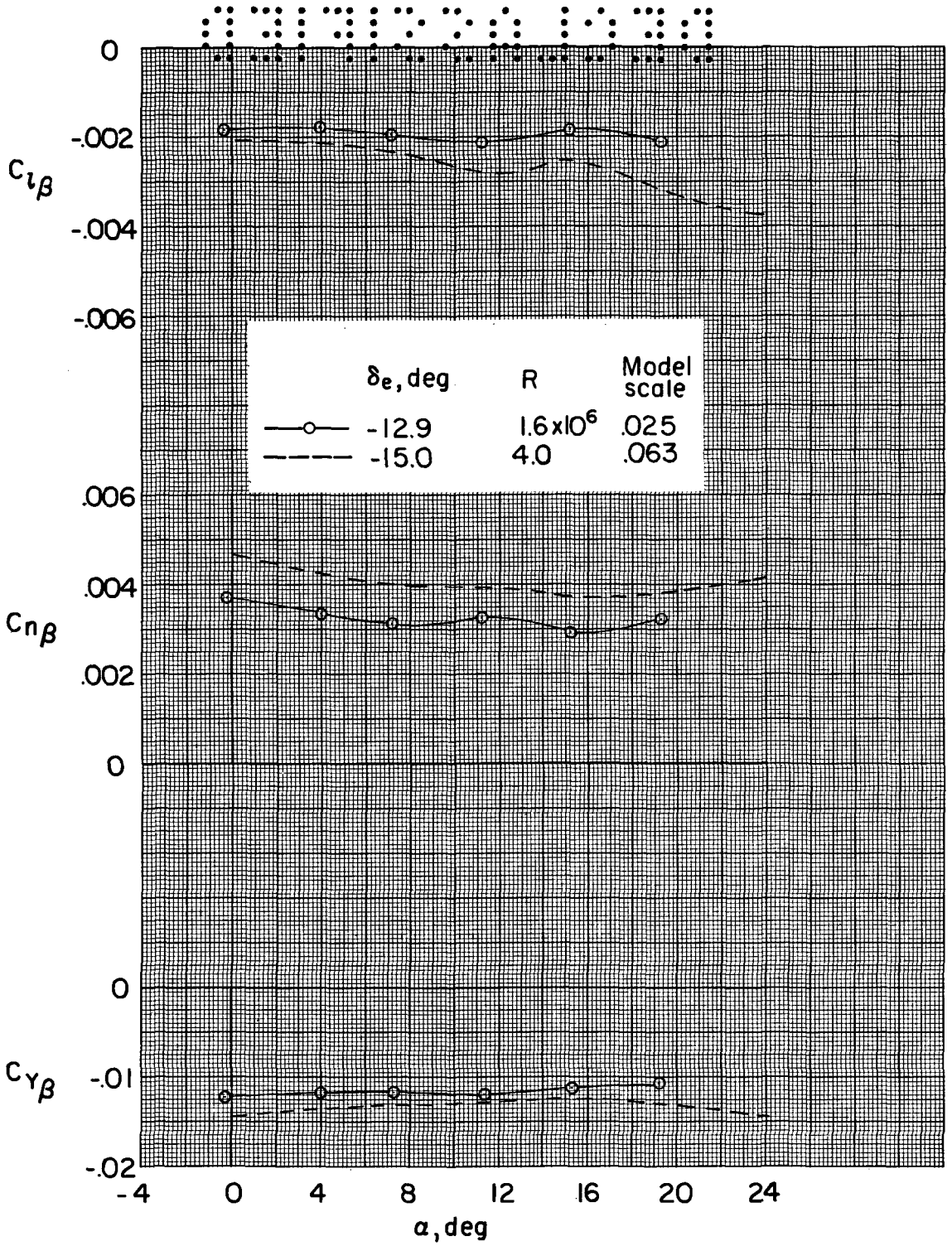


Figure 8.- Effect of Reynolds number on the lateral-directional characteristics of the HL-10 subsonic configuration in free air. M = 0.60.

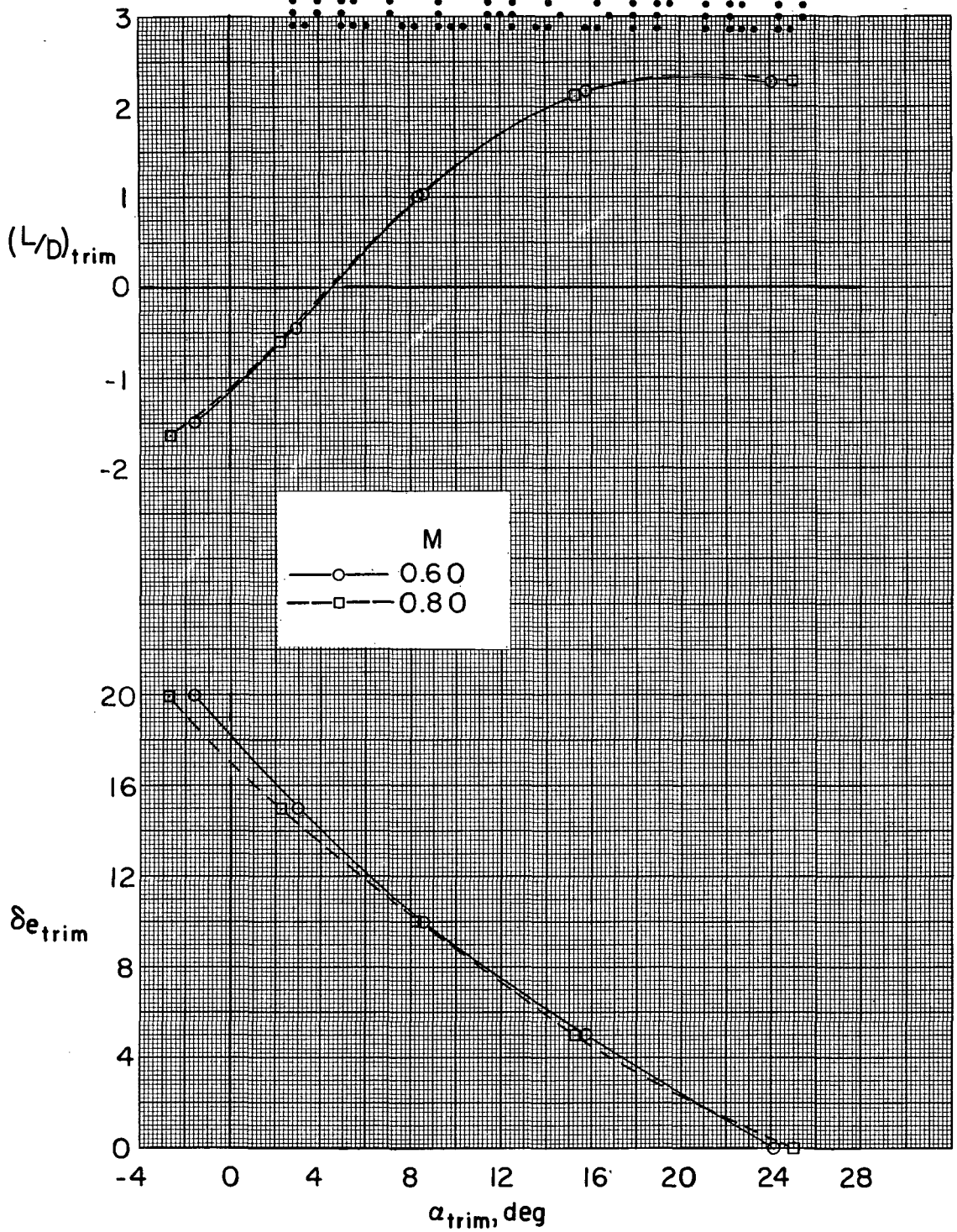


Figure 9.- Trim characteristics of the HL-10 transonic configuration in free air. 0.063-scale model.

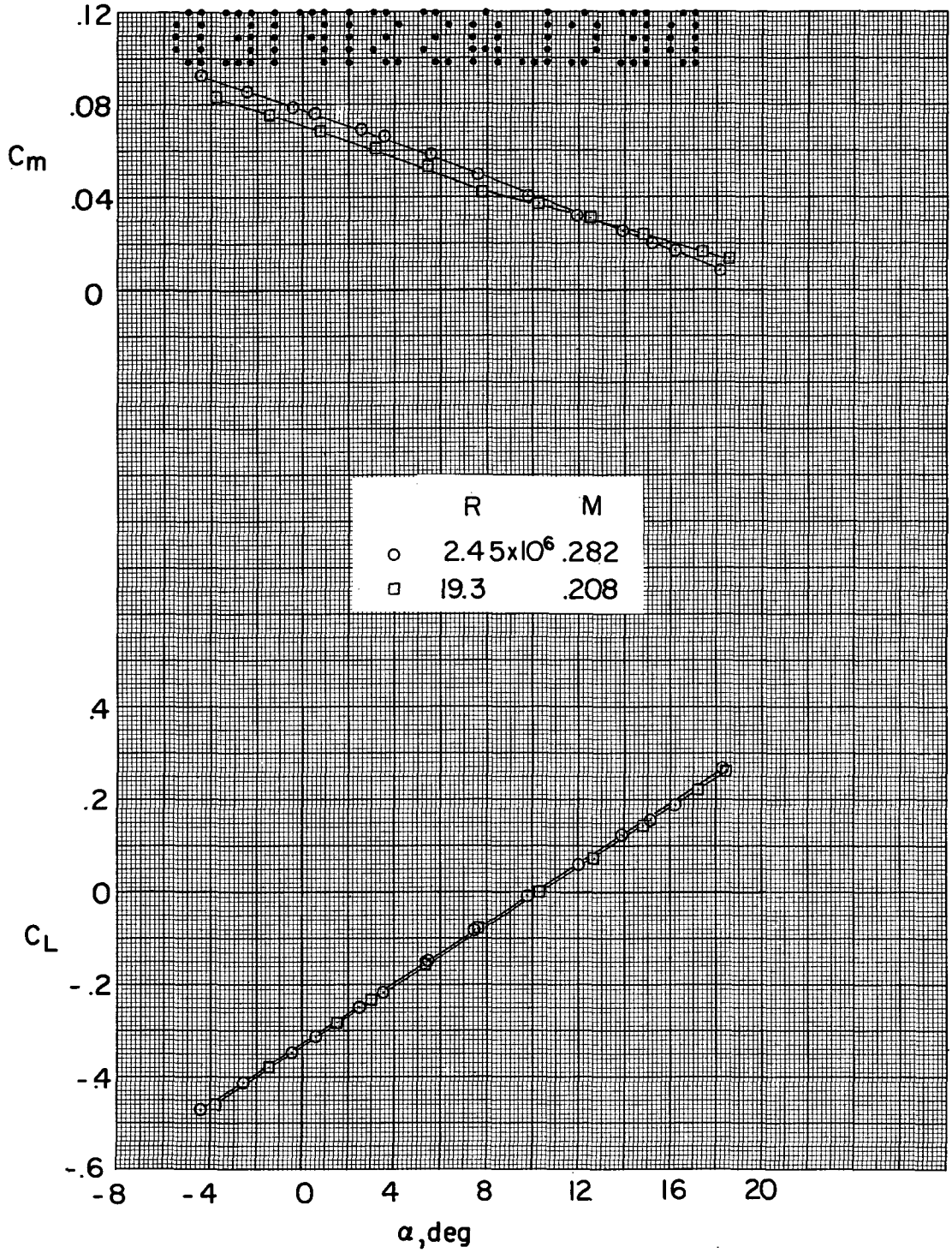


(a) $\delta_e = 0$; 0.063-scale model.

Figure 10.- Effect of Reynolds number on the longitudinal characteristics of the HL-10 transonic configuration in free air.

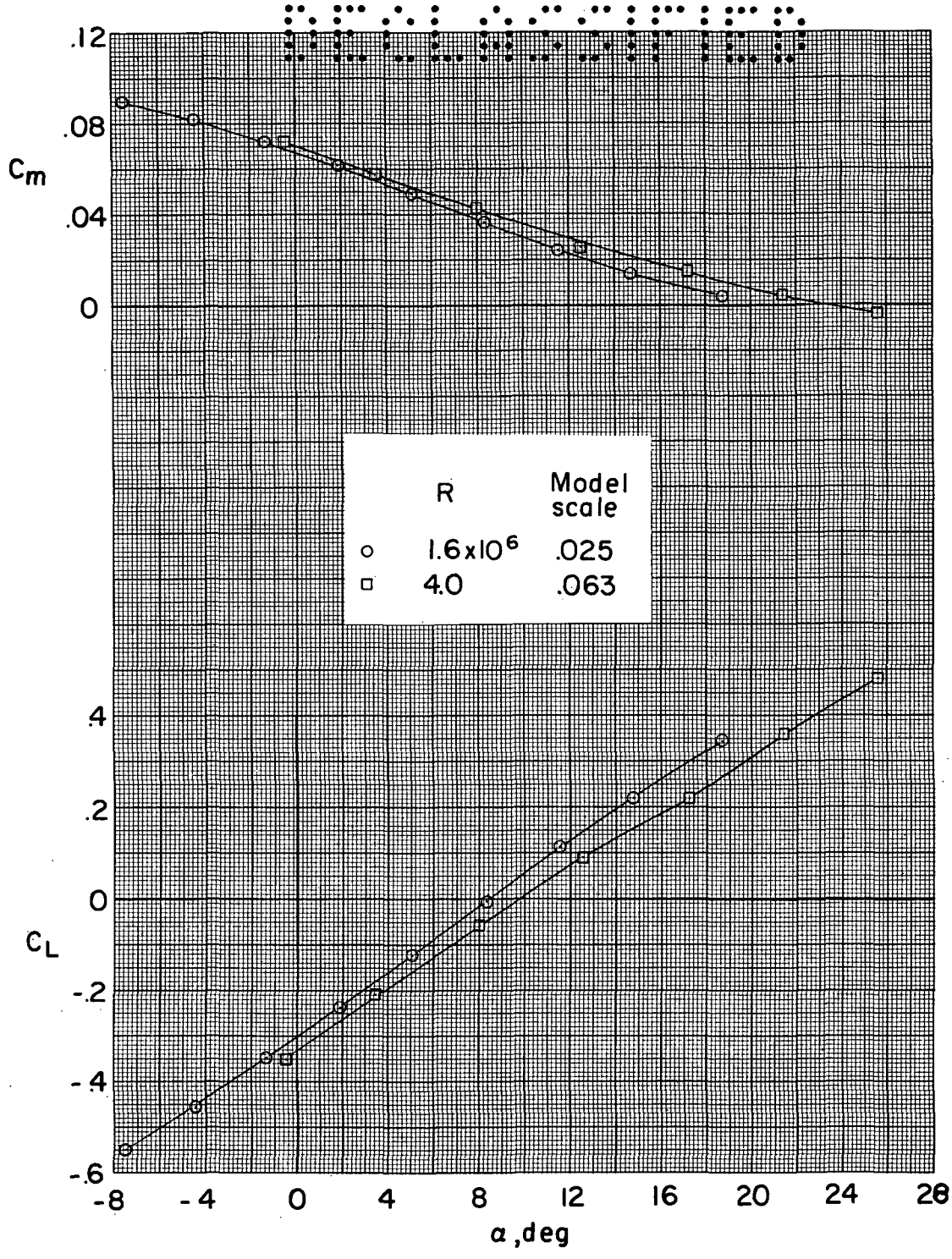


(b) $\delta_e = 0$; M = 0.60.

Figure 10.- Continued.

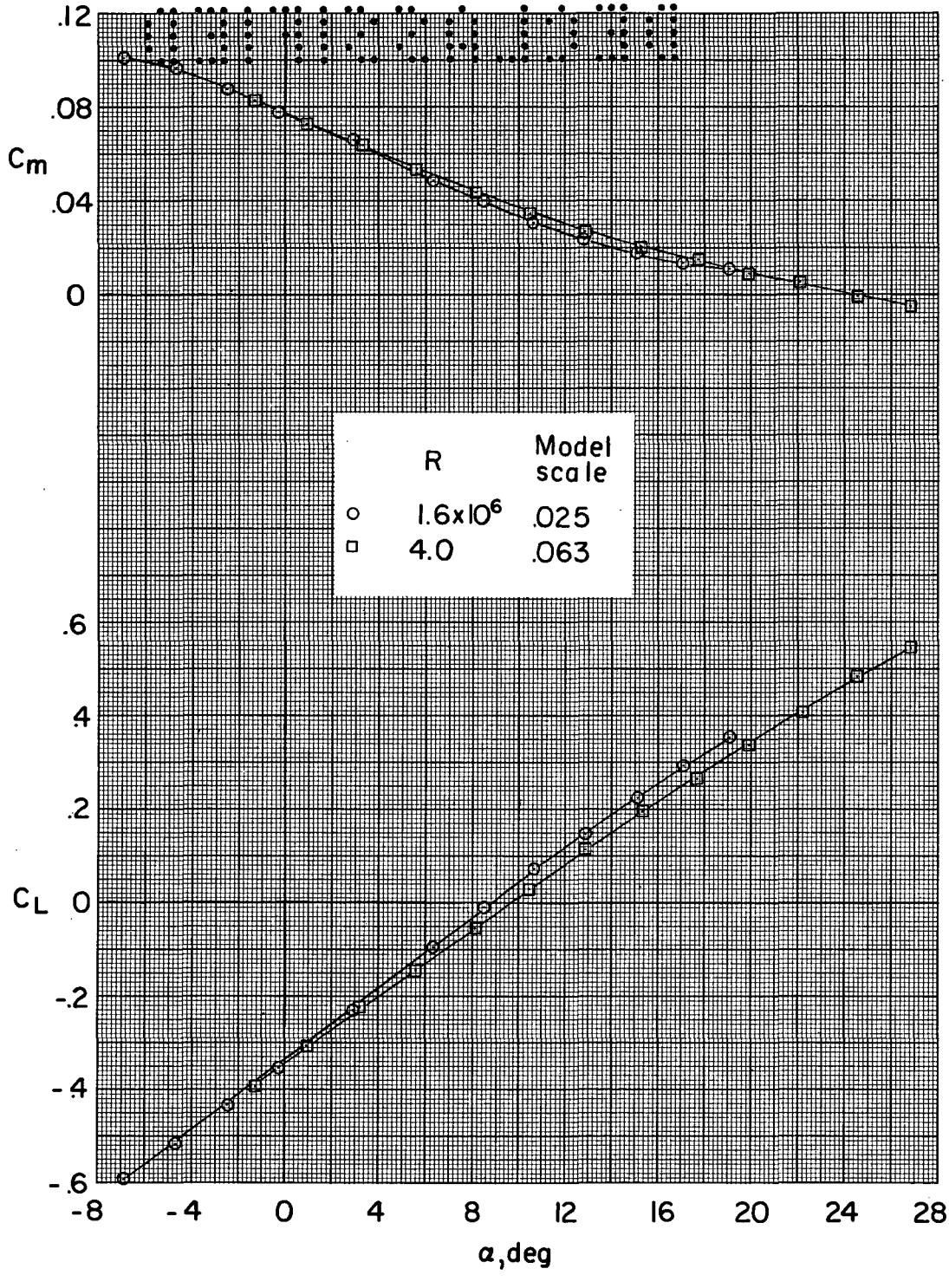


(c) $\delta_e = 0$; M = 0.80.

Figure 10.- Concluded.

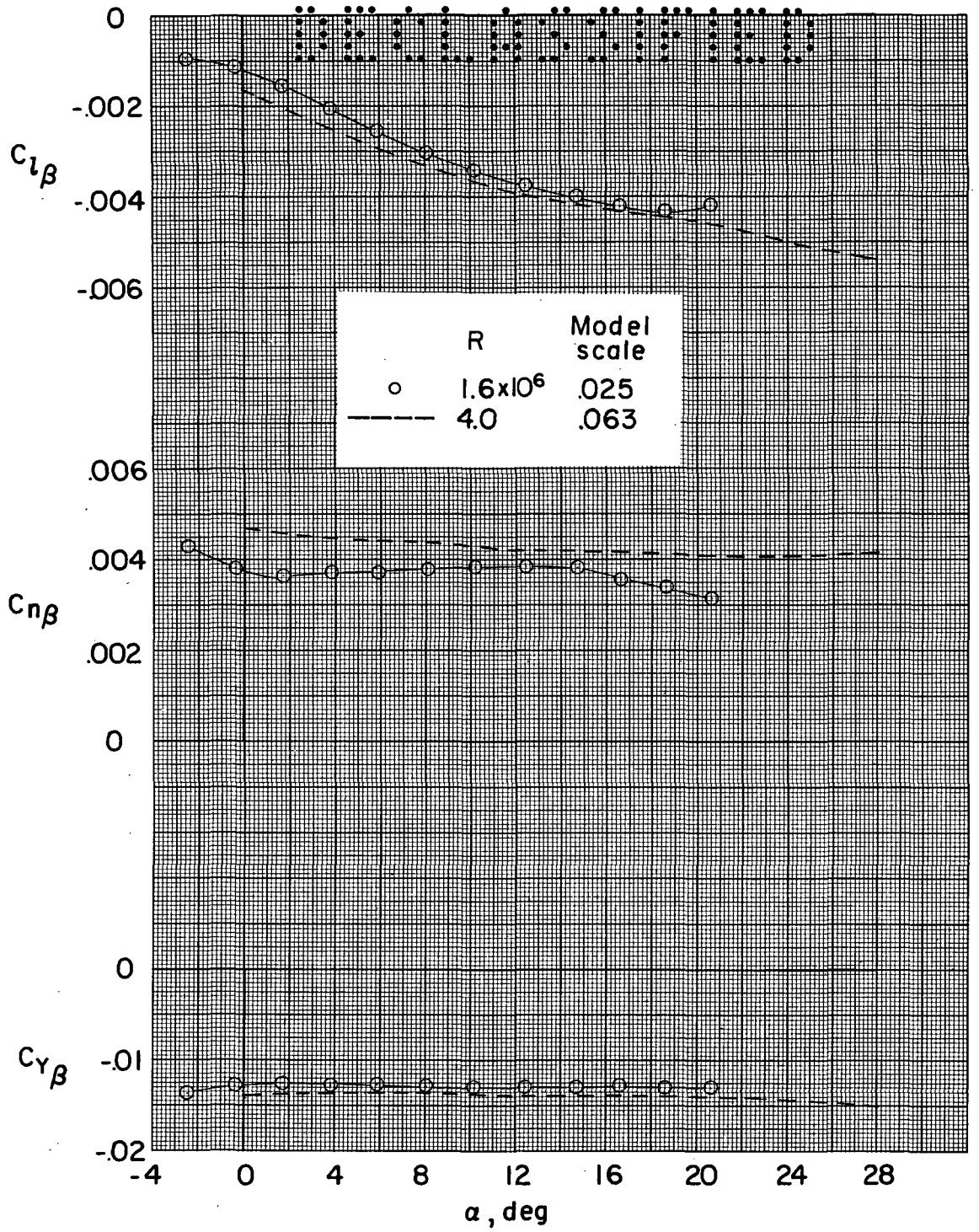


(a) M = 0.60.

Figure 11.- Effect of Reynolds number on the lateral-directional characteristics of the HL-10 transonic configuration in free air. $\delta_e = 0$.

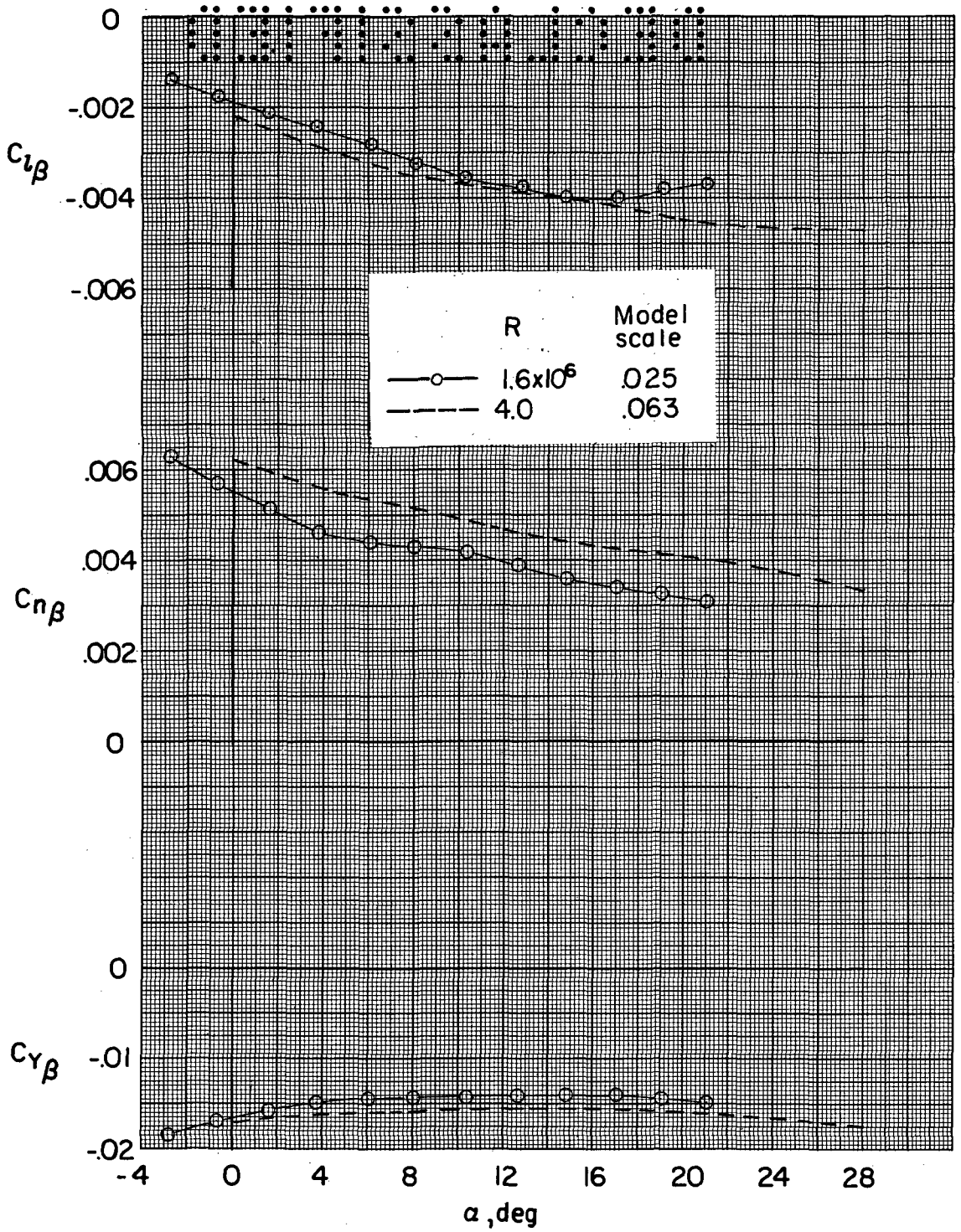


(b) M = 0.80.

Figure 11.- Concluded.

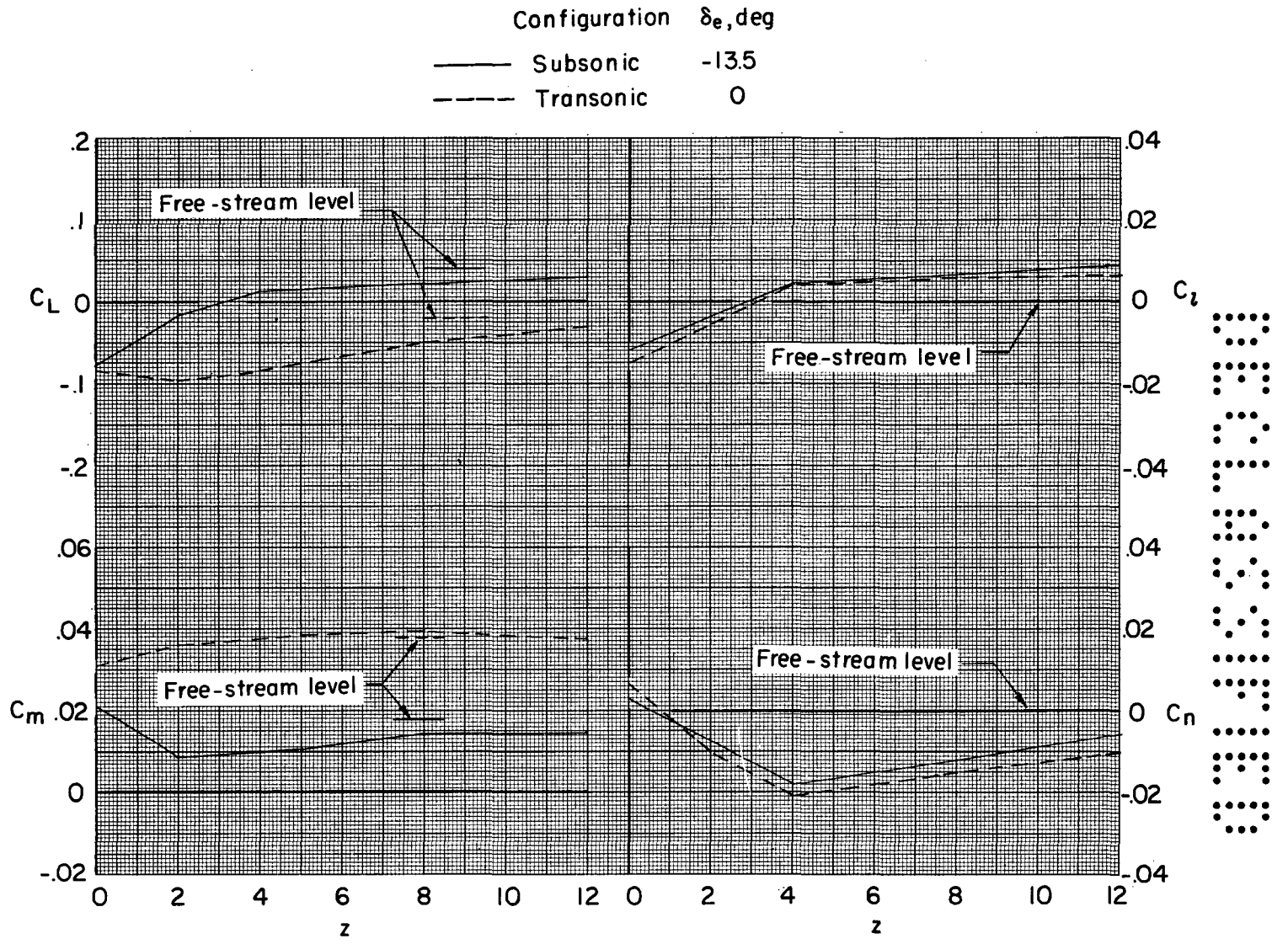


Figure 12.- Effect of separation distance on the aerodynamic coefficients of the HL-10. M = 0.60; $\alpha_{B-52}$; $\Delta\alpha = 5^0$; $\alpha_{HL-10} = 9^0$.

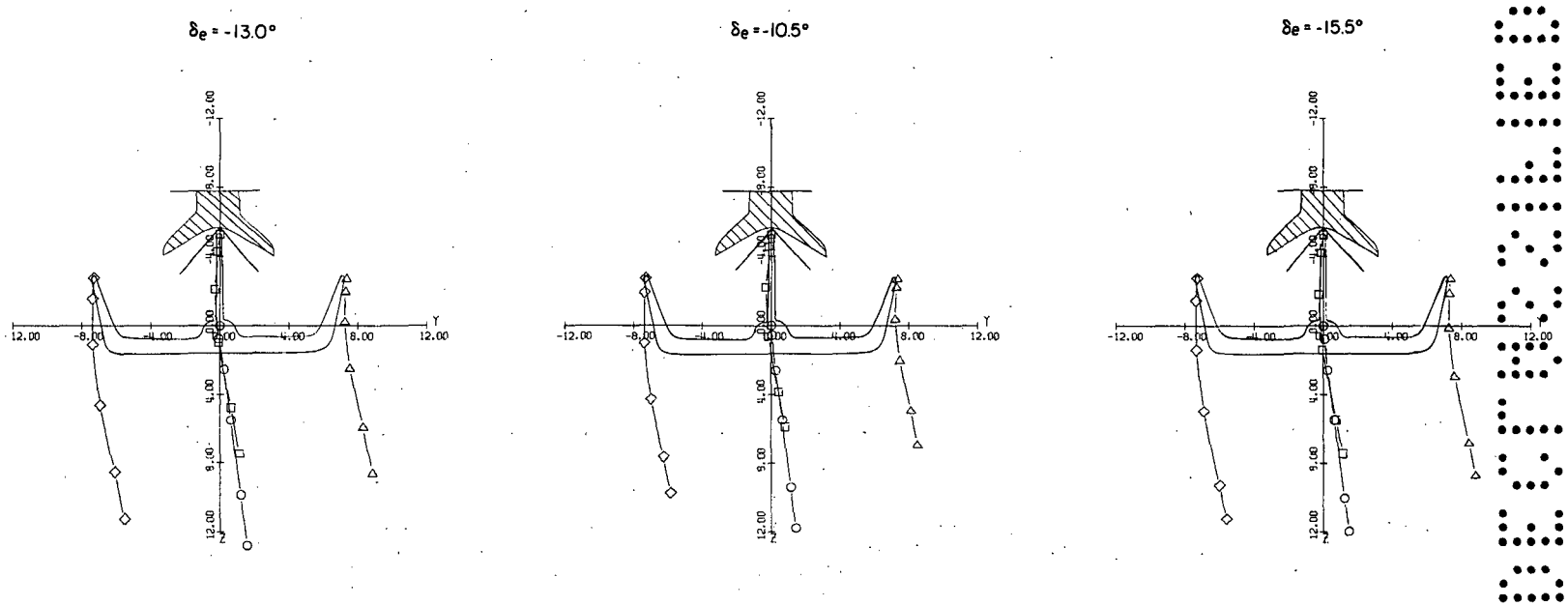


(a) Fin-tip and center-of-gravity paths. (Values along the coordinate scale are given in feet; 1 foot = 0.3048 meter.)

Figure 13.- Effect of pitch control setting $\delta_e$ on motions of HL-10 subsonic configuration after launch. $M = 0.60$; $\alpha_{B-52} = 4^0$; $\Delta\alpha = 5^0$; dampers off; $W_{B-52}$ = 240 000 pounds (1 067 568 newtons).

DECLASSIFIED

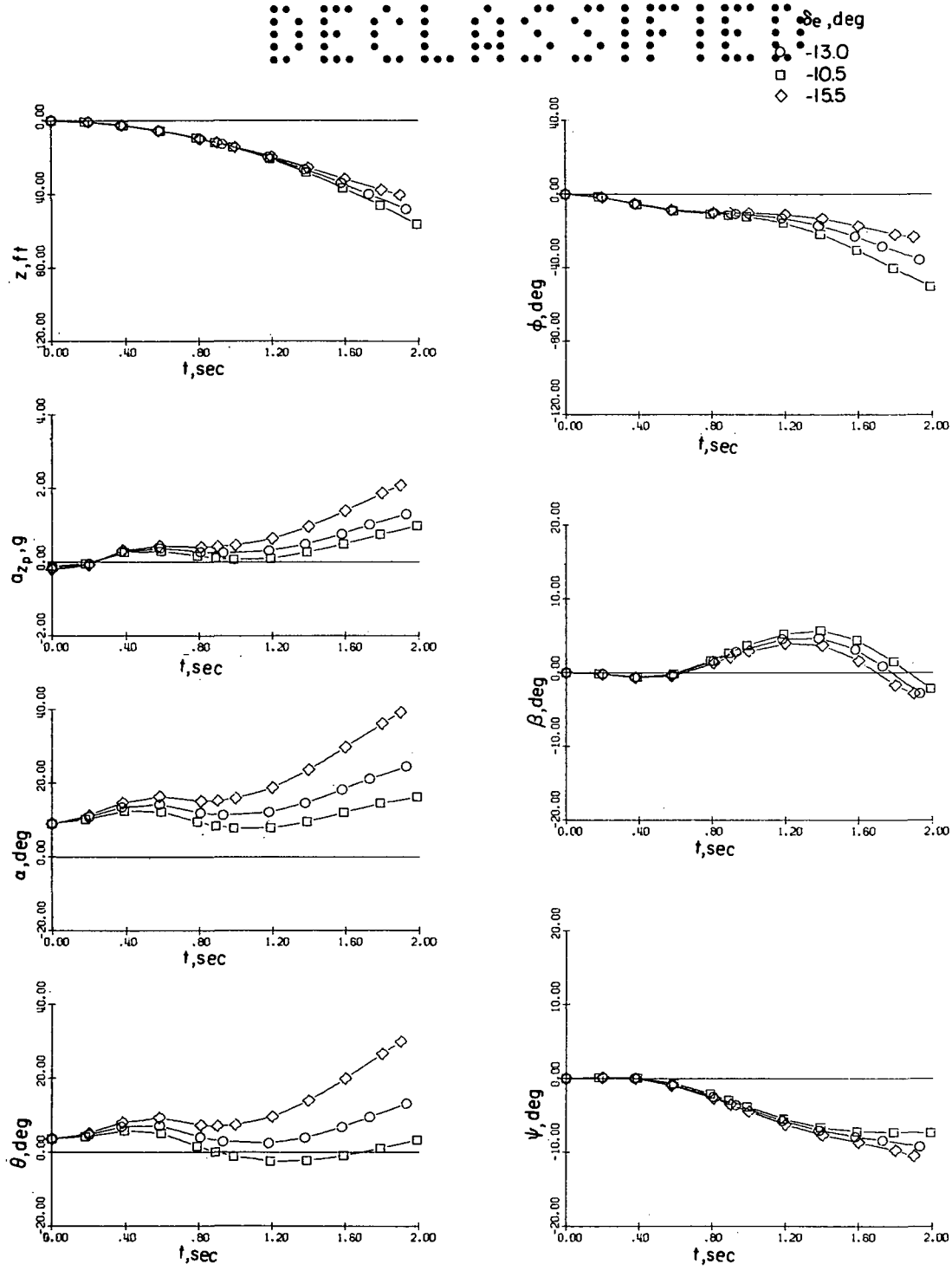


(b) Motion variables plotted against time after launch.

Figure 13.- Concluded.

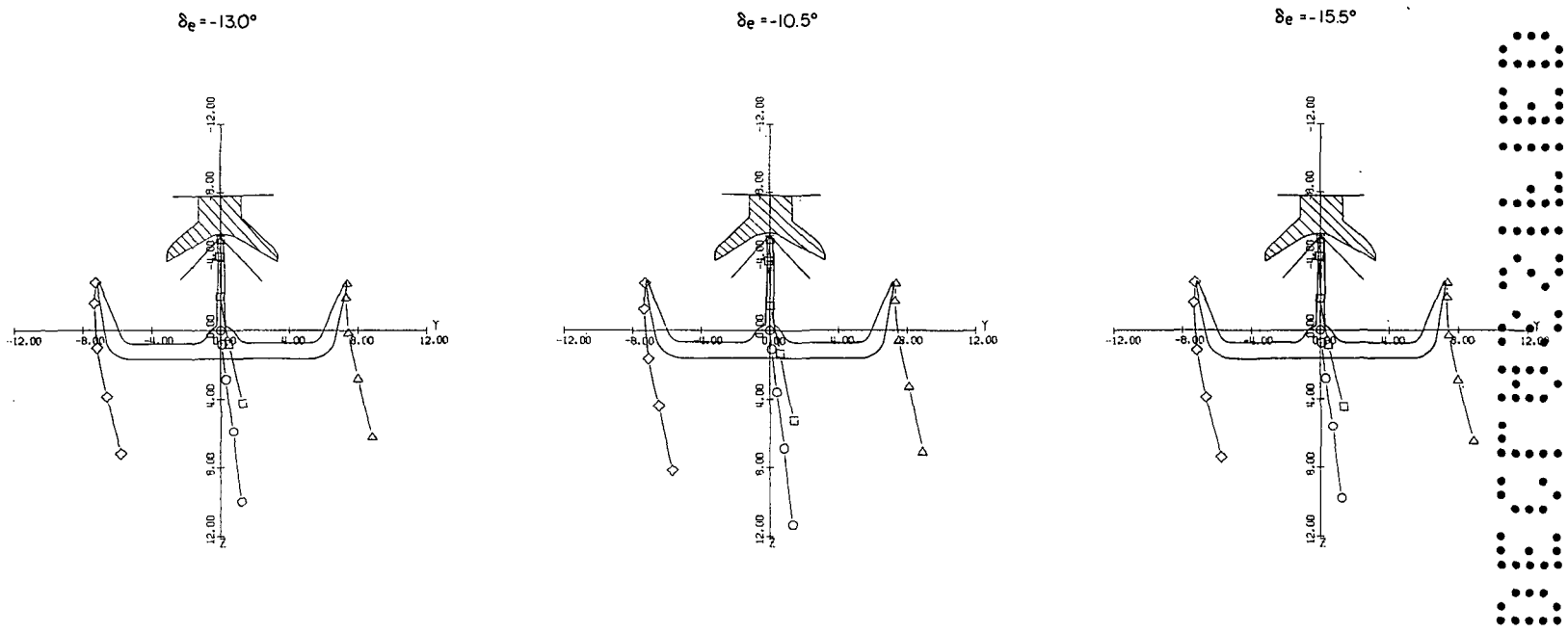


(a) Fin-tip and center-of-gravity paths. (Values along the coordinate scales are given in feet; 1 foot = 0.348 meter.)

Figure 14.- Effect of pitch control setting $\delta_e$ on motions of HL-10 subsonic configuration after launch. $M = 0.60$; $\alpha_{B-52} = 4^0$; $\Delta\alpha = 5^0$; dampers on; $W_{B-52}$ = 240 000 pounds (1 067 568 newtons).

[redacted]

DECLASSIFIED

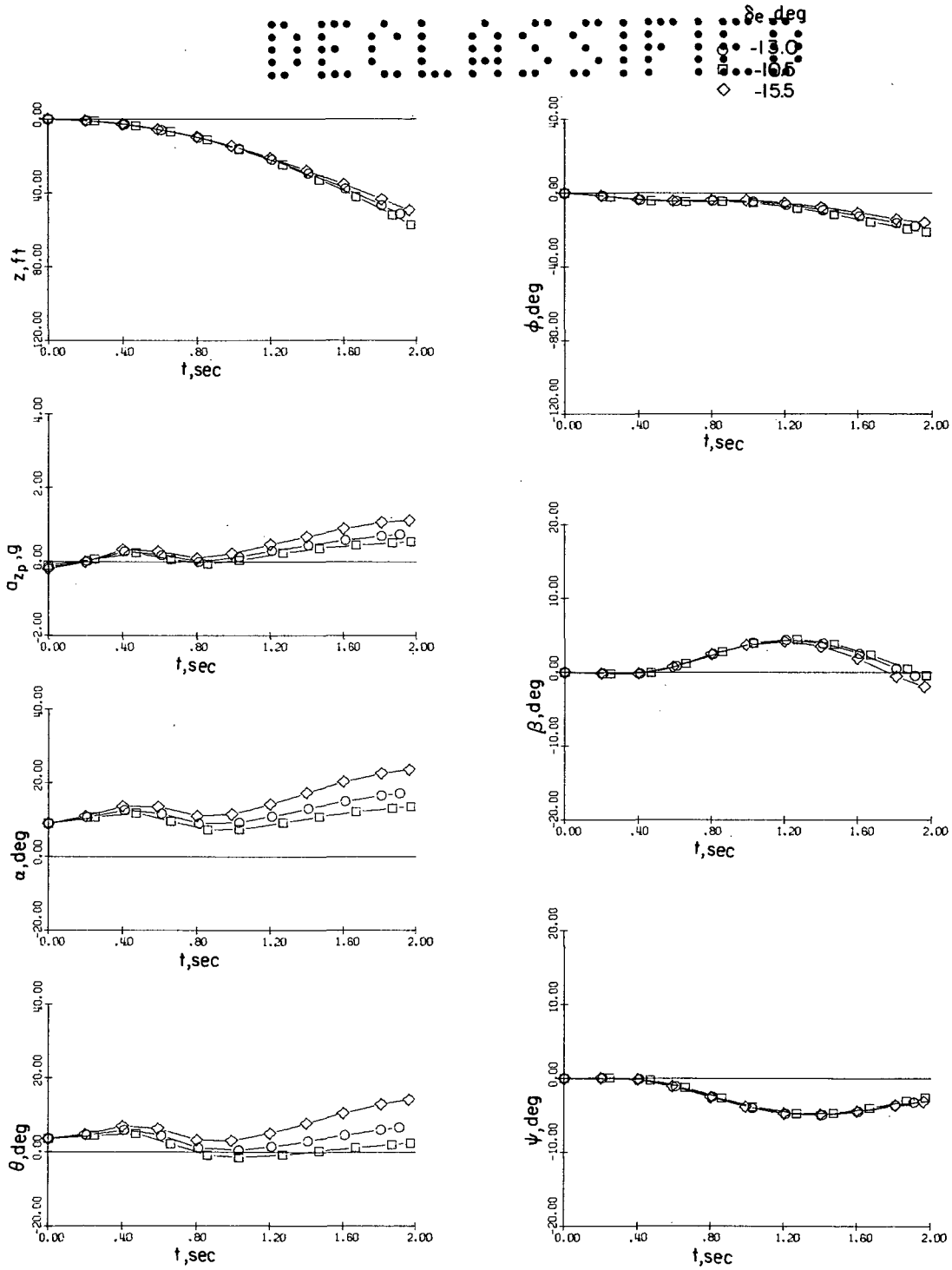


(b) Motion variables plotted against time after launch.

Figure 14.- Concluded.

[redacted]

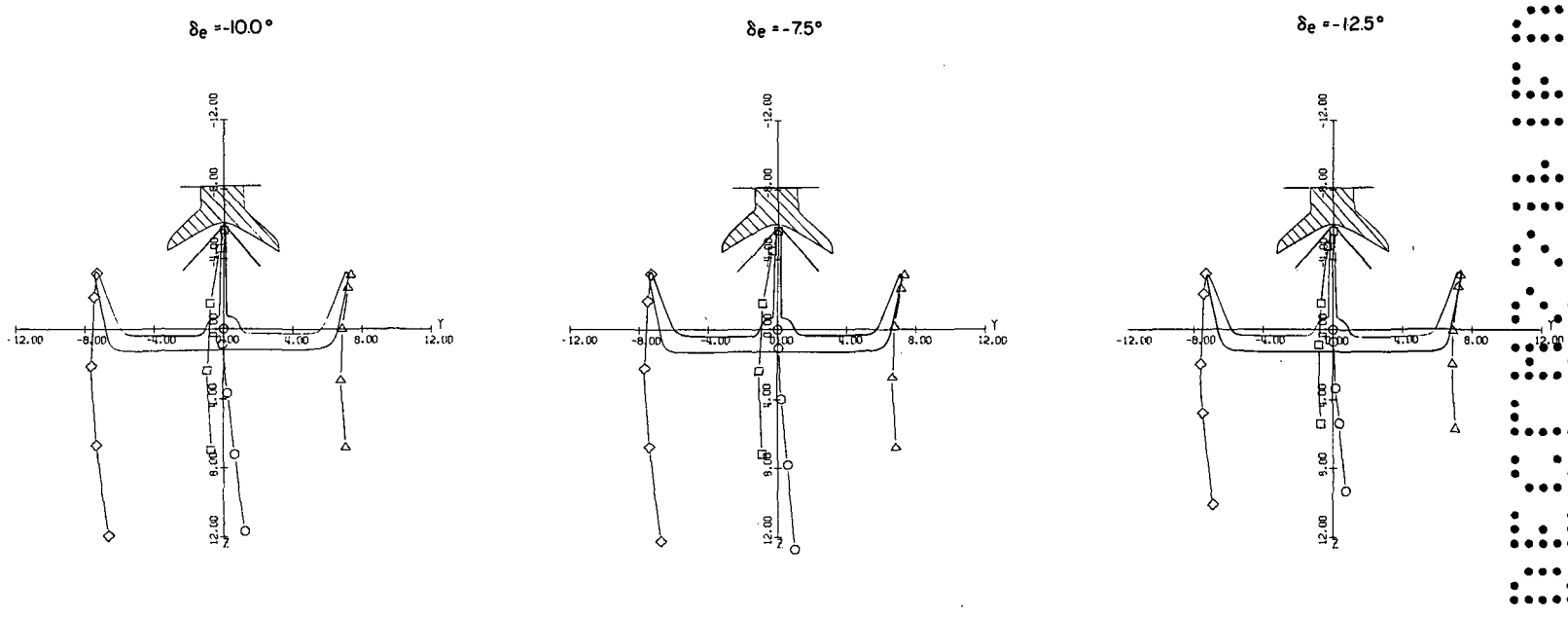


(a) Fin-tip and center-of-gravity paths. (Values along the coordinate scales are given in feet; 1 foot = 0.3048 meter.)

Figure 15.- Effect of pitch control setting $\delta_e$ on motions of HL-10 subsonic configuration after launch. $M = 0.65$; $\alpha_{B-52} = 2^0$; $\Delta\alpha = 5^0$; dampers off; $W_{B-52}$ = 240 000 pounds (1 067 568 newtons).

[redacted]

DECLASSIFIED

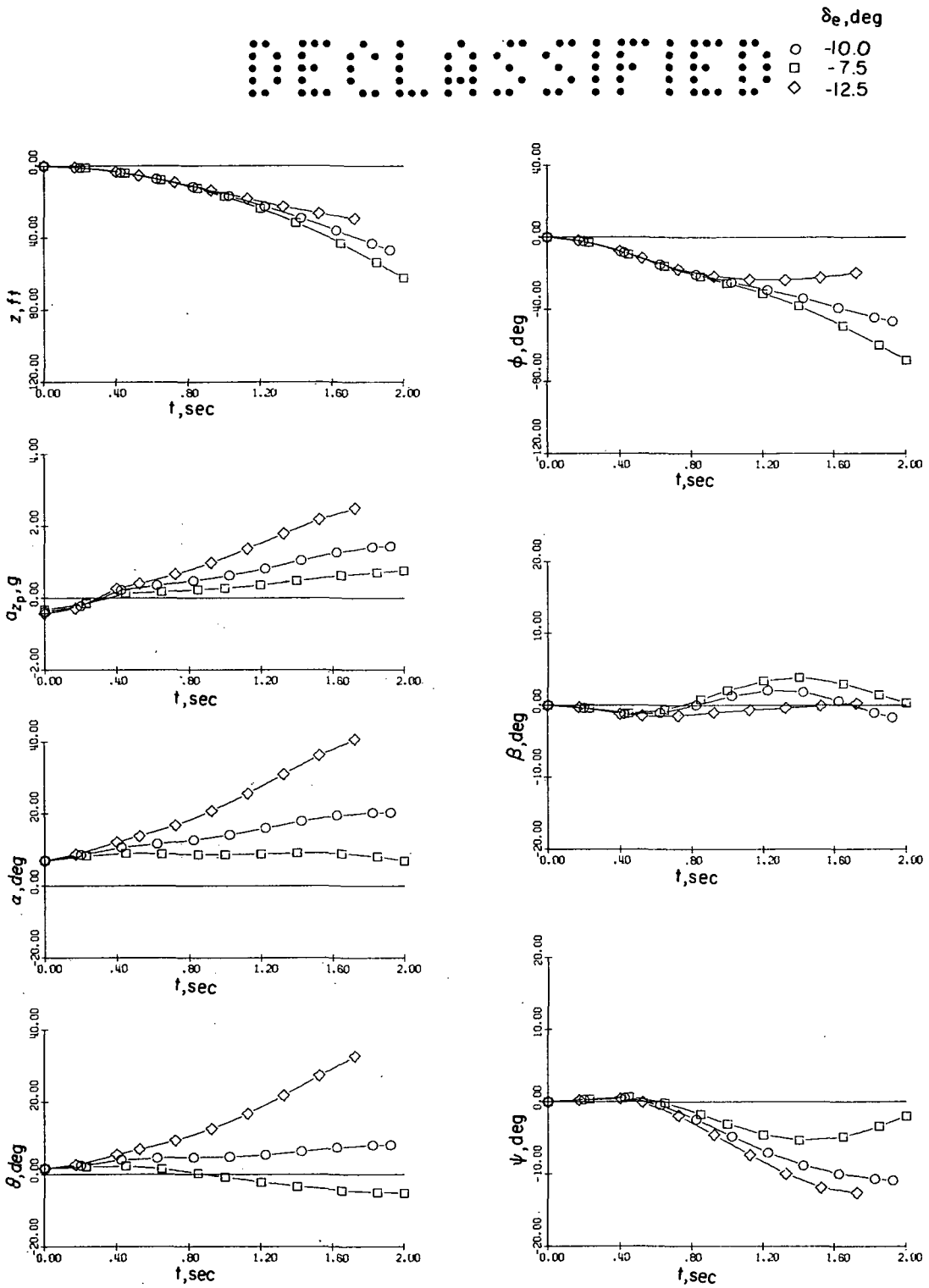


(b) Motion variables plotted against time after launch.

Figure 15.- Concluded.

[redacted]

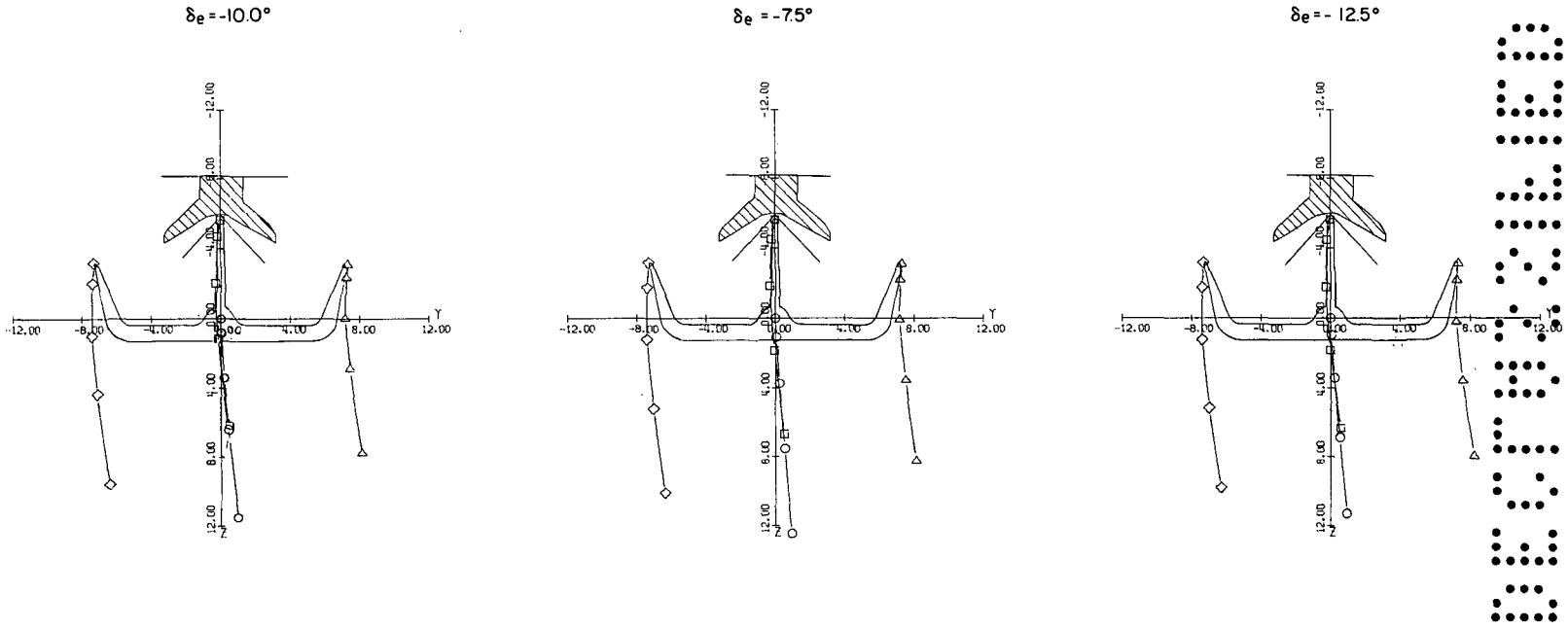


(a) Fin-tip and center-of-gravity paths. (Values along the coordinate scales are given in feet; 1 foot = 0.3048 meter.)

Figure 16.- Effect of pitch control setting $\delta_e$ on motions of HL-10 subsonic configuration after launch. $M = 0.65$; $\alpha_{B-52} = 2^0$; $\Delta\alpha = 5^0$; dampers on; $W_{B-52} = 240\,000$ pounds (1 067 568 newtons).

DECLASSIFIED

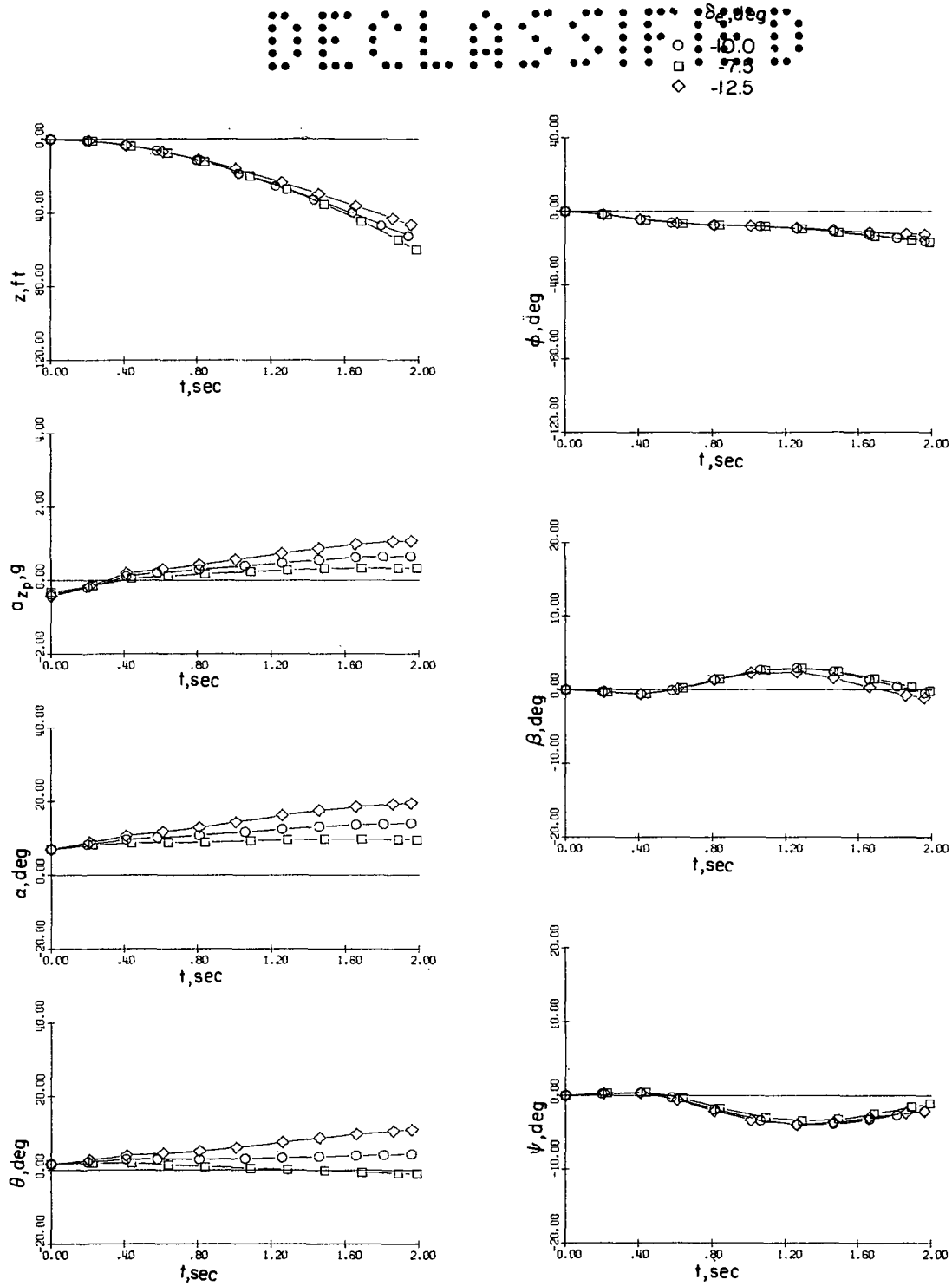


(b) Motion variables plotted against time after launch.

*Figure 16.- Concluded.*

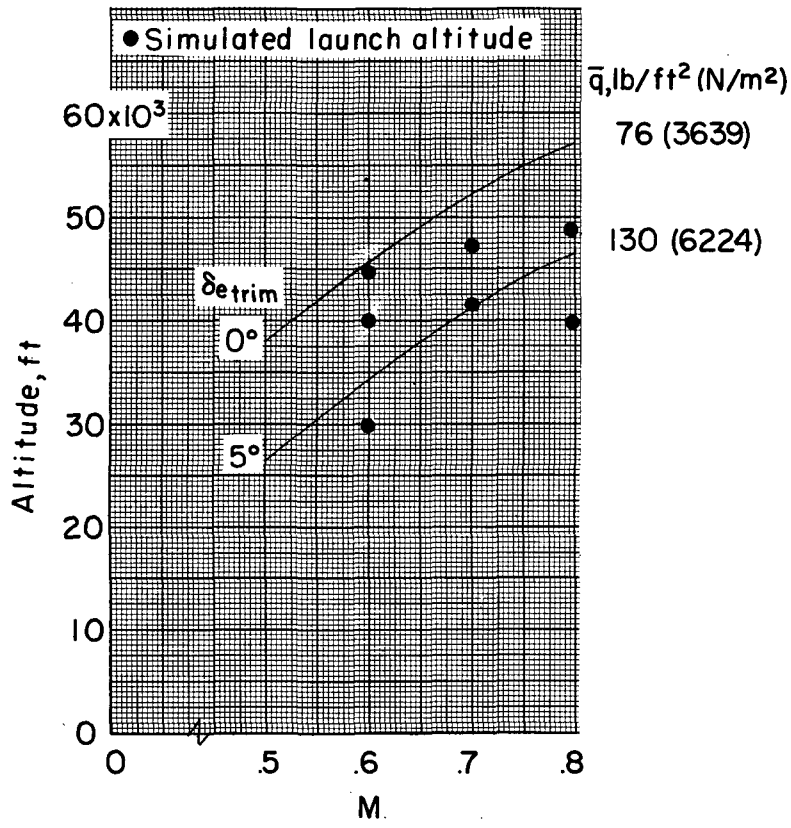


(a) $W_{HL-10}$ = 5308 pounds (23 611 newtons).

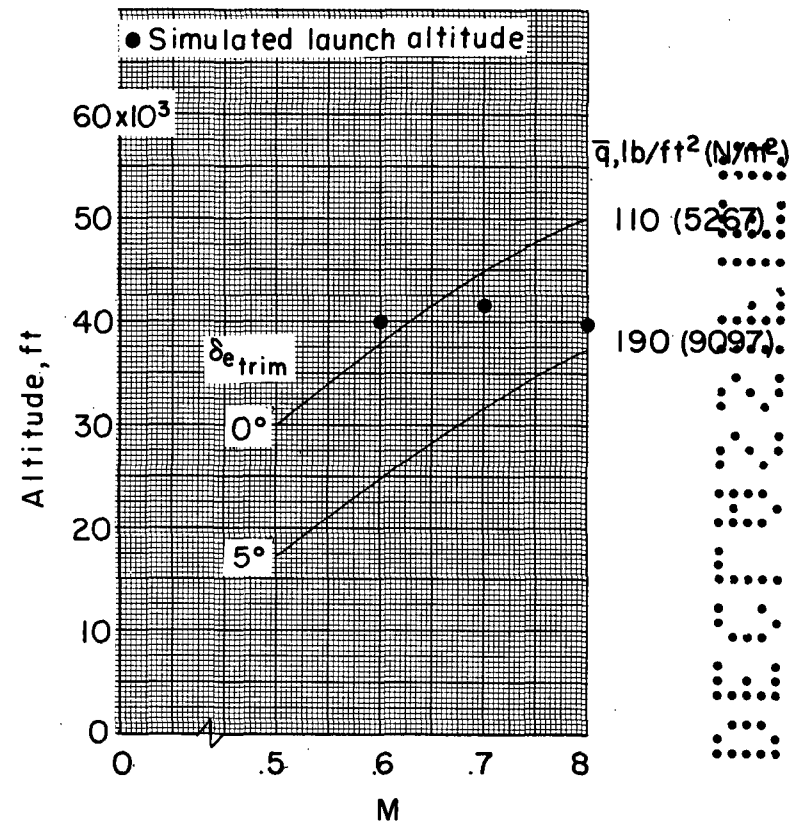


(b) $W_{HL-10}$ = 7968 pounds (35 443 newtons).

Figure 17.- Launch envelope studied for HL-10 transonic configuration. $\Delta\alpha = 5^0$.

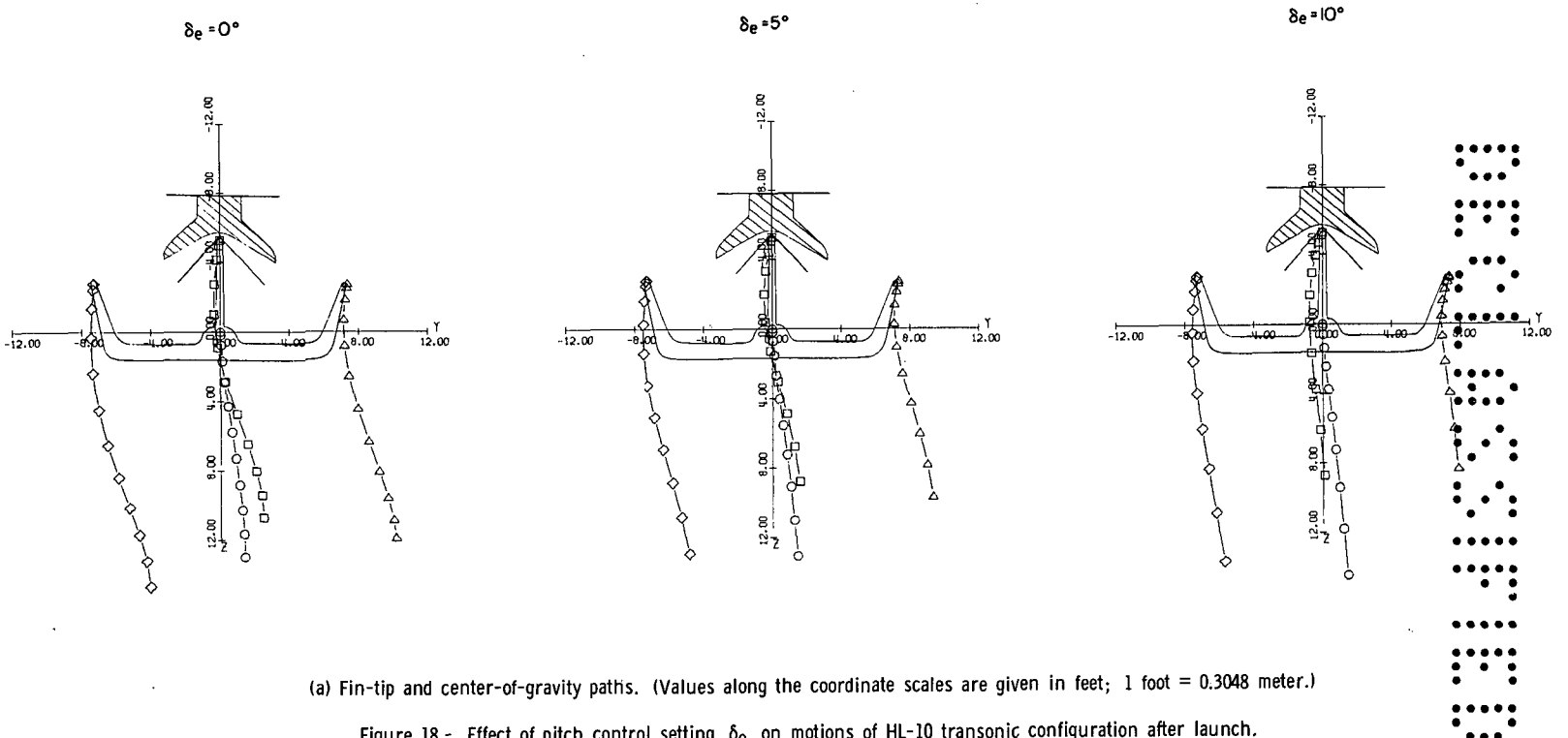


(a) Fin-tip and center-of-gravity paths. (Values along the coordinate scales are given in feet; 1 foot = 0.3048 meter.)

Figure 18.- Effect of pitch control setting $\delta_e$ on motions of HL-10 transonic configuration after launch. $M = 0.60$; $\alpha_{B-52} = 4^0$; $\Delta\alpha = 5^0$; dampers off; $W_{B-52} = 250\,000$ pounds (1 112 050 newtons).

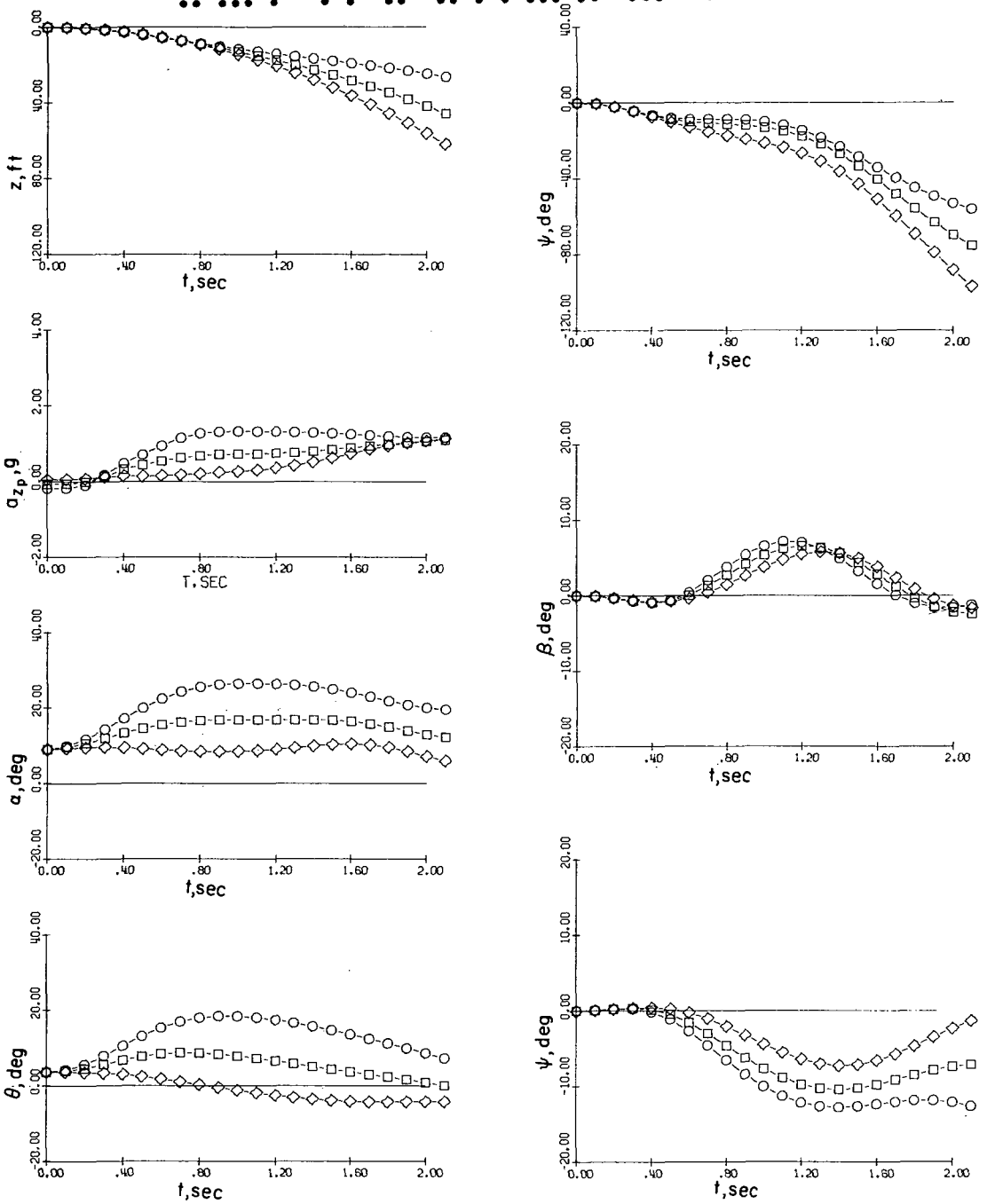


(b) Motion variables plotted against time after launch.

Figure 18.- Concluded.

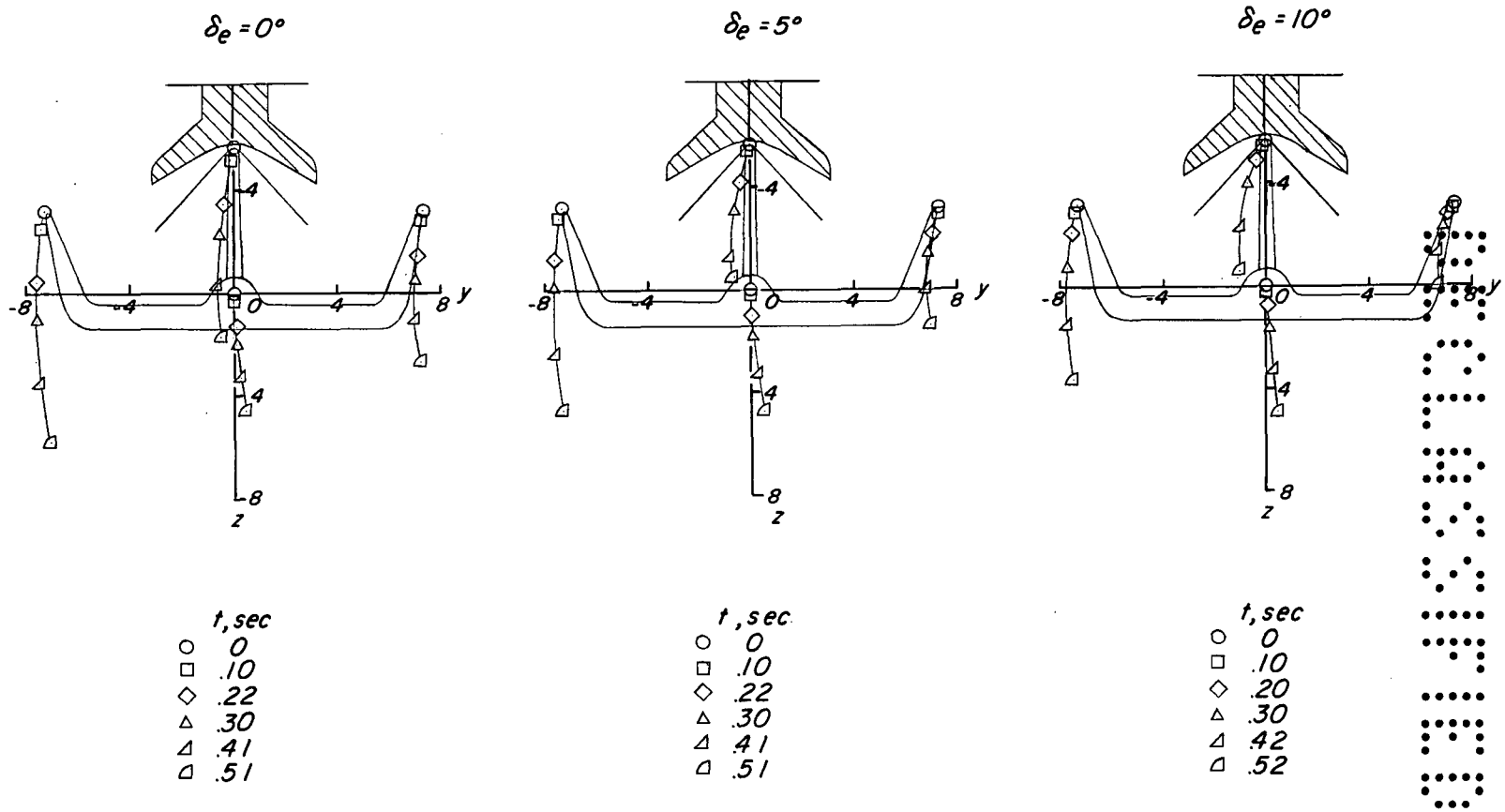


(a) Fin-tip and center-of-gravity paths. (Values along the coordinate scales are given in feet; 1 foot = 0.3048 meter.)

Figure 19.- Effect of pitch control setting $\delta_e$ on motions of HL-10 transonic configuration after launch. $M = 0.60$; $\alpha_{B-52} = 2^0$; $\Delta\alpha = 5^0$; dampers off; $W_{B-52} = 250\,000$ pounds (1 112 050 newtons).

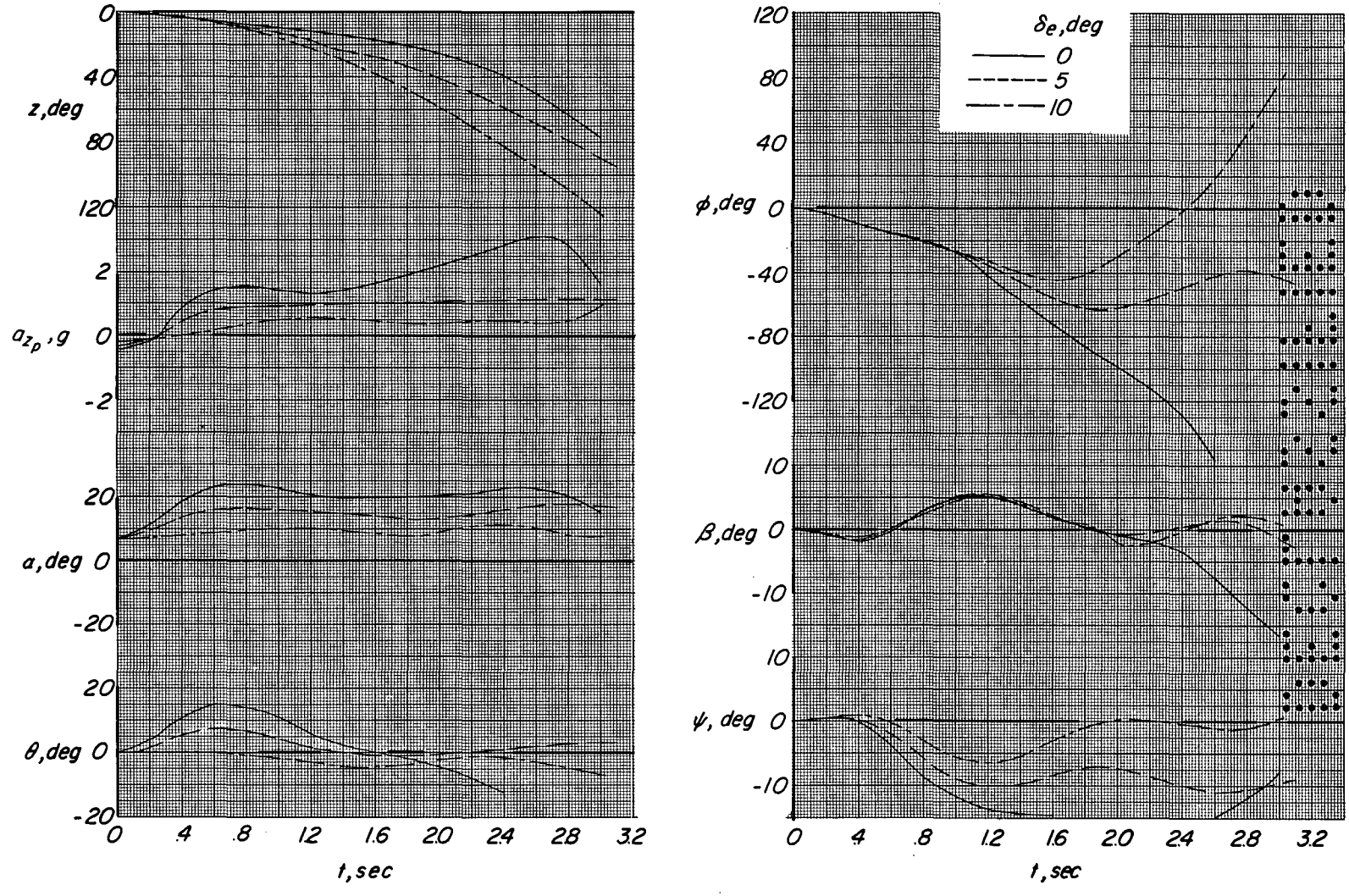


(b) Motion variables plotted against time after launch.

Figure 19.- Concluded.

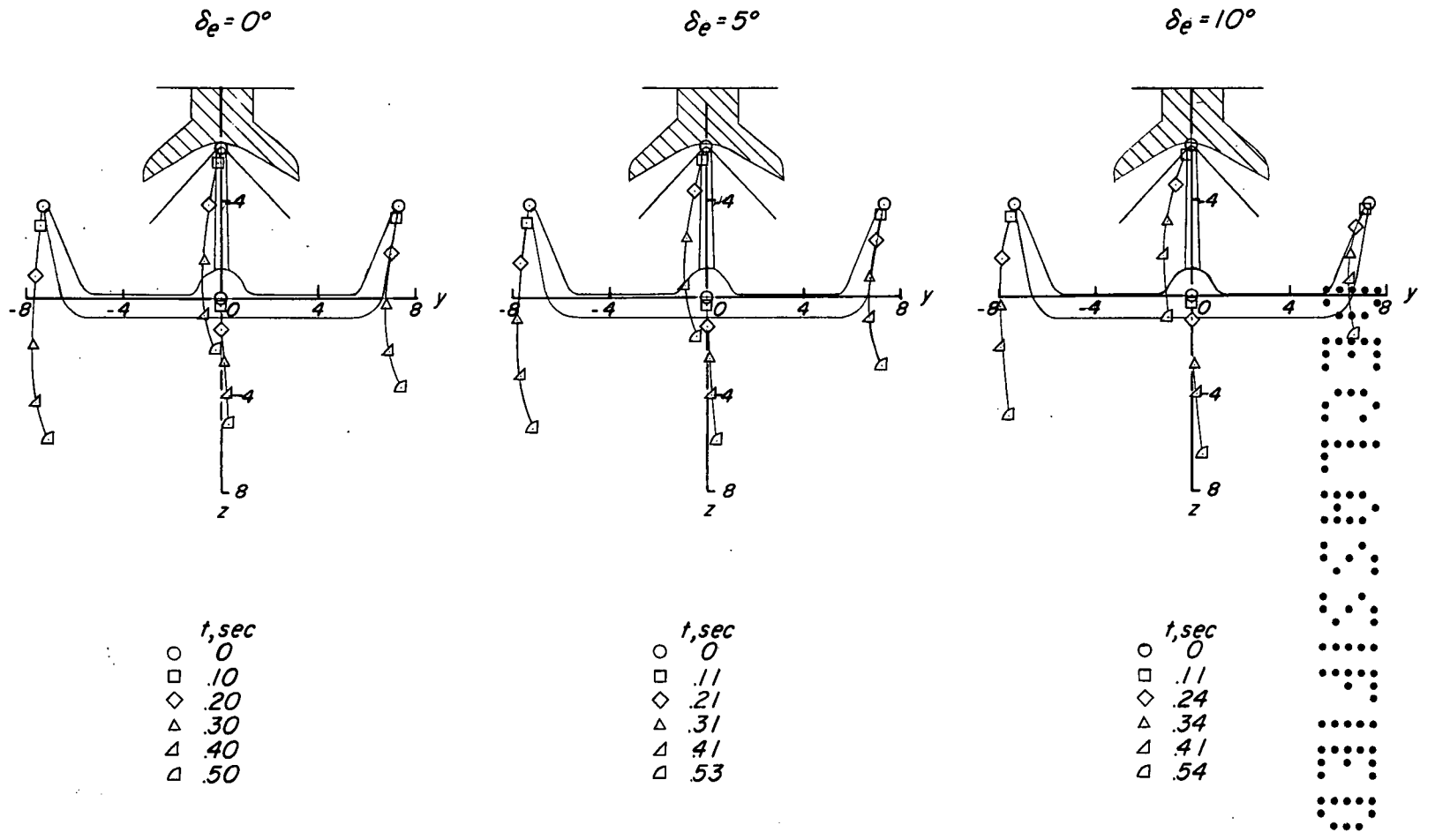


(a) Fin-tip and center-of-gravity paths. (Values along the coordinate scales are given in feet; 1 foot = 0.3048 meter.)

Figure 20.- Effect of pitch control setting $\delta_e$ on motions of HL-10 transonic configuration after launch. $M = 0.60$; $\alpha_{B-52} = -1^0$; $\Delta\alpha = 5^0$; dampers off; $W_{B-52} = 250\,000$ pounds (1 112 050 newtons).

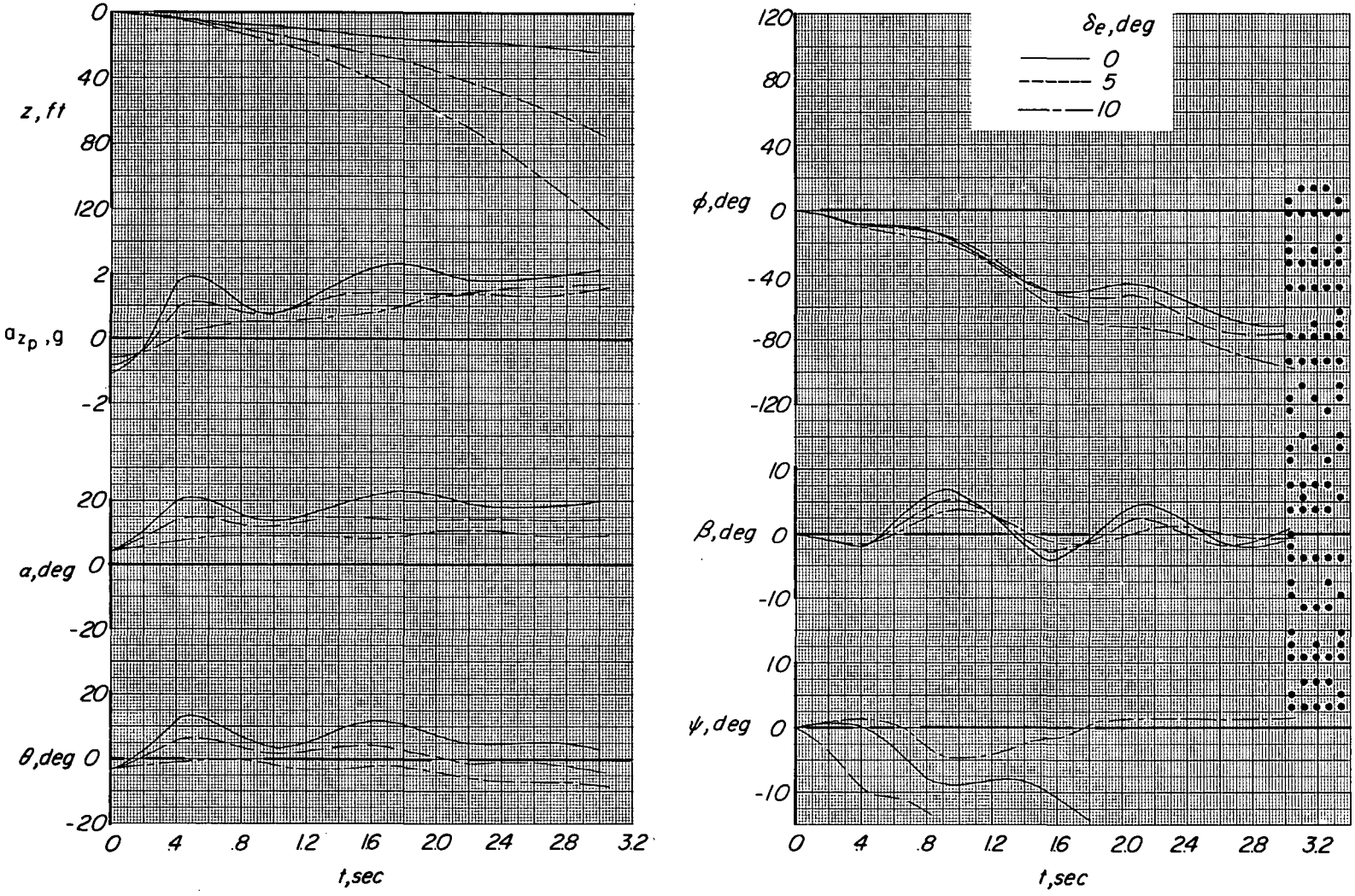


(b) Motion variables plotted against time after launch.

Figure 20.- Concluded.

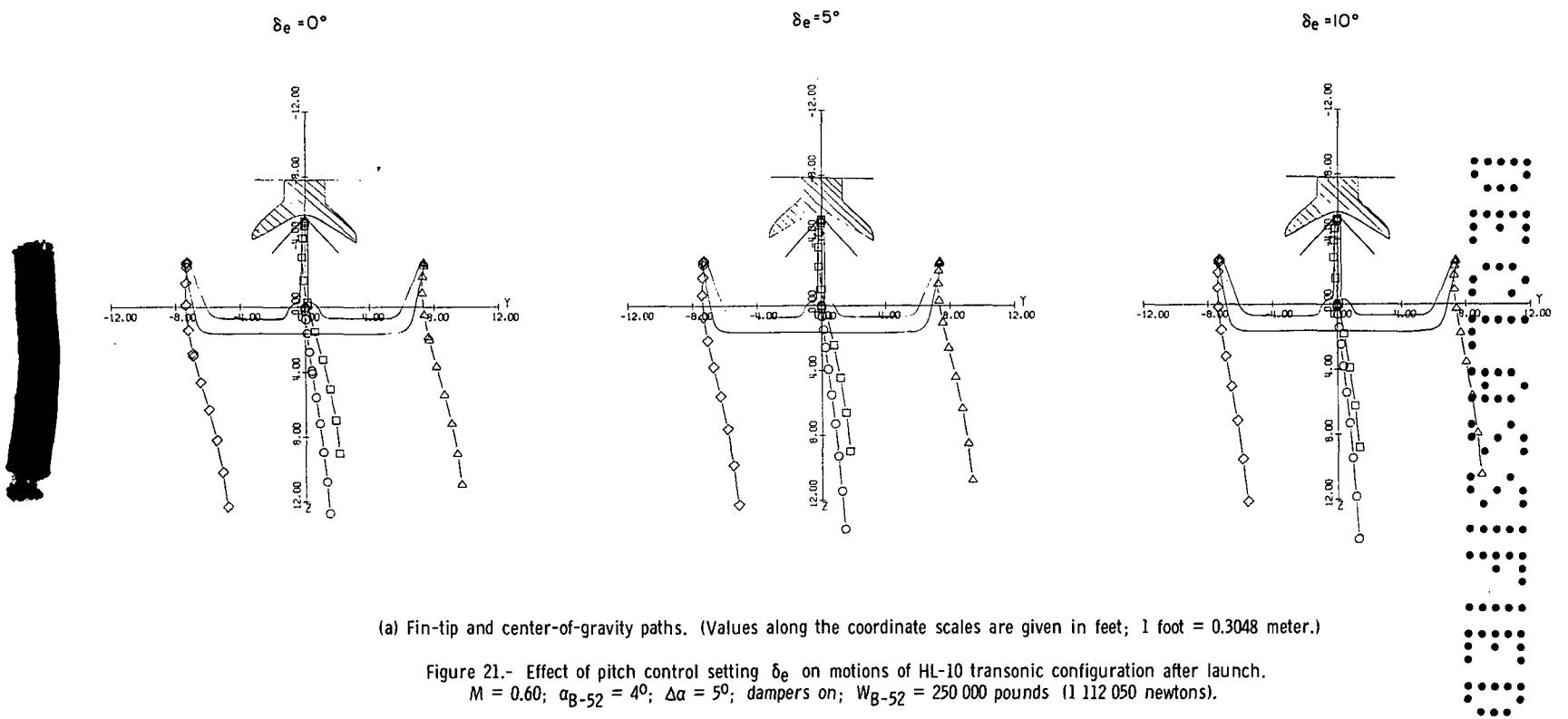


(a) Fin-tip and center-of-gravity paths. (Values along the coordinate scales are given in feet; 1 foot = 0.3048 meter.)

Figure 21.- Effect of pitch control setting $\delta_e$ on motions of HL-10 transonic configuration after launch. $M = 0.60$; $\alpha_{B-52} = 4^0$; $\Delta\alpha = 5^0$; *dampers on*; $W_{B-52}$ = 250 000 pounds (1 112 050 newtons).

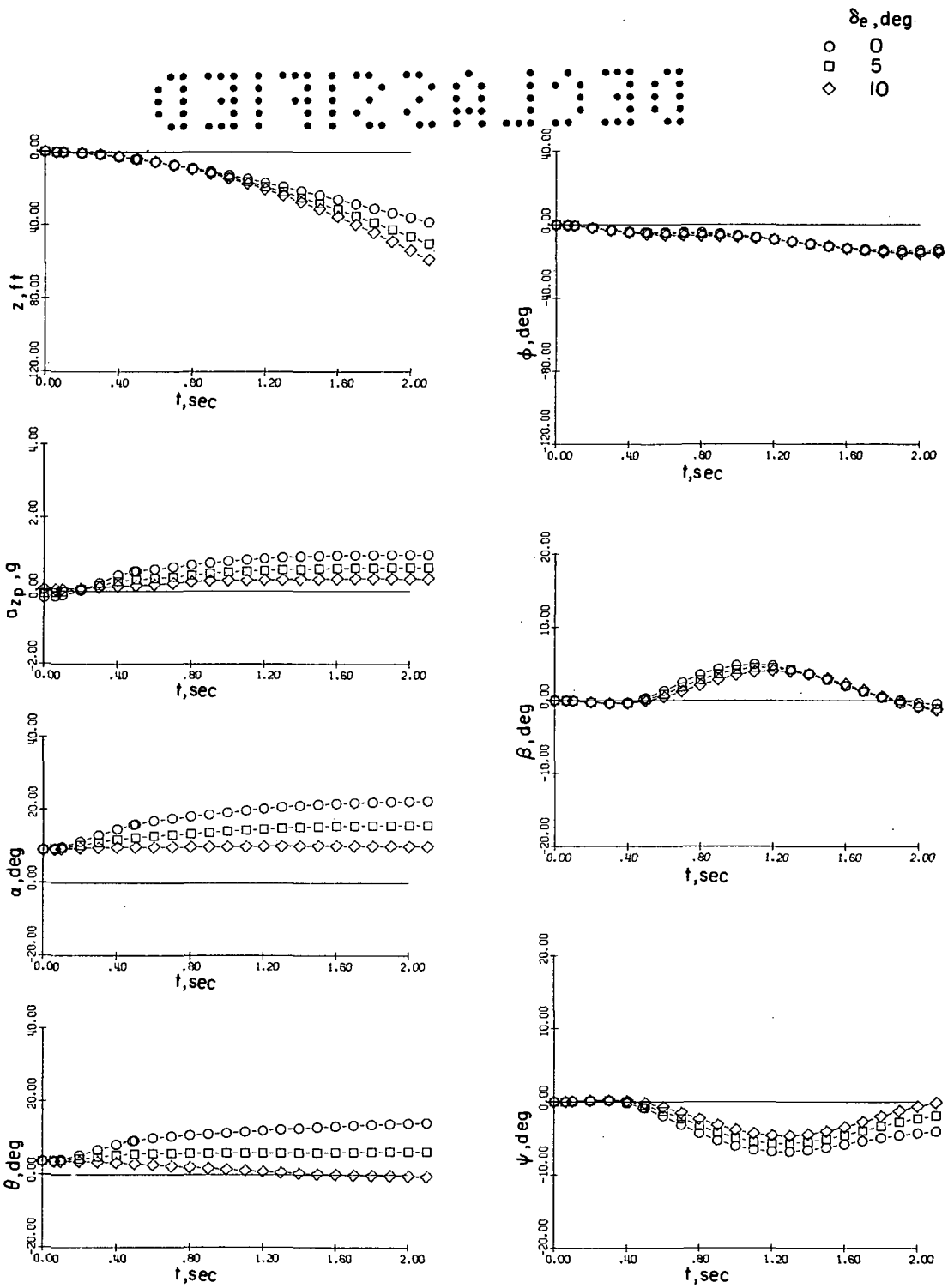


(b) Motion variables plotted against time after launch.

Figure 21.- Concluded.

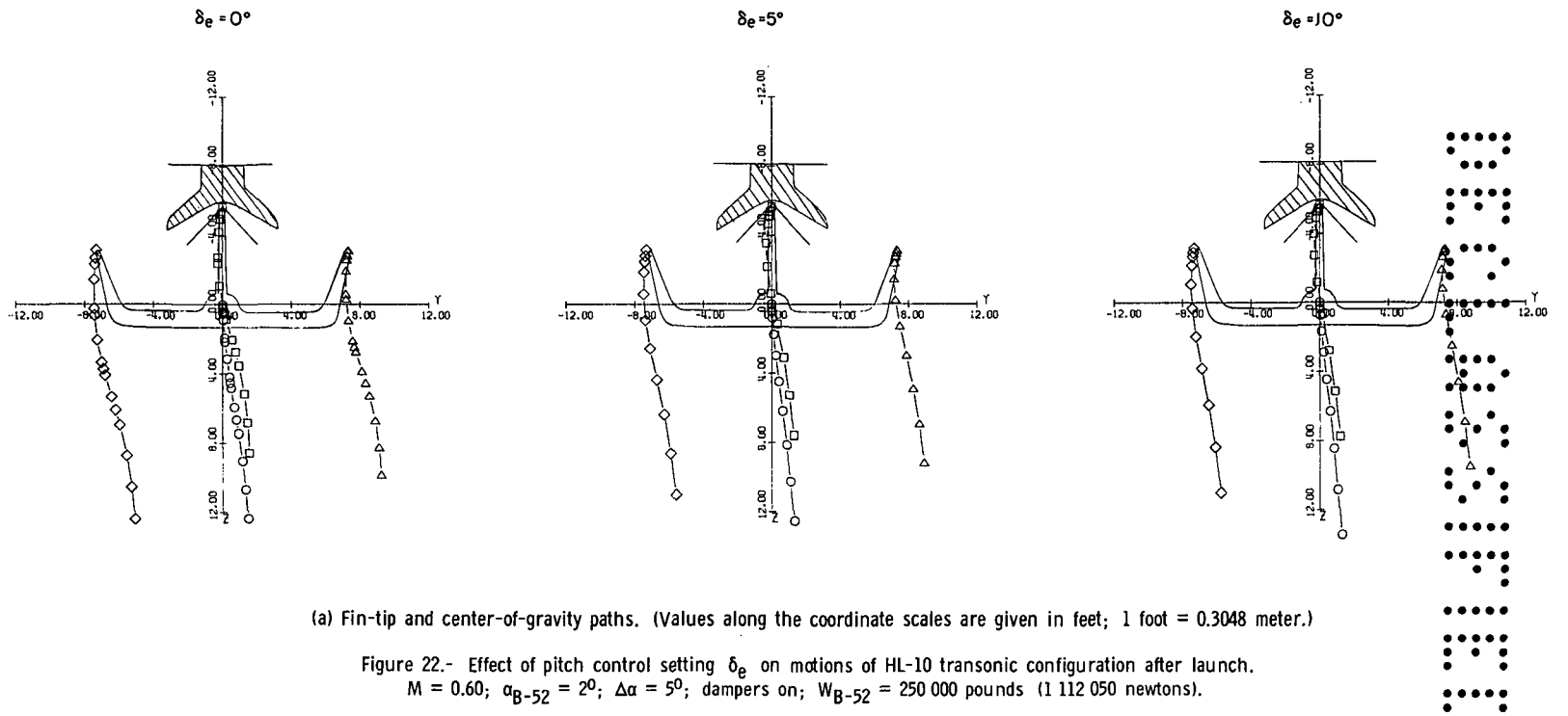


(a) Fin-tip and center-of-gravity paths. (Values along the coordinate scales are given in feet; 1 foot = 0.3048 meter.)

Figure 22.- Effect of pitch control setting $\delta_e$ on motions of HL-10 transonic configuration after launch. M = 0.60; $\alpha_{B-52} = 2^0$; $\Delta\alpha = 5^0$; dampers on; $W_{B-52}$ = 250 000 pounds (1 112 050 newtons).

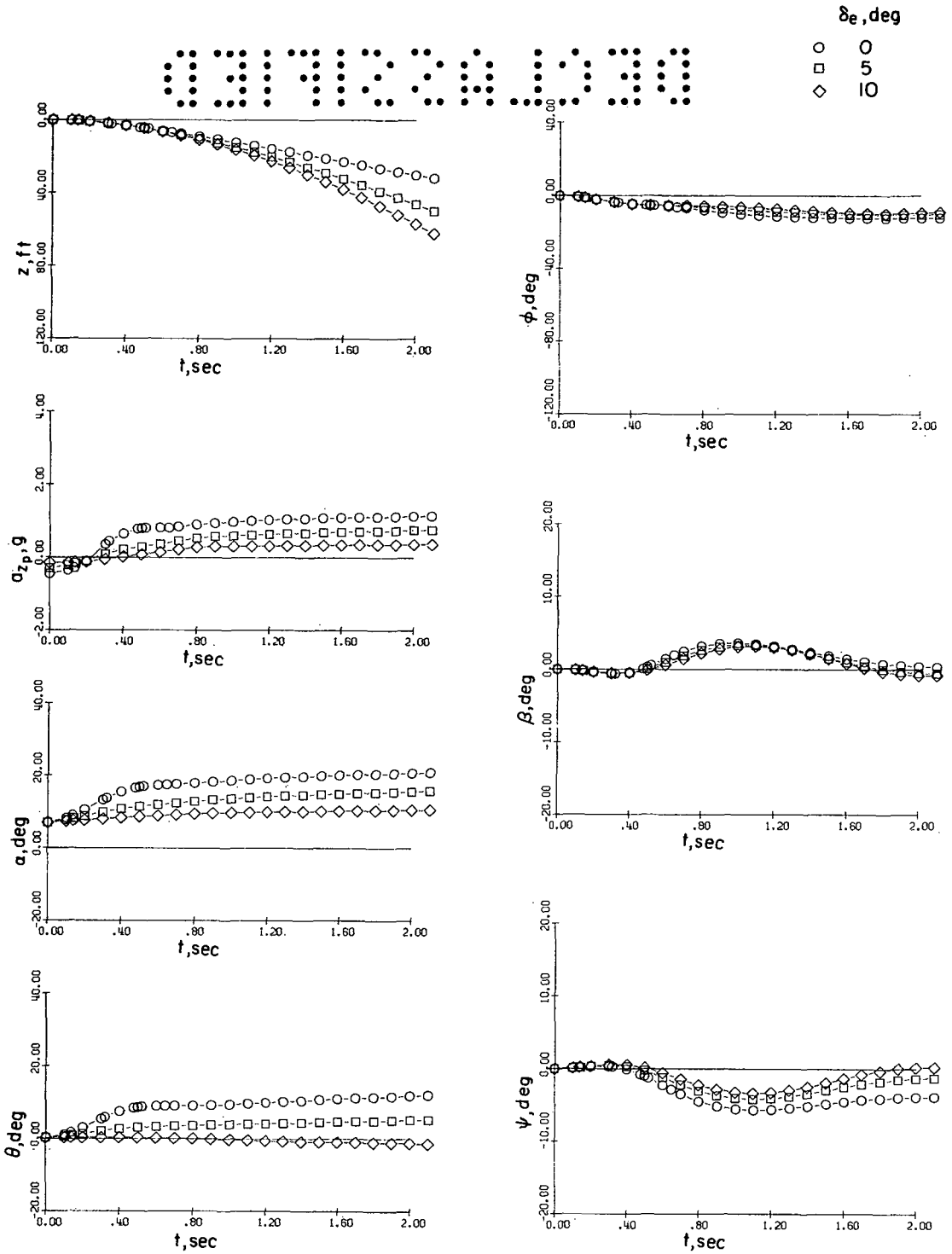


(b) Motion variables plotted against time after launch.

Figure 22.- Concluded.

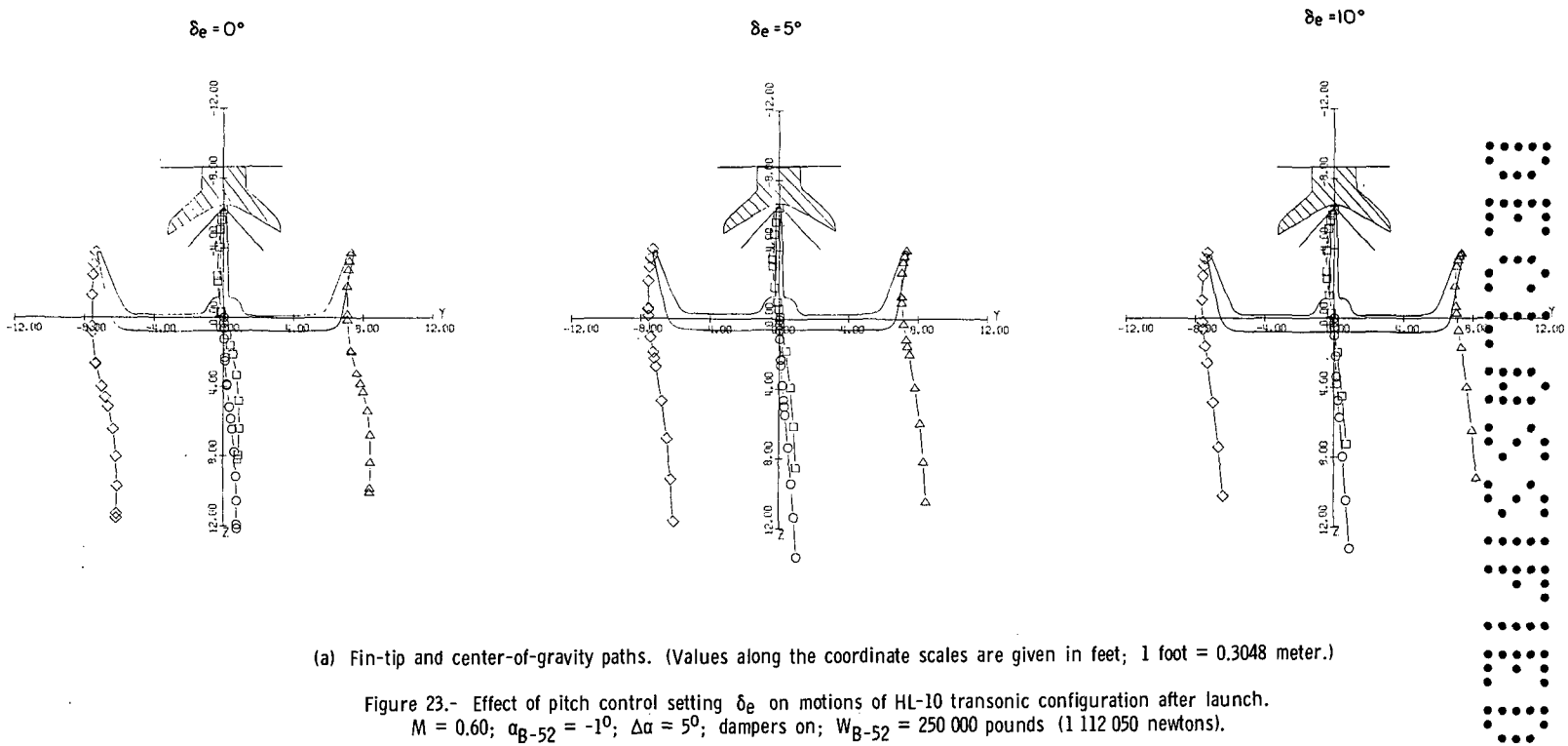


(a) Fin-tip and center-of-gravity paths. (Values along the coordinate scales are given in feet; 1 foot = 0.3048 meter.)

Figure 23.- Effect of pitch control setting $\delta_e$ on motions of HL-10 transonic configuration after launch. $M = 0.60$; $\alpha_{B-52} = -1^0$; $\Delta\alpha = 5^0$; dampers on; $W_{B-52} = 250\,000$ pounds (1 112 050 newtons).

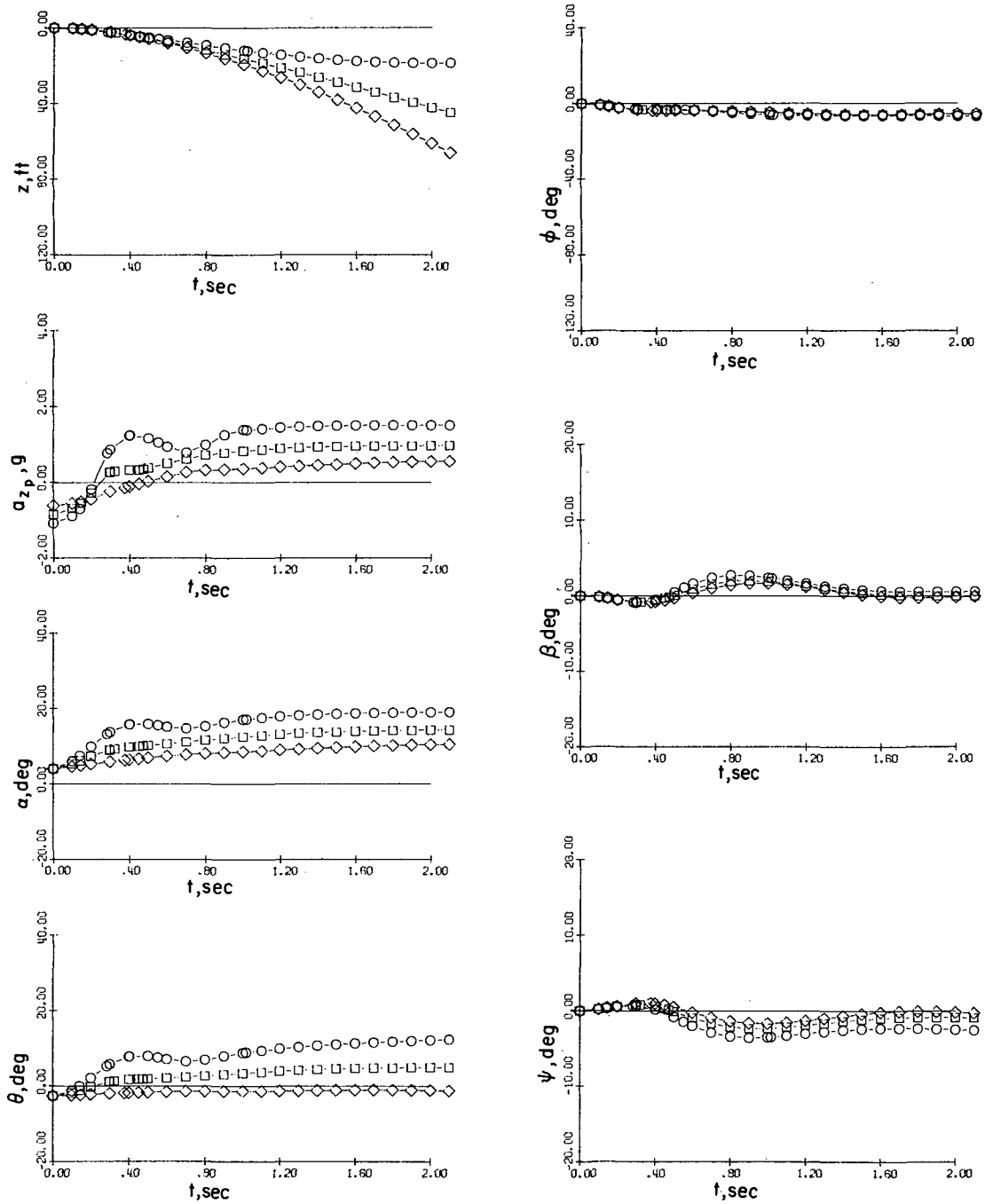


(b) Motion variables plotted against time after launch.

Figure 23.- Concluded.

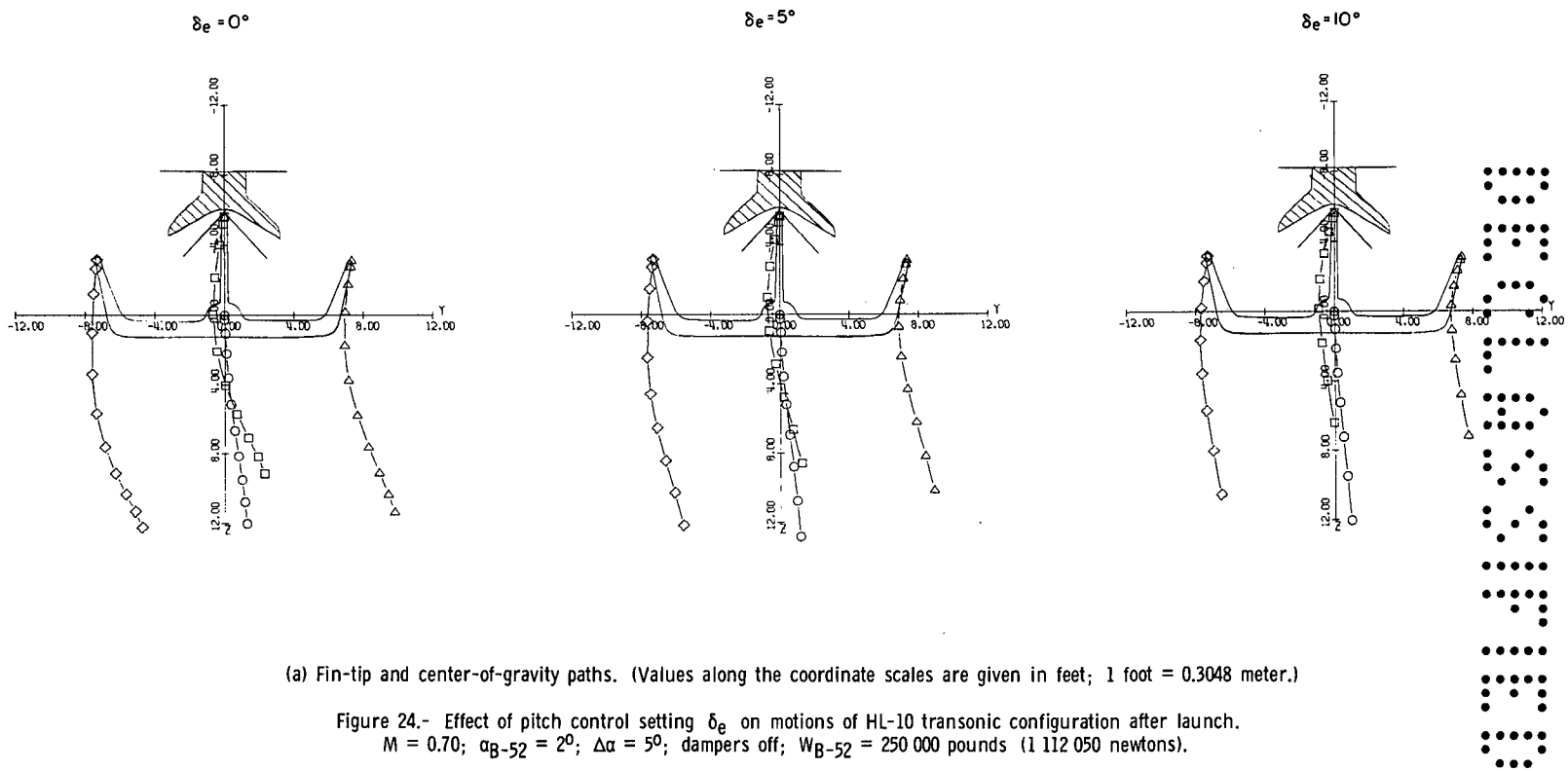


(a) Fin-tip and center-of-gravity paths. (Values along the coordinate scales are given in feet; 1 foot = 0.3048 meter.)

Figure 24.- Effect of pitch control setting $\delta_e$ on motions of HL-10 transonic configuration after launch. $M = 0.70$; $\alpha_{B-52} = 2^0$; $\Delta\alpha = 5^0$; dampers off; $W_{B-52} = 250\,000$ pounds (1 112 050 newtons).

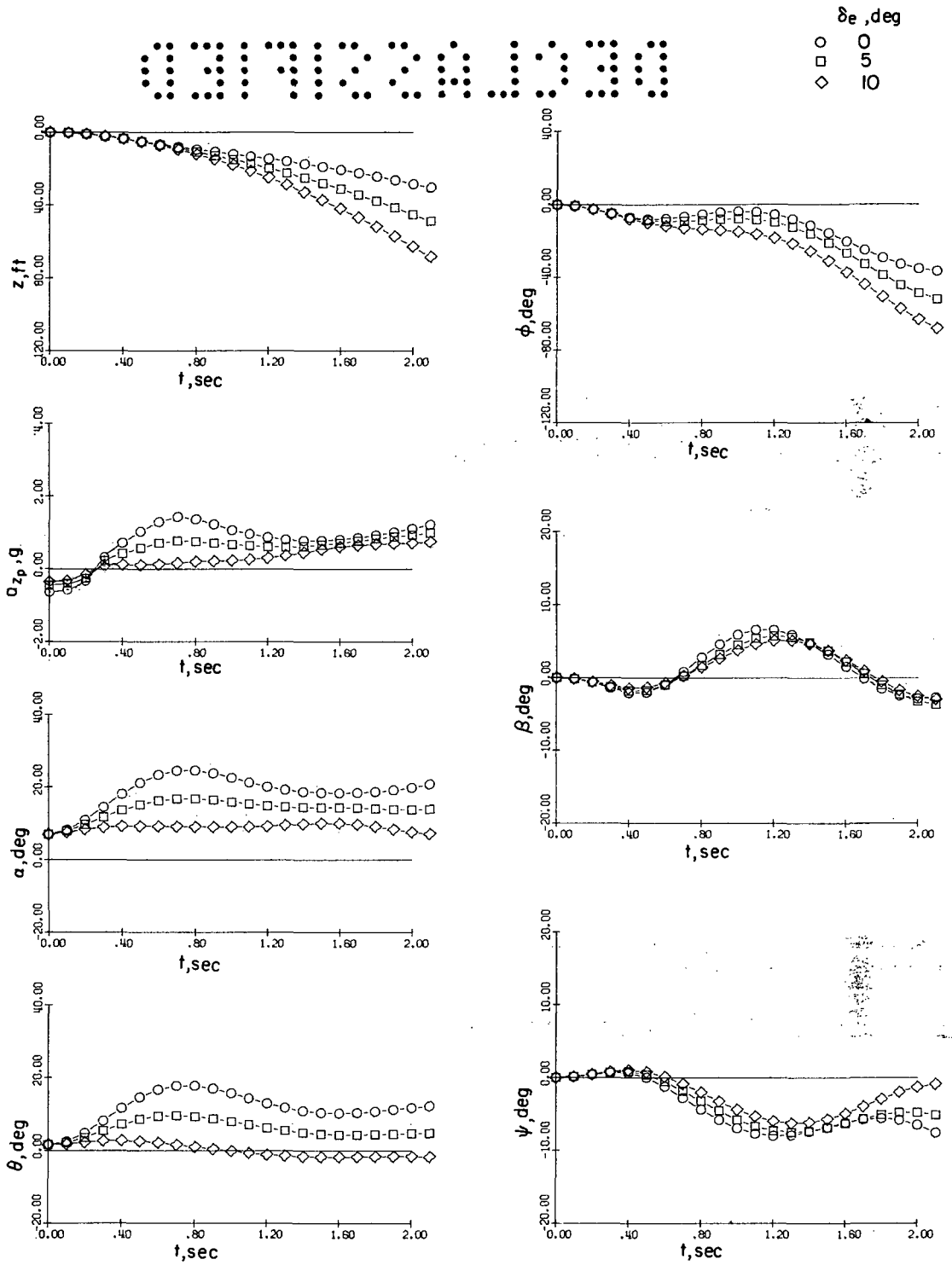


(b) Motion variables plotted against time after launch.

Figure 24.- Concluded.

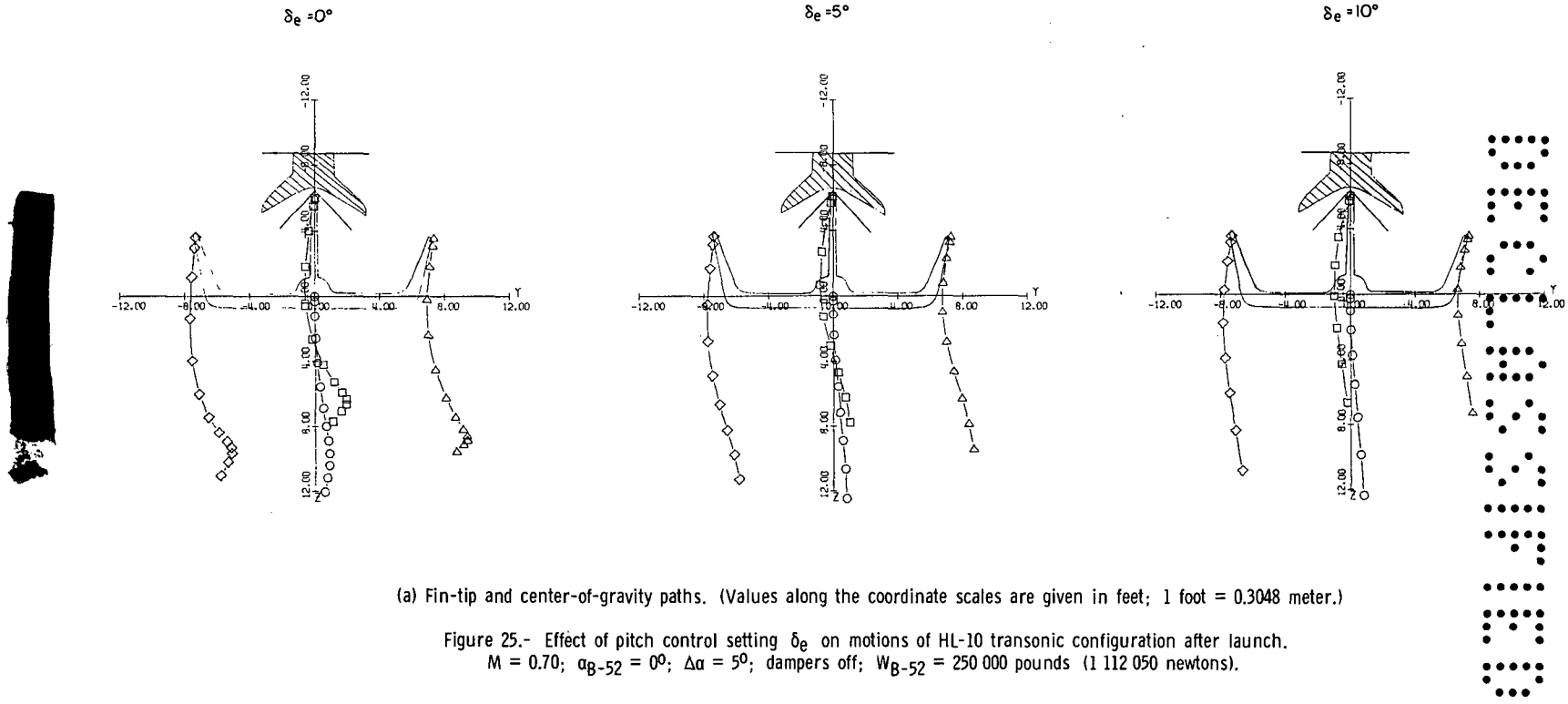


(a) Fin-tip and center-of-gravity paths. (Values along the coordinate scales are given in feet; 1 foot = 0.3048 meter.)

Figure 25.- Effect of pitch control setting $\delta_e$ on motions of HL-10 transonic configuration after launch. M = 0.70; $\alpha_{B-52} = 0^0$; $\Delta\alpha = 5^0$; dampers off; $W_{B-52}$ = 250 000 pounds (1 112 050 newtons).

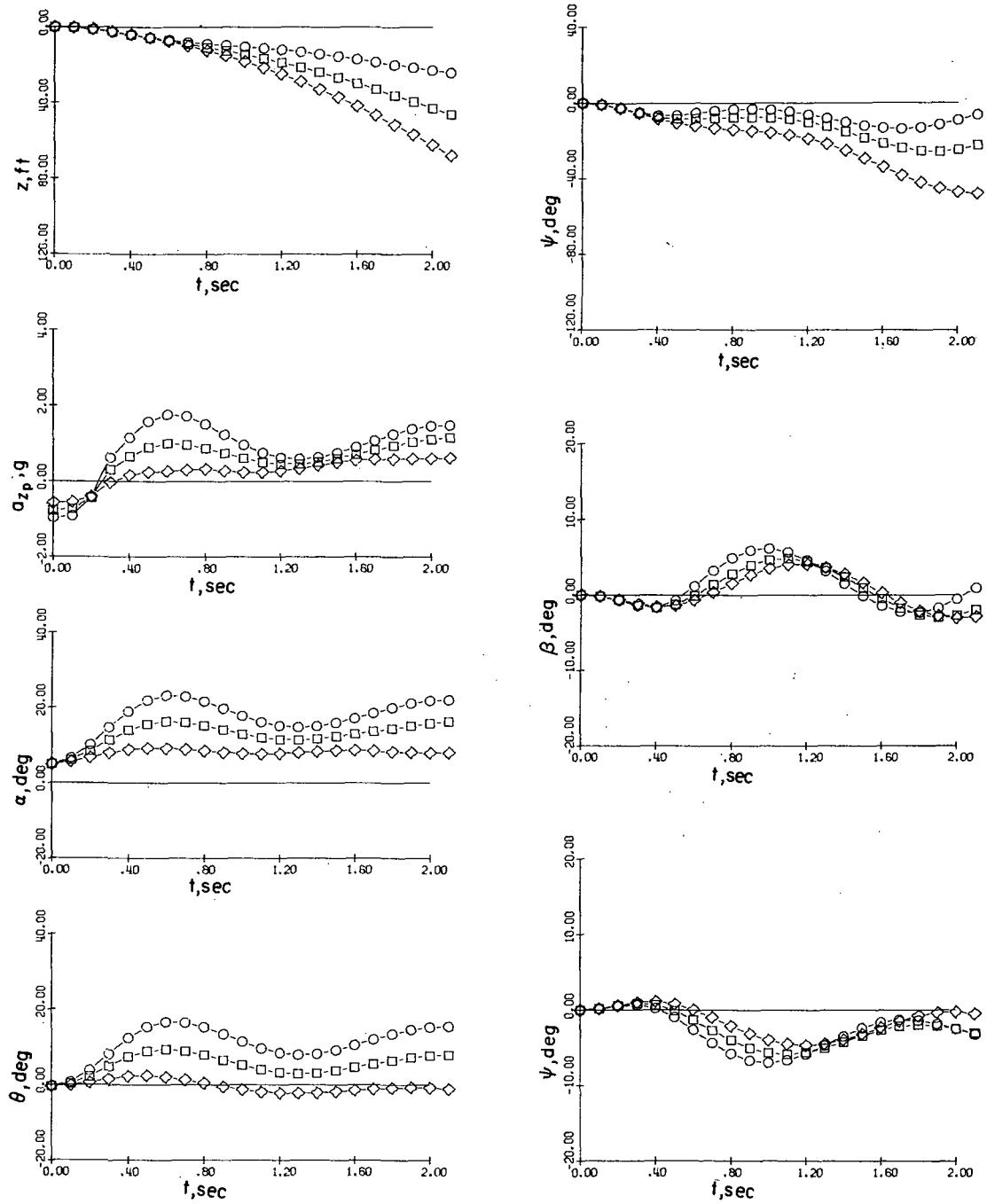


(b) Motion variables plotted against time after launch.

Figure 25.- Concluded.

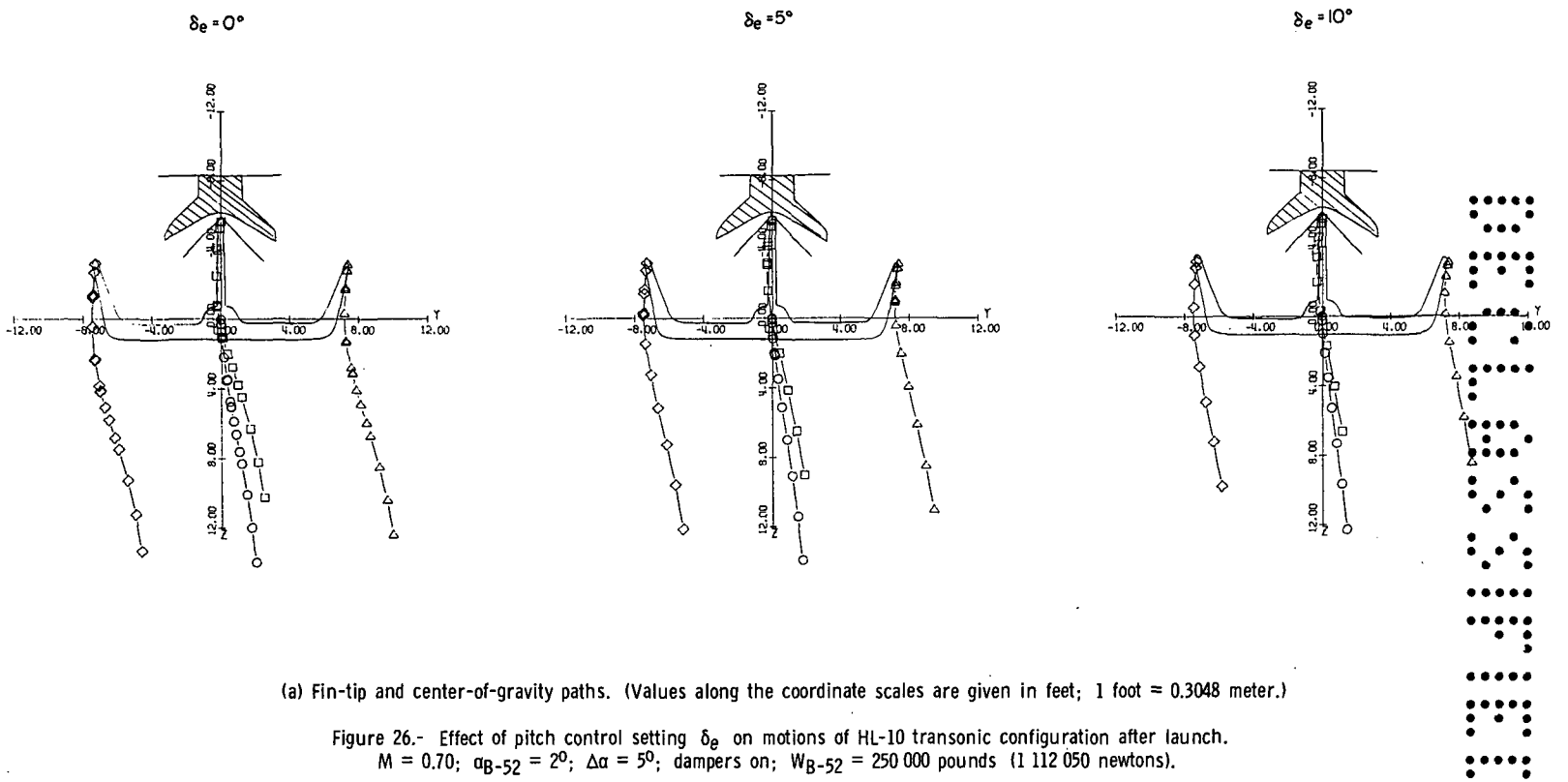


(a) Fin-tip and center-of-gravity paths. (Values along the coordinate scales are given in feet; 1 foot = 0.3048 meter.)

Figure 26.- Effect of pitch control setting $\delta_e$ on motions of HL-10 transonic configuration after launch. $M = 0.70$; $\alpha_{B-52} = 2^0$; $\Delta\alpha = 5^0$; dampers on; $W_{B-52} = 250\,000$ pounds (1 112 050 newtons).

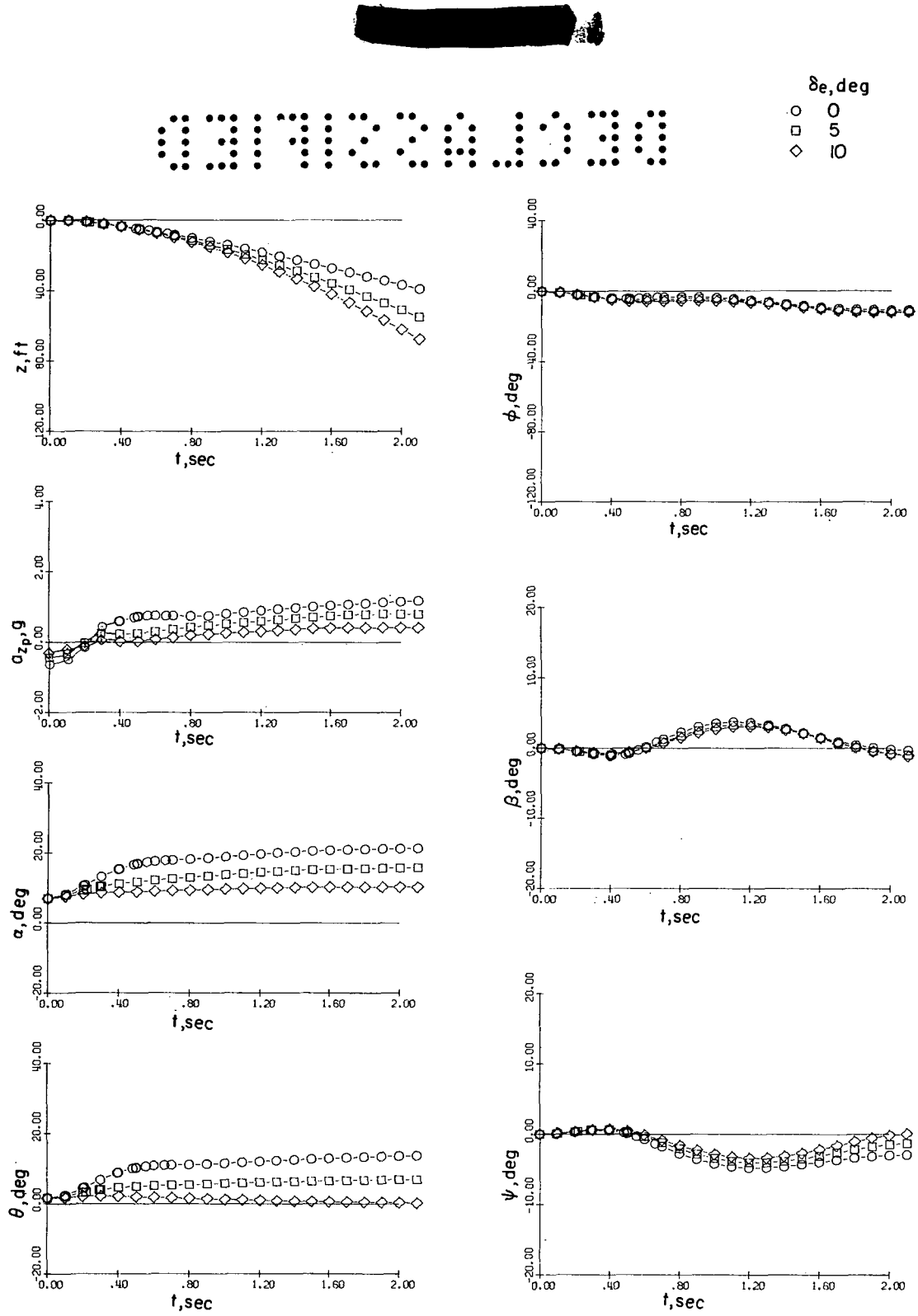


(b) Motion variables plotted against time after launch.

Figure 26.- Concluded.

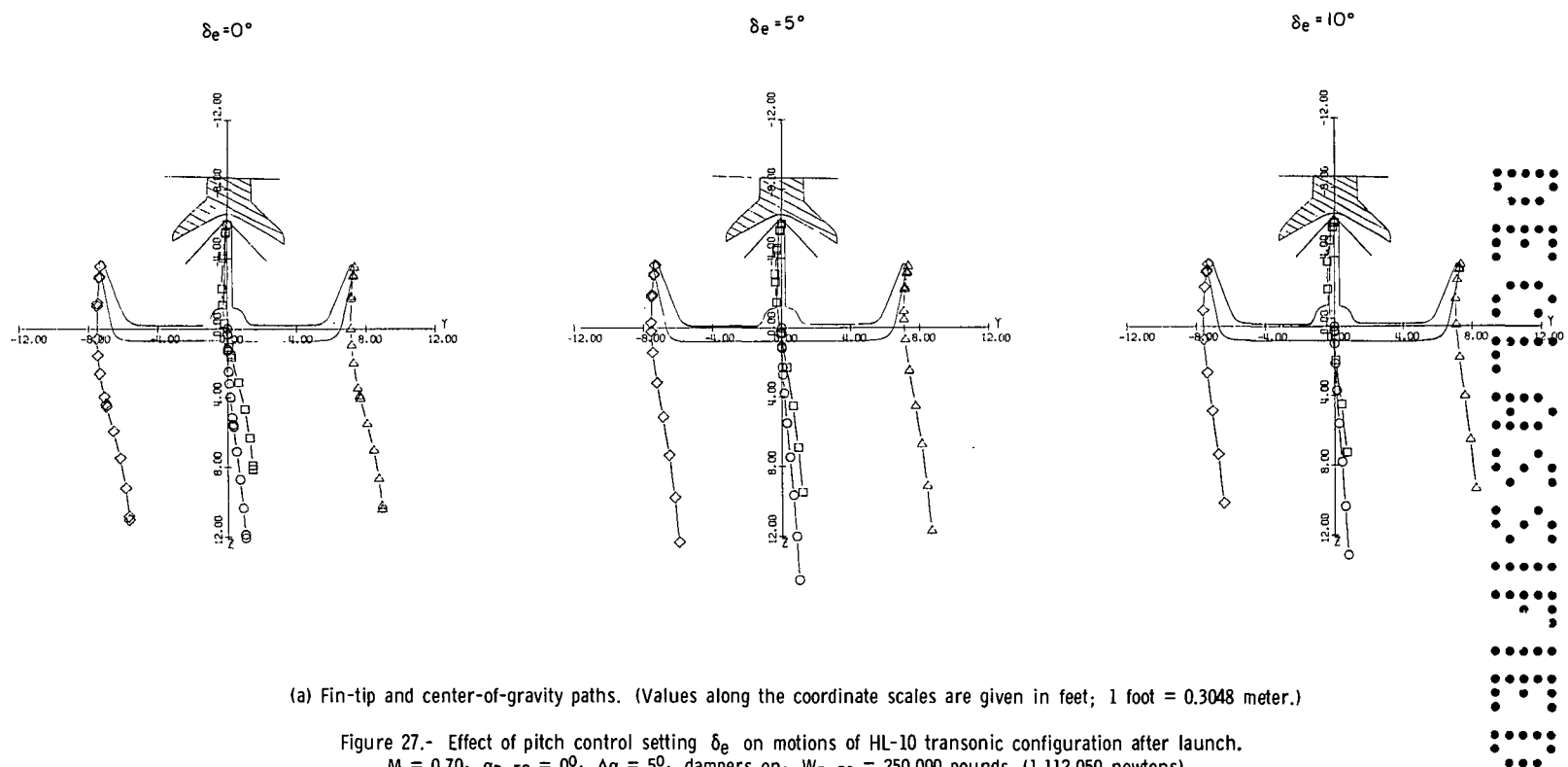


(a) Fin-tip and center-of-gravity paths. (Values along the coordinate scales are given in feet; 1 foot = 0.3048 meter.)

Figure 27.- Effect of pitch control setting $\delta_e$ on motions of HL-10 transonic configuration after launch. $M = 0.70$; $\alpha_{B-52} = 0^0$; $\Delta\alpha = 5^0$; dampers on; $W_{B-52} = 250\,000$ pounds (1 112 050 newtons).

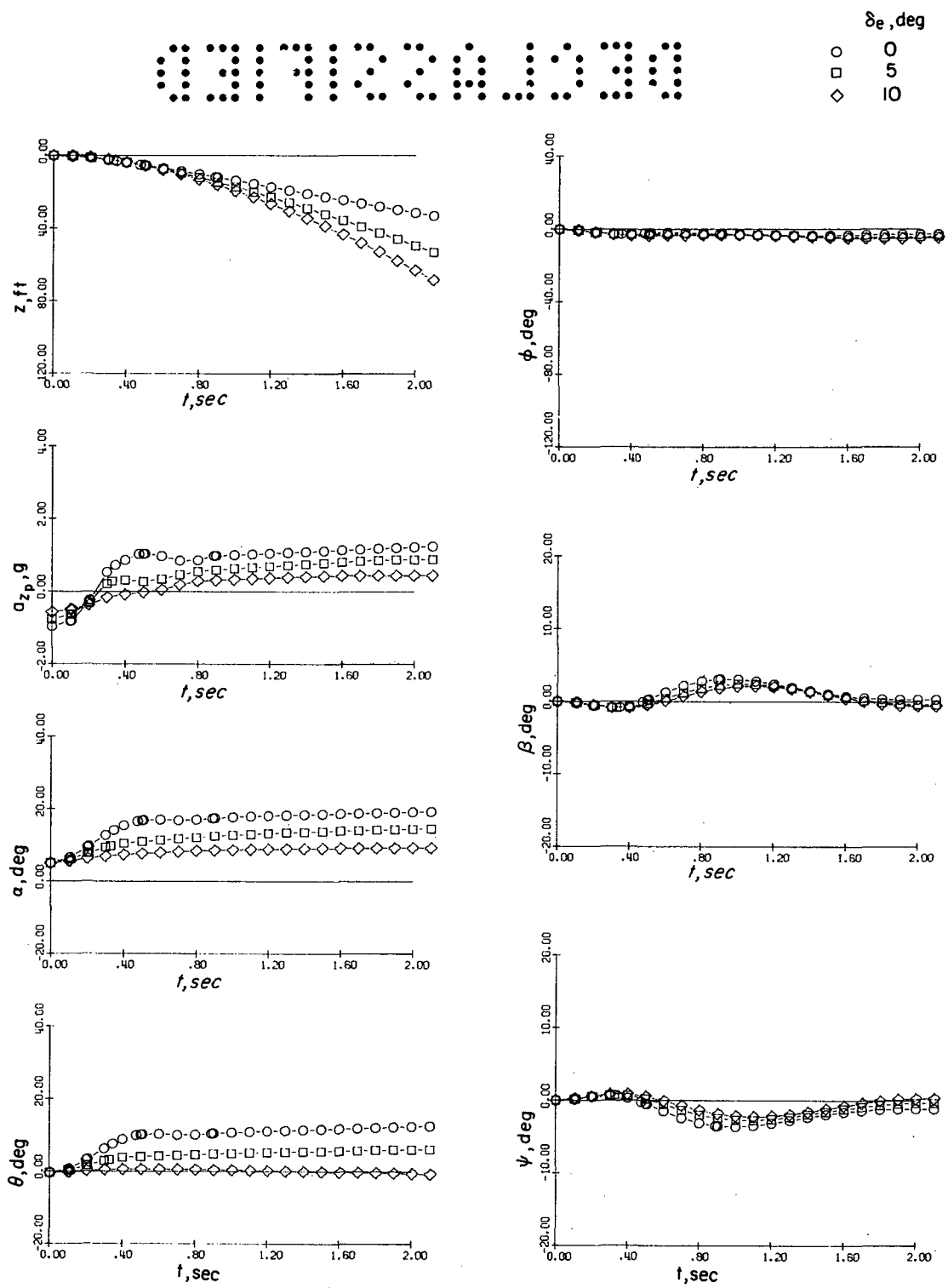


(b) Motion variables plotted against time after launch.

Figure 27.- Concluded.

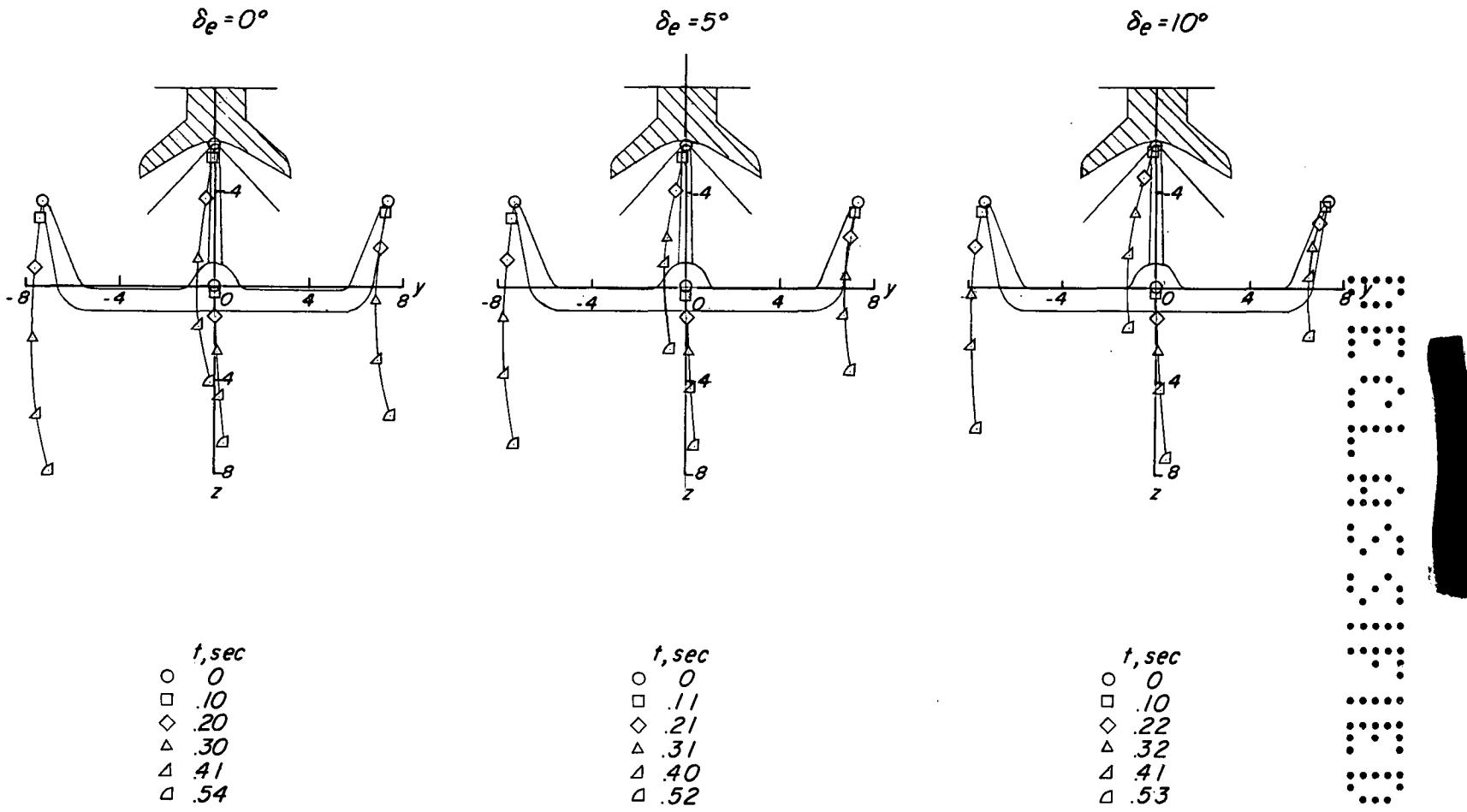


(a) Fin-tip and center-of-gravity paths. (Values along the coordinate scales are given in feet; 1 foot = 0.3048 meter.)

Figure 28.- Effect of pitch control setting $\delta_e$ on motions of HL-10 transonic configuration after launch. $M = 0.80$; $\alpha_{B-52} = 0^o$; $\Delta\alpha = 5^o$; dampers off; $W_{B-52} = 250\,000$ pounds (1 112 050 newtons).

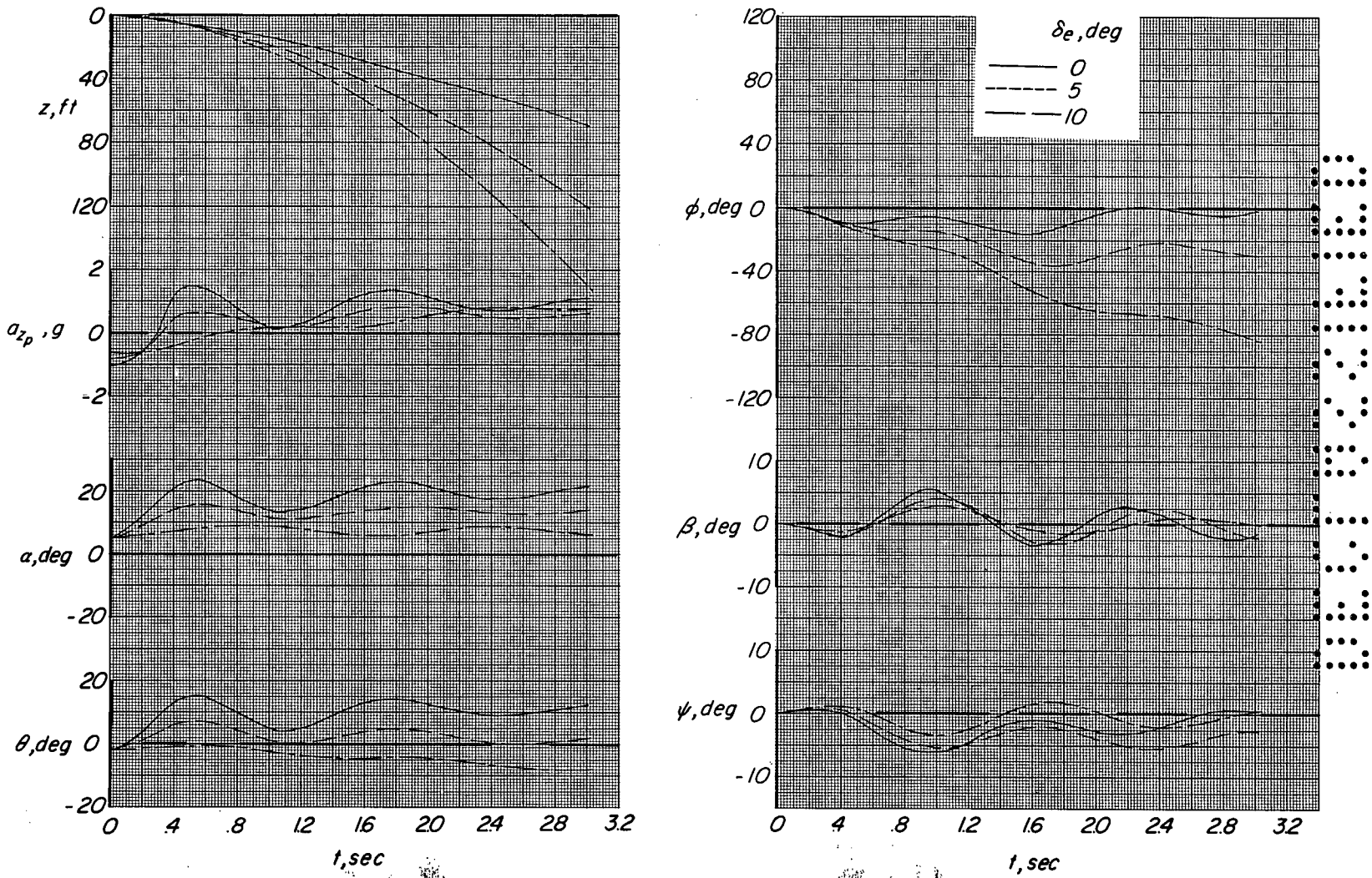


(b) Motion variables plotted against time after launch.

Figure 28.- Concluded.

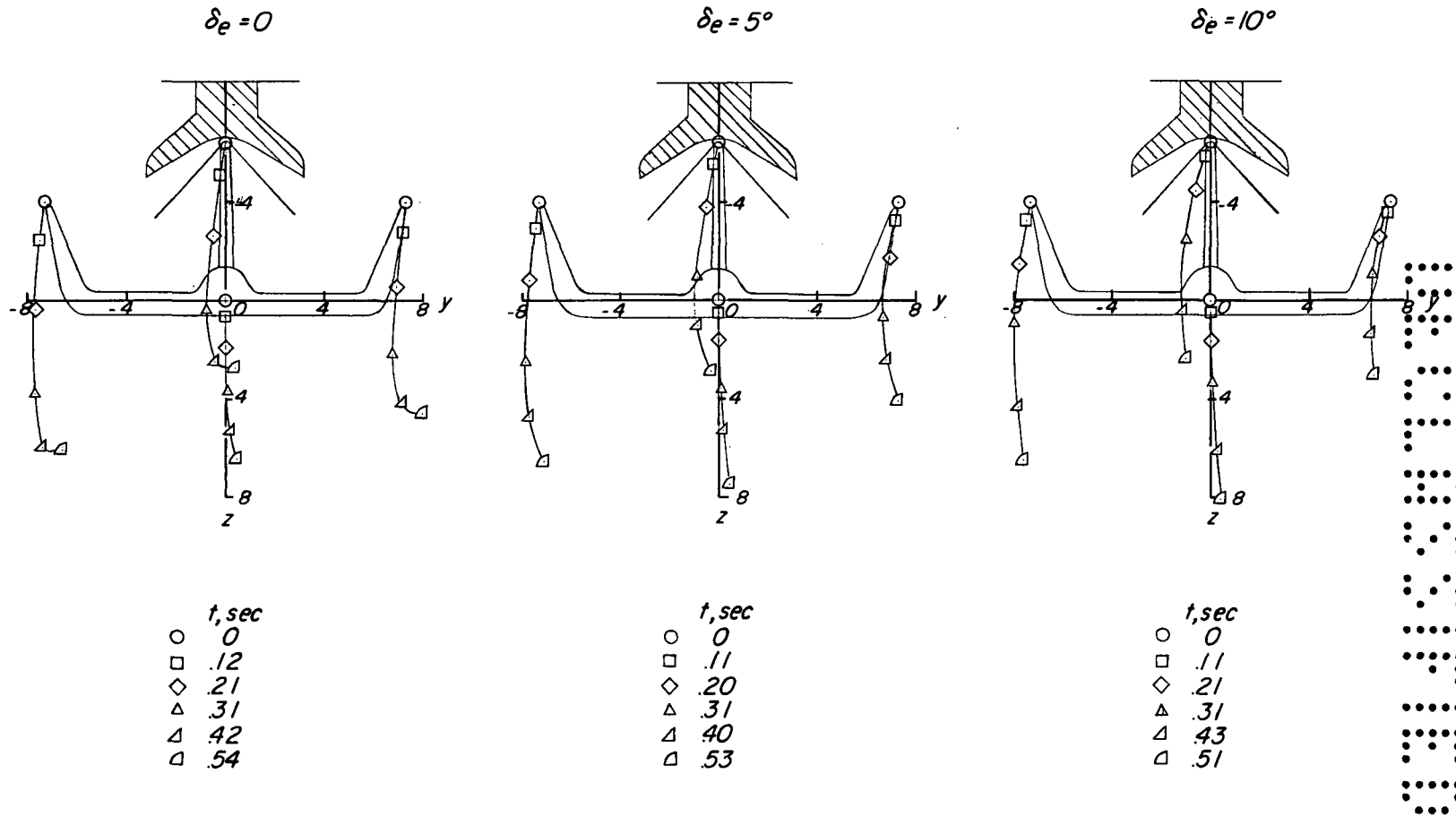


(a) Fin-tip and center-of-gravity paths. (Values along the coordinate scales are given in feet; 1 foot = 0.3048 meter.)

Figure 29.- Effect of pitch control setting $\delta_e$ on motions of HL-10 transonic configuration after launch. $M = 0.80$; $\alpha_{B-52} = -2^0$; $\Delta\alpha = 5^0$; dampers off; $W_{B-52} = 250\,000$ pounds (1 112 050 newtons).

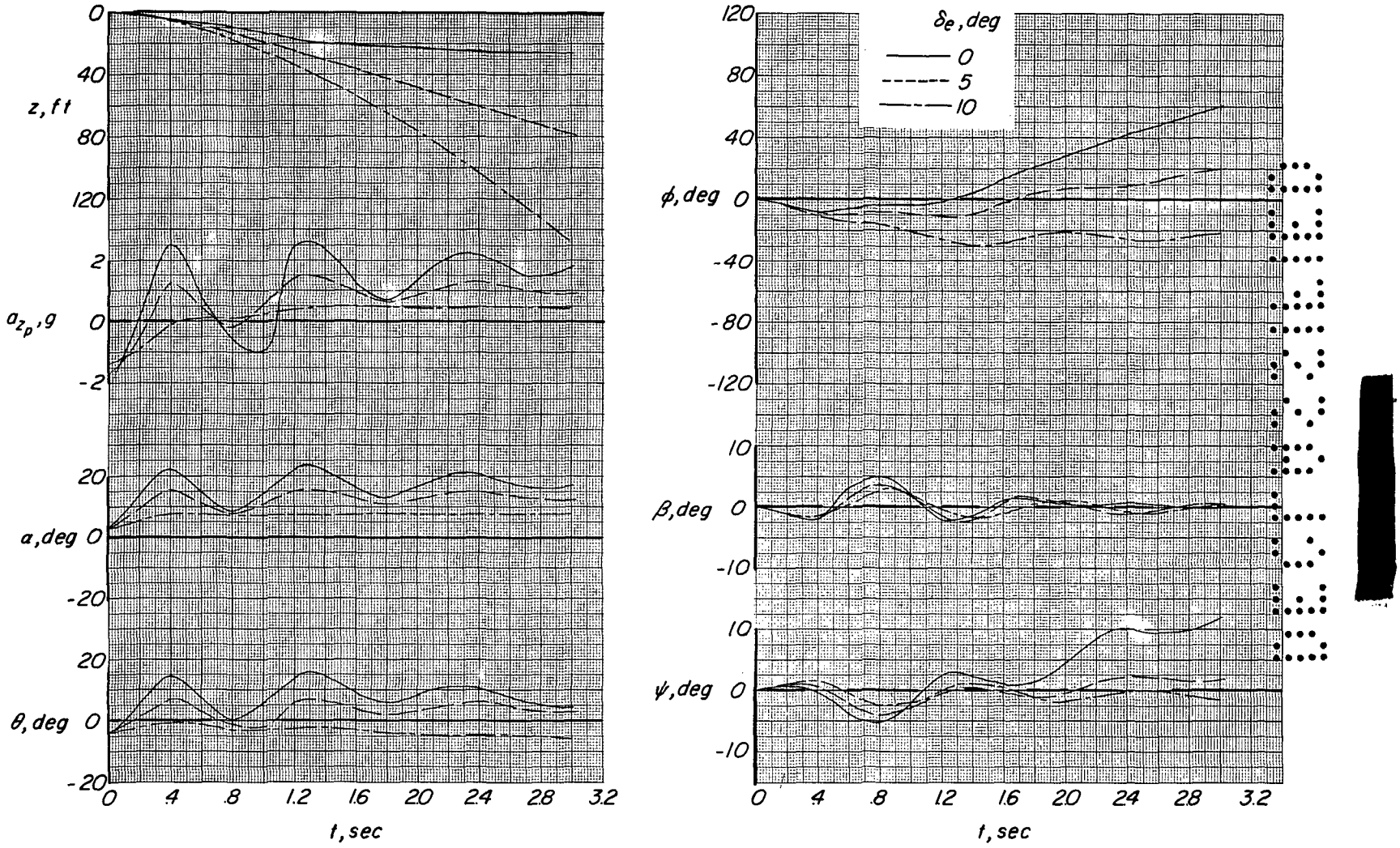


(b) Motion variables plotted against time after launch.

Figure 29.- Concluded.

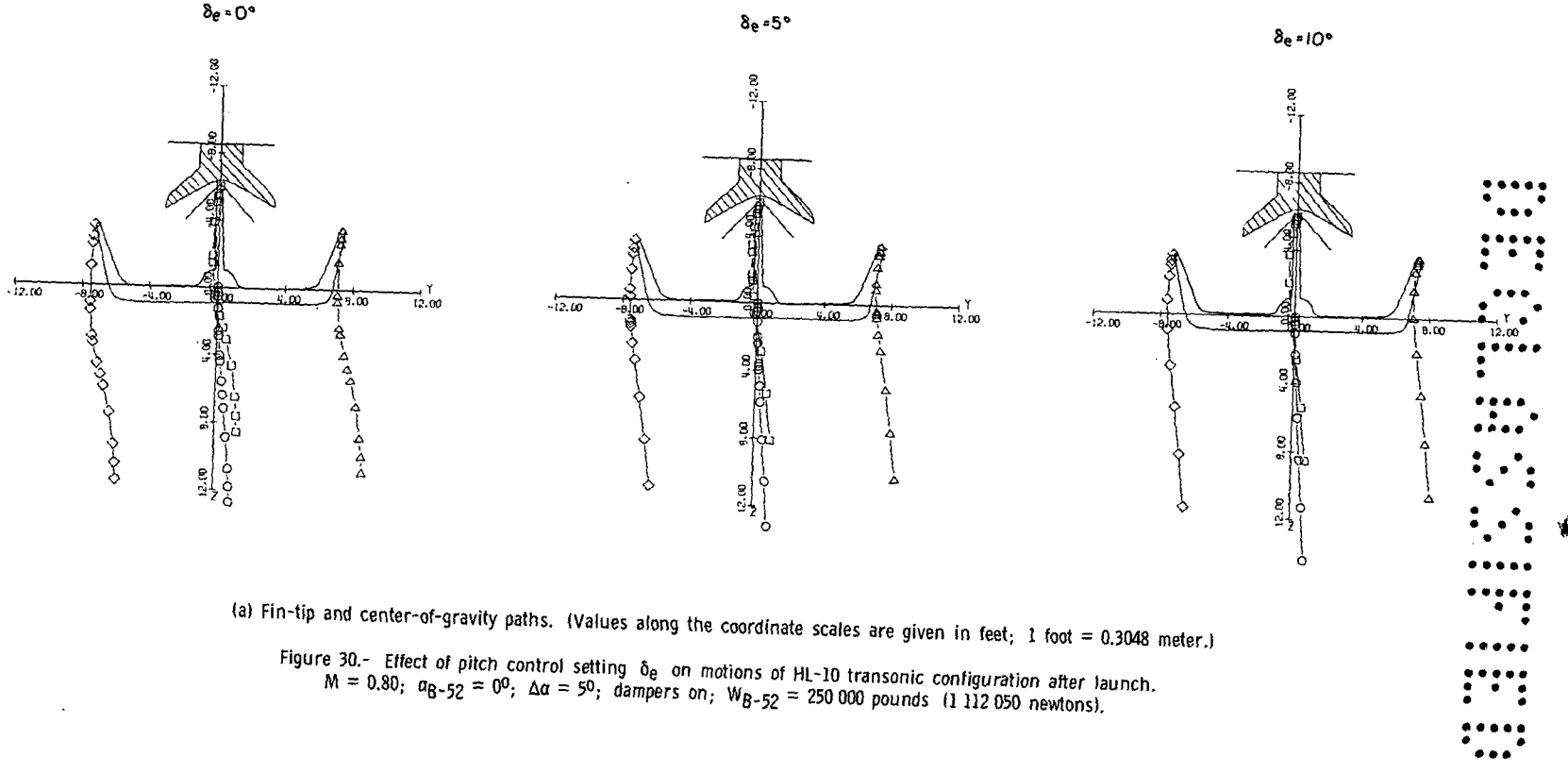


(a) Fin-tip and center-of-gravity paths. (Values along the coordinate scales are given in feet; 1 foot = 0.3048 meter.)

Figure 30.- Effect of pitch control setting $\delta_e$ on motions of HL-10 transonic configuration after launch. $M = 0.80$; $\alpha_{B-52} = 0^0$; $\Delta\alpha = 5^0$; dampers on; $W_{B-52} = 250\,000$ pounds (1 112 050 newtons).

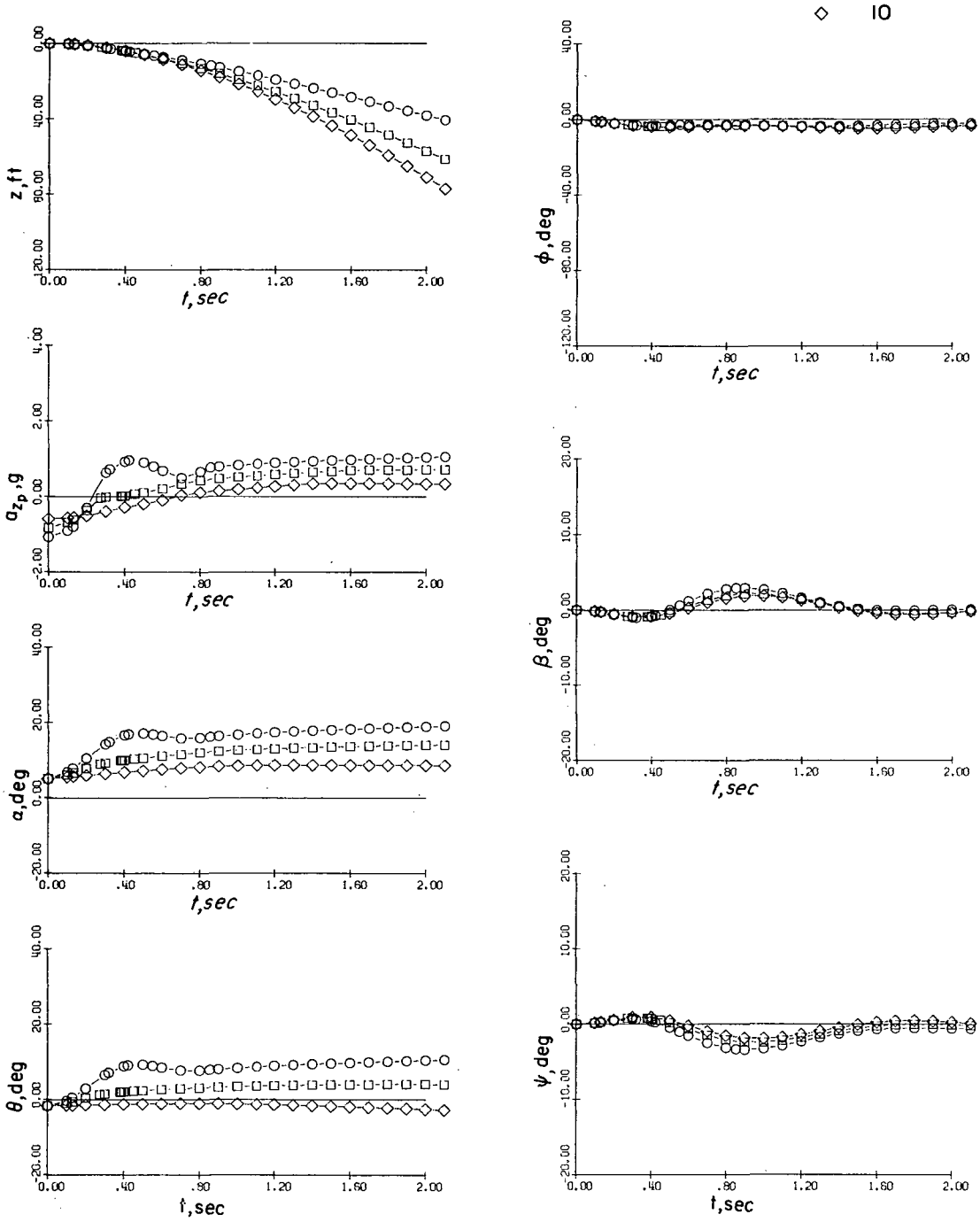


(b) Motion variables plotted against time after launch.

Figure 30.- Concluded.

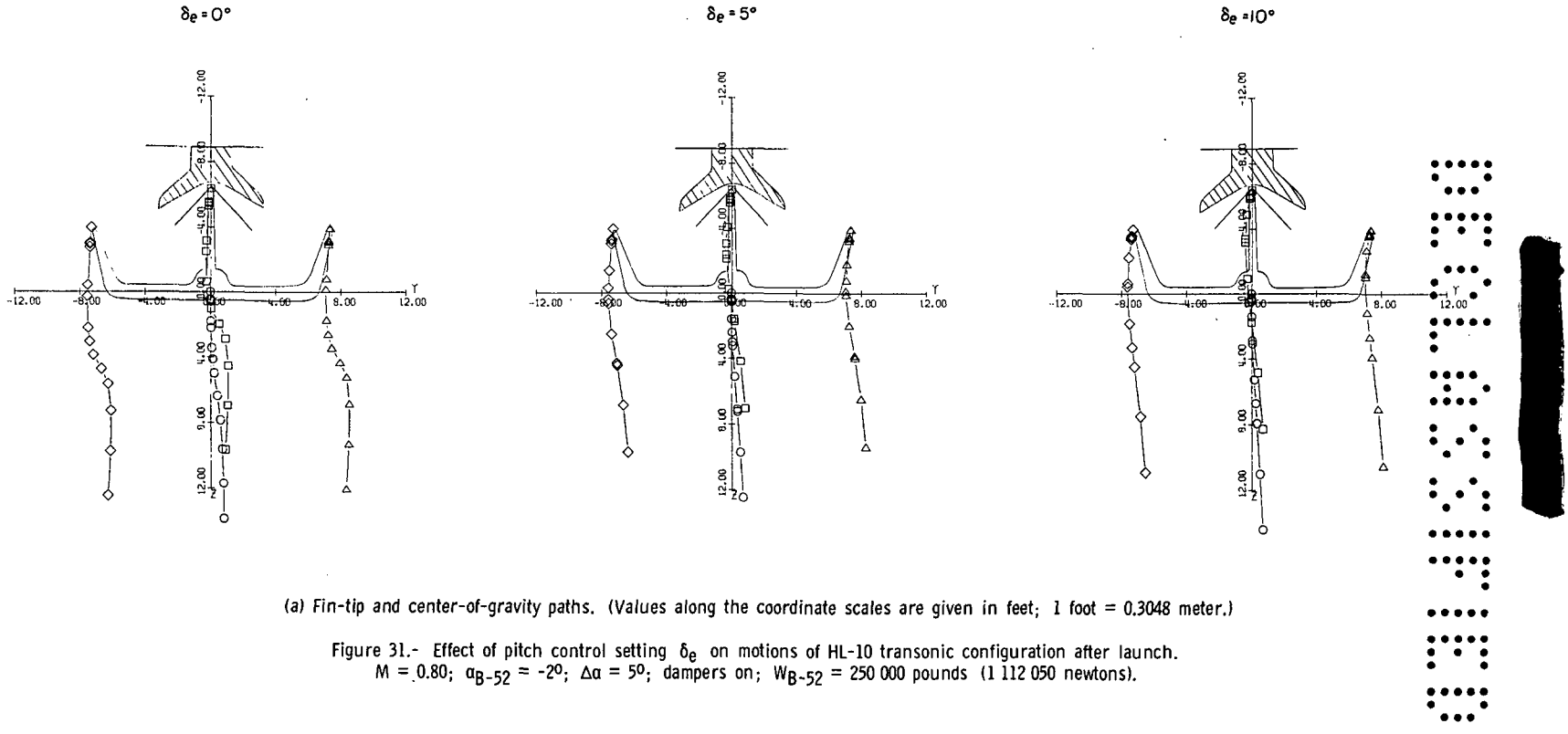


(a) Fin-tip and center-of-gravity paths. (Values along the coordinate scales are given in feet; 1 foot = 0.3048 meter.)

Figure 31.- Effect of pitch control setting $\delta_e$ on motions of HL-10 transonic configuration after launch. $M = 0.80$; $\alpha_{B-52} = -2°$; $\Delta\alpha = 5°$; dampers on; $W_{B-52} = 250\,000$ pounds (1 112 050 newtons).

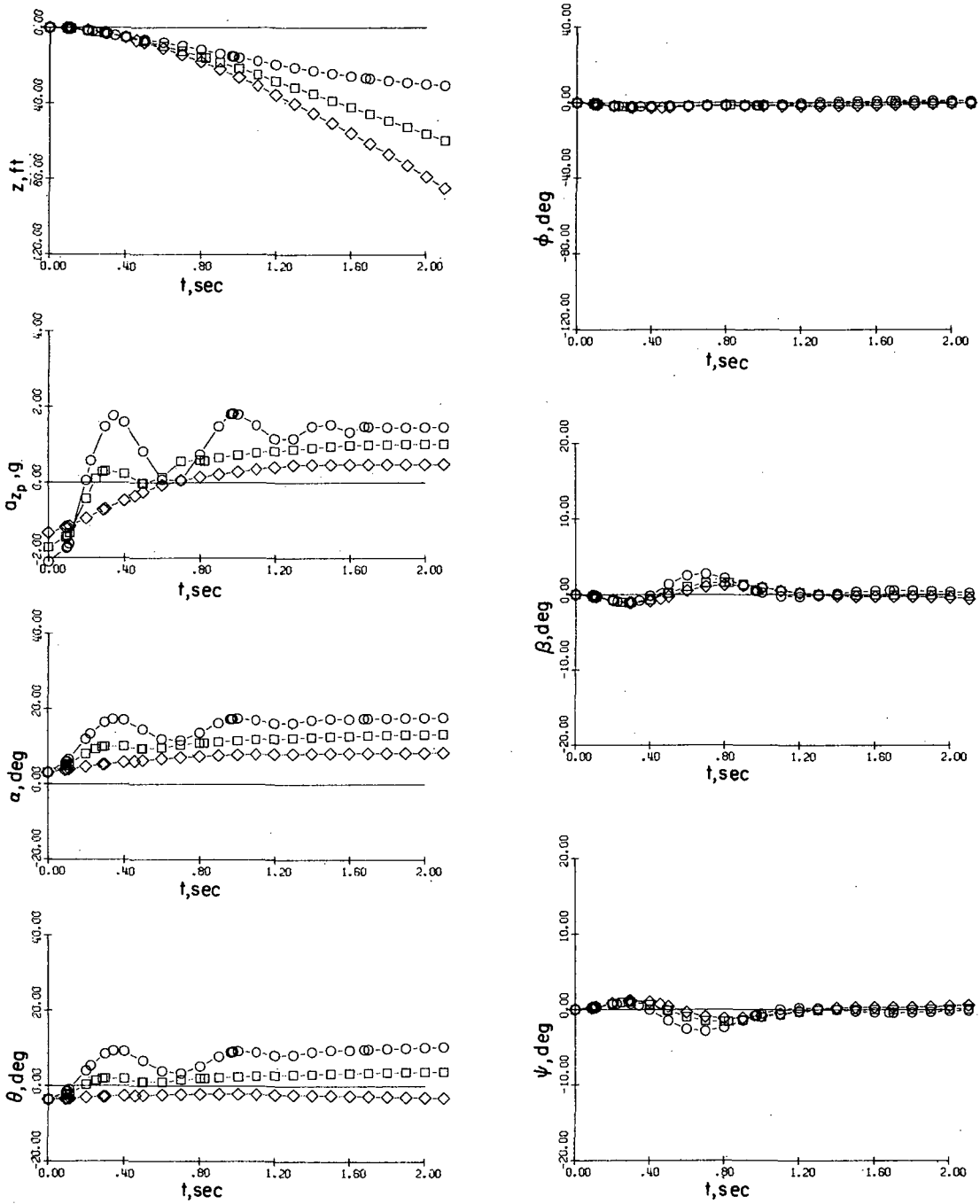


(b) Motion variables plotted against time after launch.

Figure 31.- Concluded.

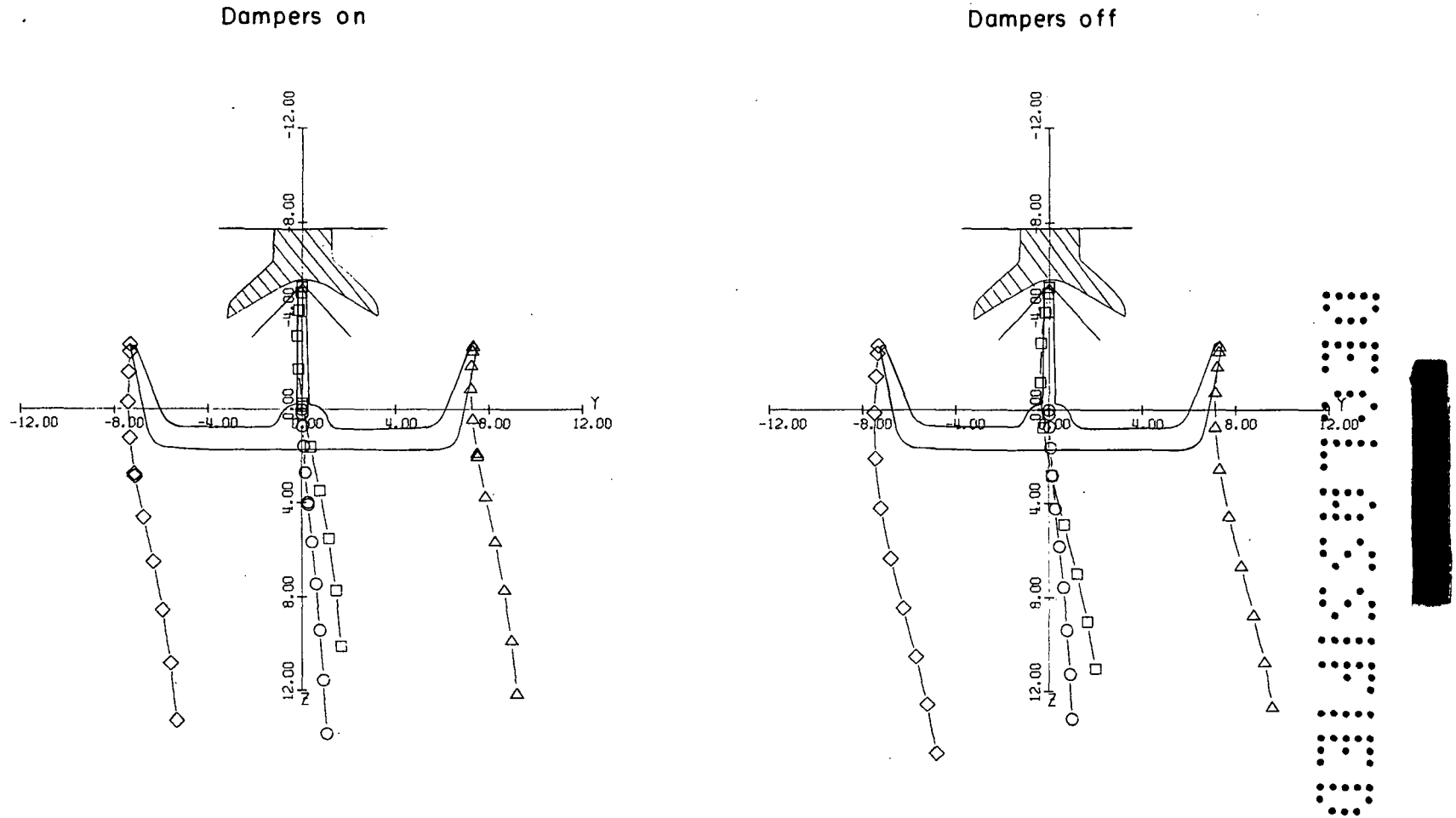


(a) Fin-tip and center-of-gravity paths. (Values along the coordinate scales are given in feet; 1 foot = 0.3048 meter.)

Figure 32.- Effect of damper operation on motions of the heavyweight HL-10 transonic configuration after launch. $W_{HL-10}$ = 7968 pounds (35 443 newtons); M = 0.60; $\alpha_{B-52} = 4^{0}$; $\Delta\alpha = 5^{0}$; $W_{B-52}$ = 250 000 pounds (1 112 050 newtons); $\delta_e = 0^{0}$.

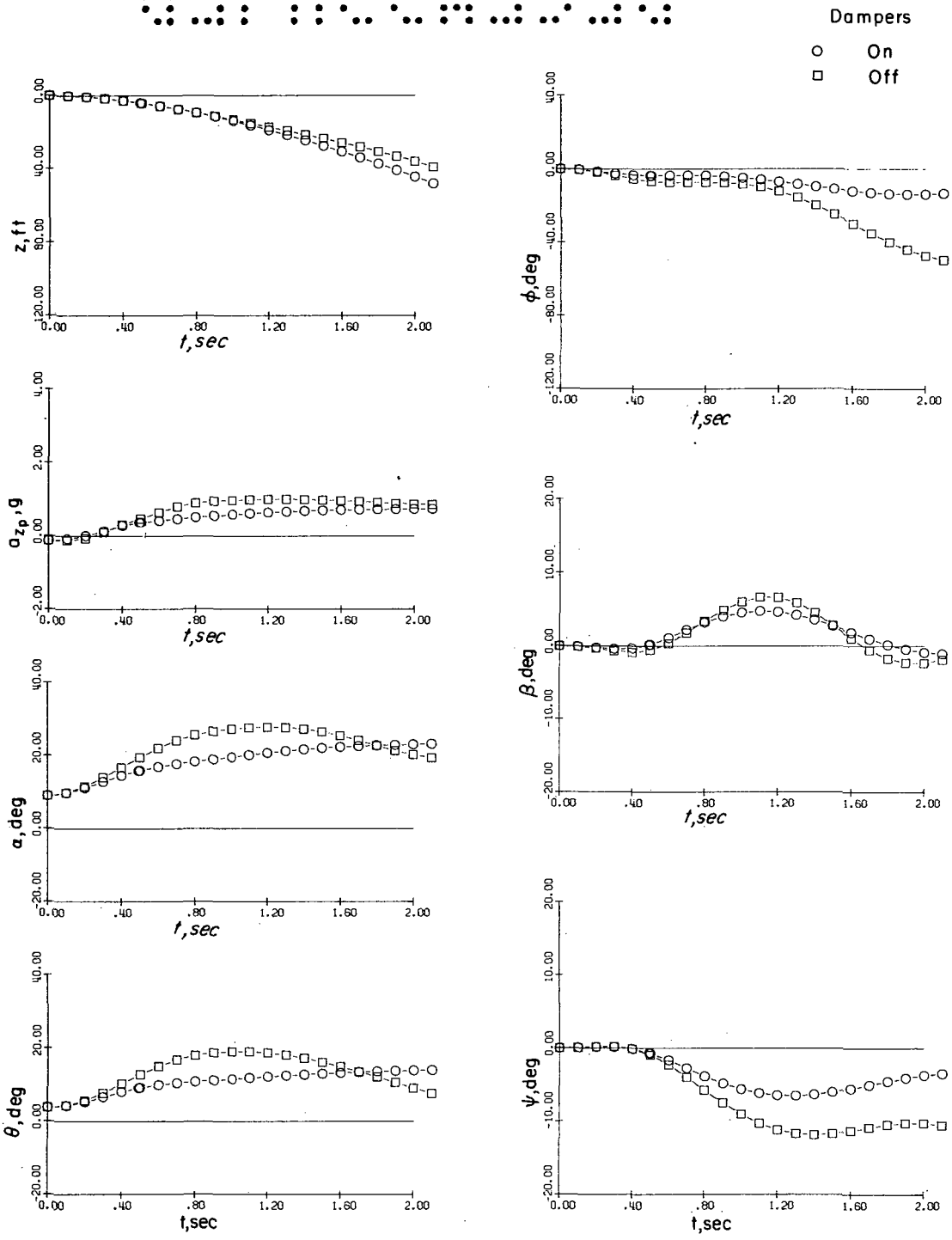


(b) Motion variables plotted against time after launch.

Figure 32.- Concluded.

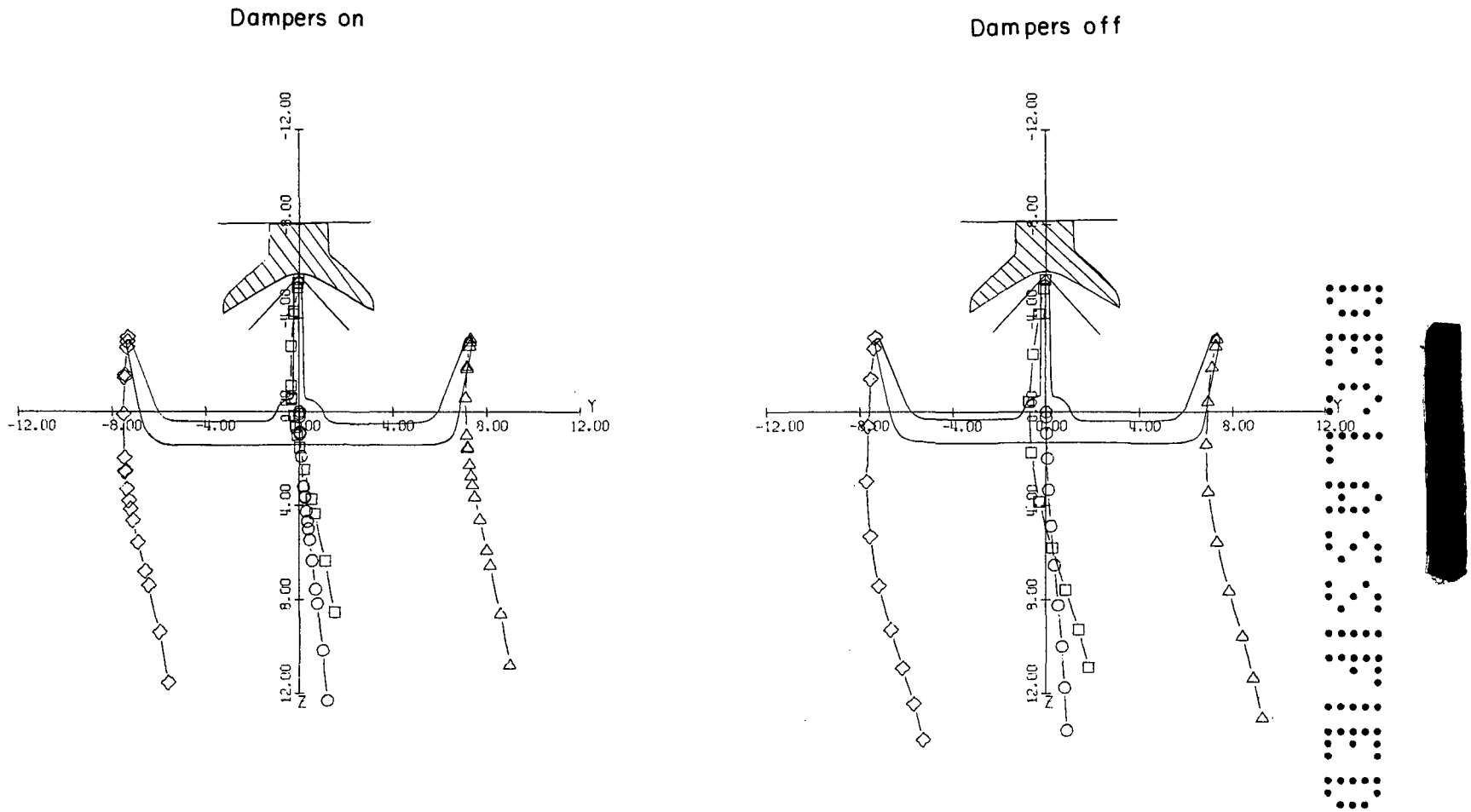


(a) Fin-tip and center-of-gravity paths. (Values along the coordinate scales are given in feet; 1 foot = 0.3048 meter.)

Figure 33.- Effect of damper operation on motions of the heavyweight HL-10 transonic configuration after launch. $W_{HL-10}$ = 7968 pounds (35 443 newtons); M = 0.70; $\alpha_{B-52} = 2^0$; $\Delta\alpha = 5^0$; $W_{B-52}$ = 250 000 pounds (1 112 050 newtons); $\delta_e = 0^0$.

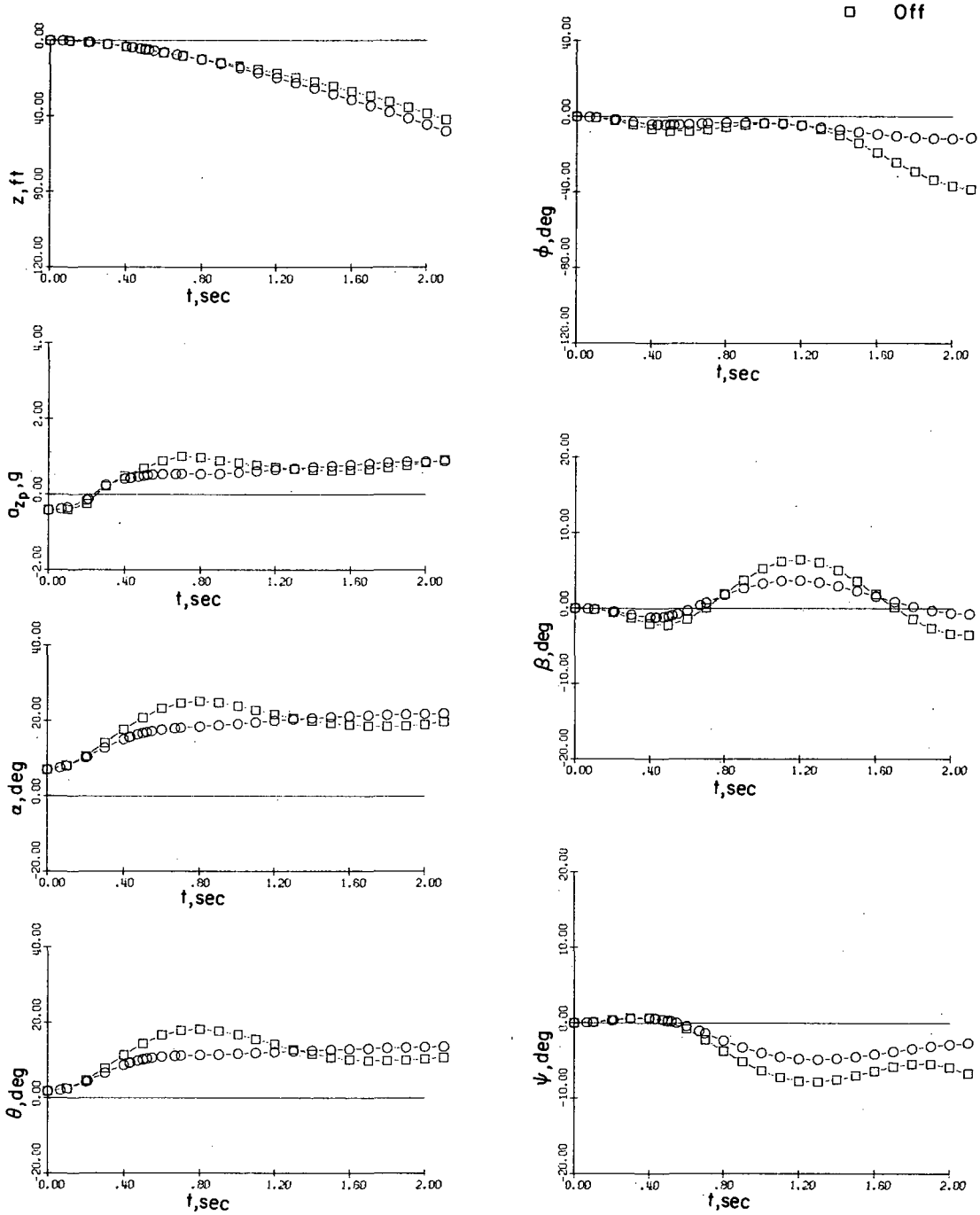


(b) Motion variables plotted against time after launch.

Figure 33.- Concluded.

DECLASSIFIED

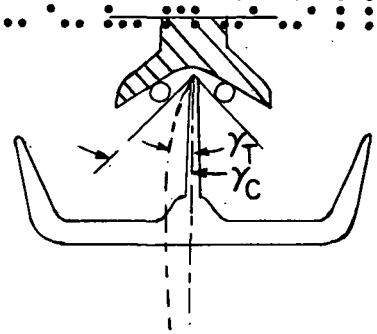


| | M | $\alpha_{B-52}$ | Dampers |
|---|---|---|---|
| ○ | .60 | 4 | Off |
| □ | .65 | 2 | Off |
| ● | .60 | 4 | On |
| ■ | .65 | 2 | On |

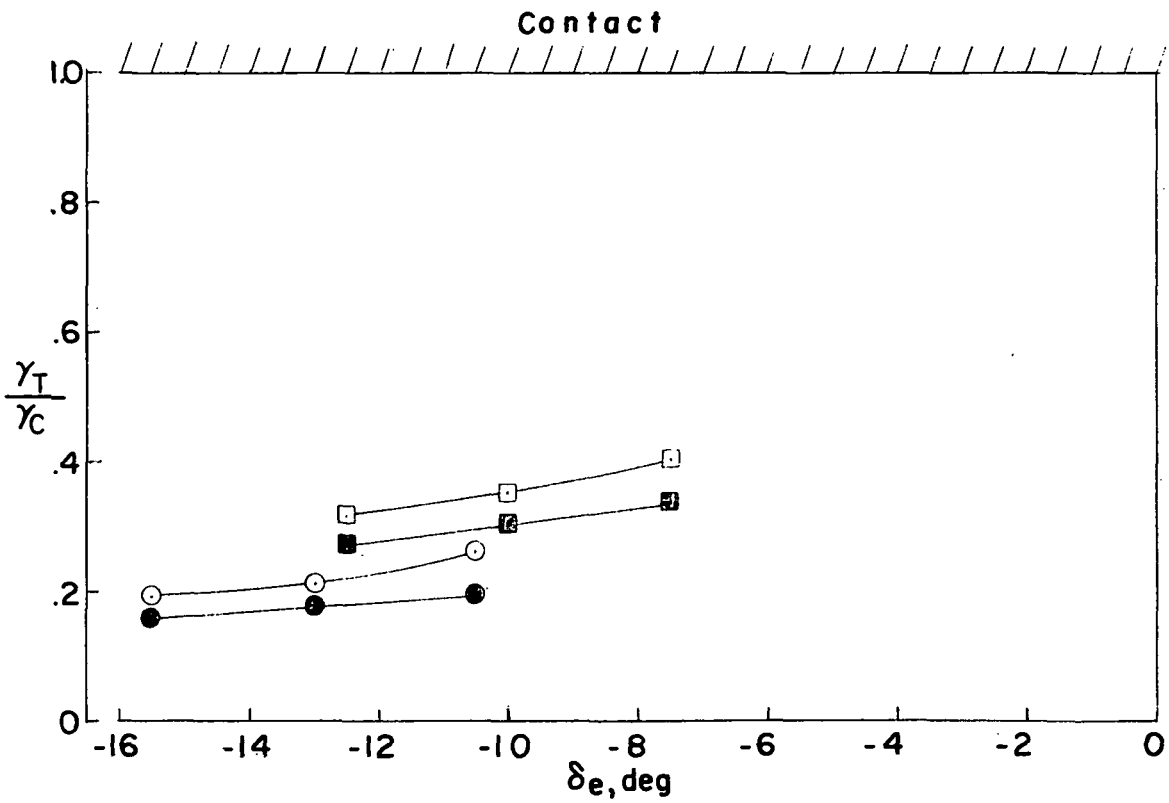


Figure 34.- Summary of the effect of launch variables on the path of the HL-10 center fin (subsonic configuration).

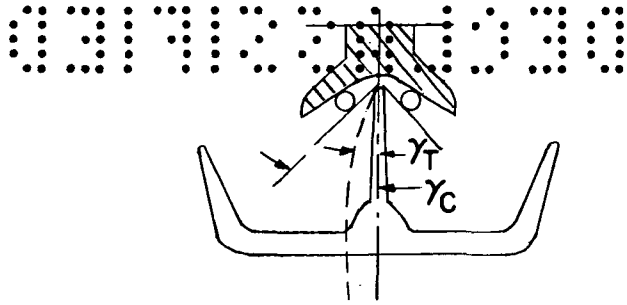


| | $\alpha_{B-52}$ | Dampers |
|---|---|---|
| ○ | 4 | Off |
| □ | 2 | Off |
| ◇ | -1 | Off |
| ● | 4 | On |
| ■ | 2 | On |
| ◆ | -1 | On |

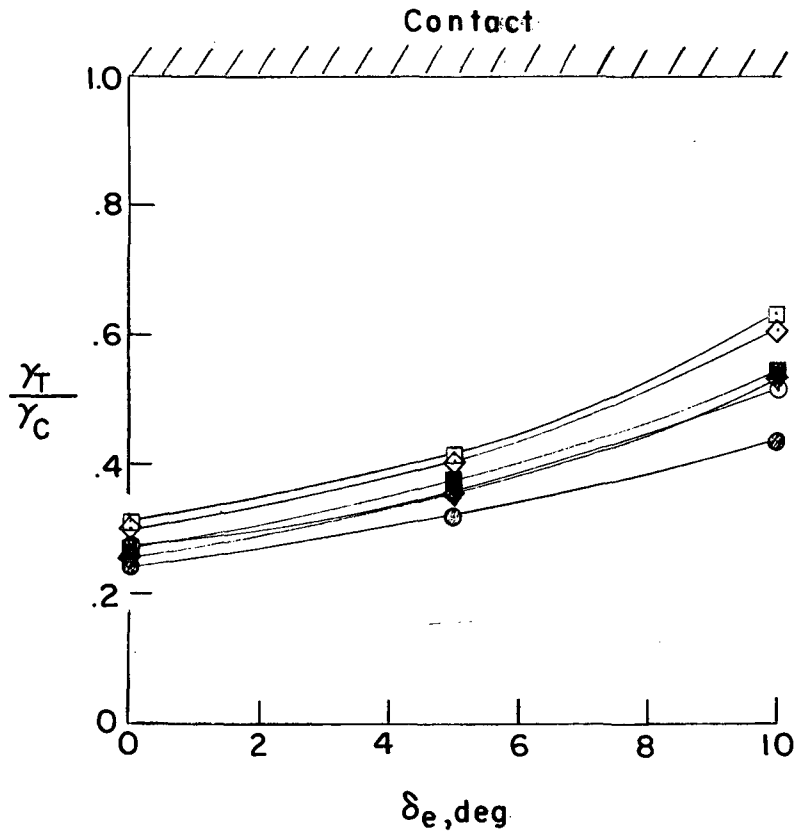


(a) M = 0.60.

Figure 35.- Summary of the effect of launch variables on the path of the HL-10 center fin (transonic configuration).

DECLASSIFIED

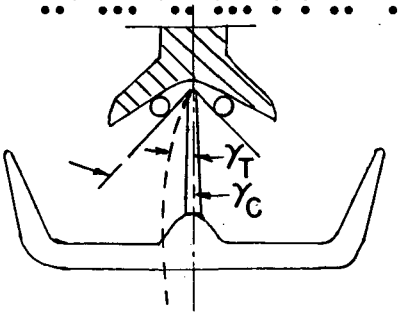


| | $\alpha_{B-52}$ | Dampers |
|---|---|---|
| ○ | 2 | Off |
| □ | 0 | Off |
| ● | 2 | On |
| ■ | 0 | On |

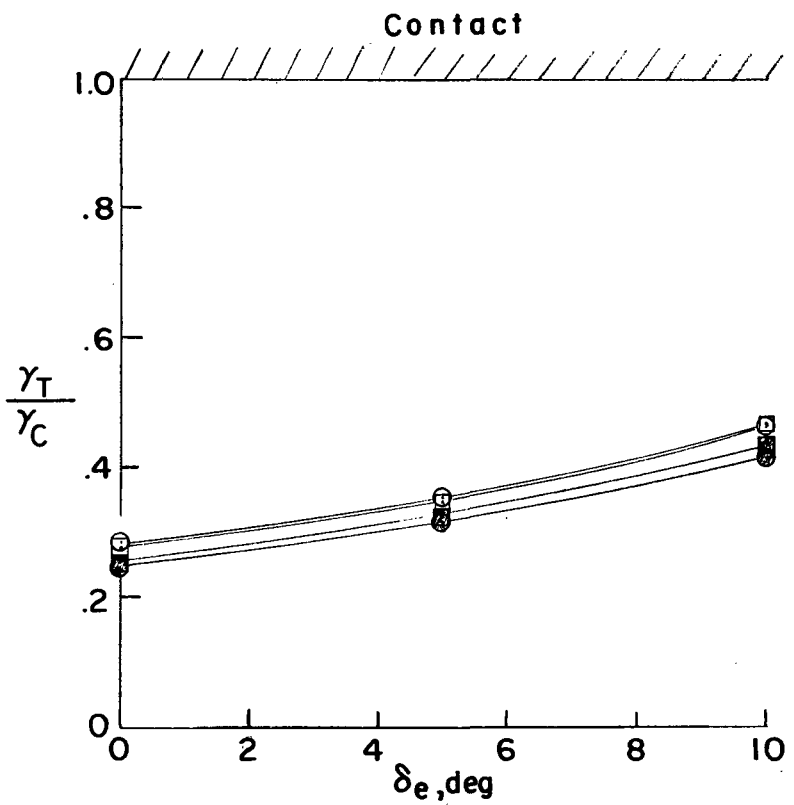


(b) M = 0.70.

Figure 35.- Continued.

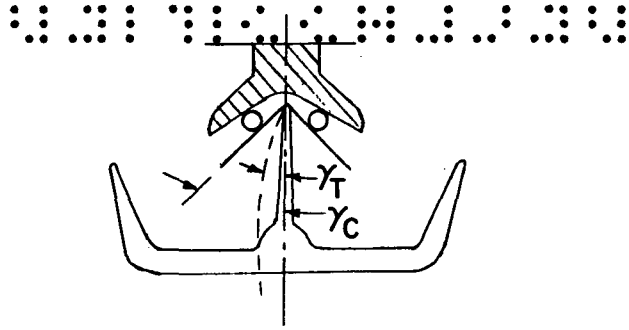


| | $\alpha_{B-52}$ | Dampers |
|---|---|---|
| ○ | 0 | Off |
| □ | -2 | Off |
| ● | 0 | On |
| ■ | -2 | On |

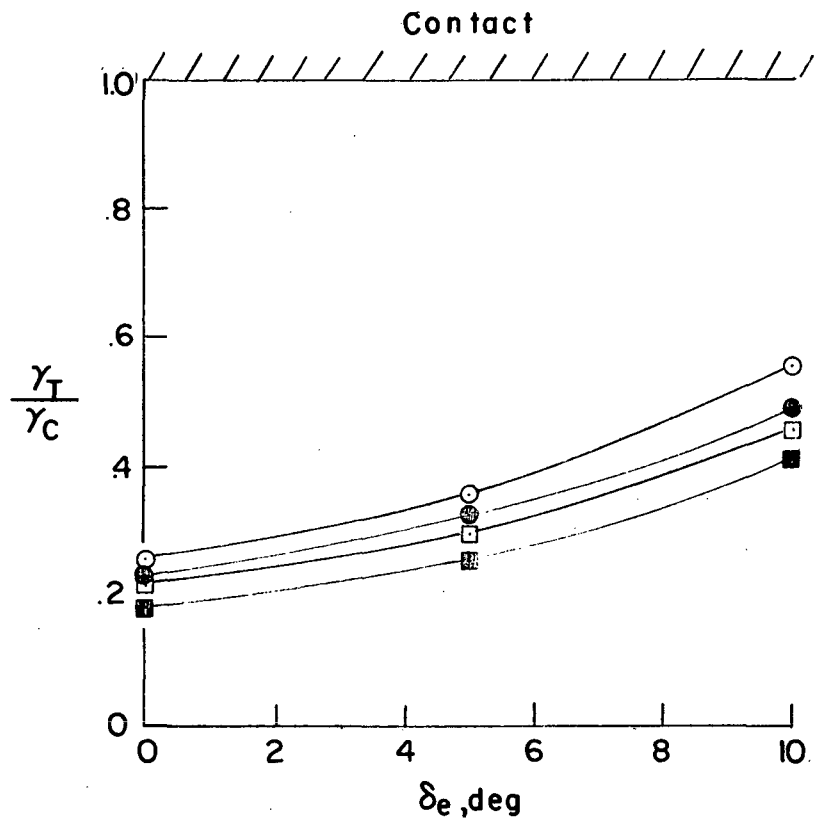


(c) $M = 0.80$.

Figure 35.- Concluded.

[redacted]

*"The aeronautical and space activities of the United States shall be conducted so as to contribute . . . to the expansion of human knowledge of phenomena in the atmosphere and space. The Administration shall provide for the widest practicable and appropriate dissemination of information concerning its activities and the results thereof."*

—NATIONAL AERONAUTICS AND SPACE ACT OF 1958

# NASA SCIENTIFIC AND TECHNICAL PUBLICATIONS

**TECHNICAL REPORTS:** Scientific and technical information considered important, complete, and a lasting contribution to existing knowledge.

**TECHNICAL NOTES:** Information less broad in scope but nevertheless of importance as a contribution to existing knowledge.

**TECHNICAL MEMORANDUMS:** Information receiving limited distribution because of preliminary data, security classification, or other reasons.

**CONTRACTOR REPORTS:** Scientific and technical information generated under a NASA contract or grant and considered an important contribution to existing knowledge.

**TECHNICAL TRANSLATIONS:** Information published in a foreign language considered to merit NASA distribution in English.

**SPECIAL PUBLICATIONS:** Information derived from or of value to NASA activities. Publications include conference proceedings, monographs, data compilations, handbooks, sourcebooks, and special bibliographies.

**TECHNOLOGY UTILIZATION PUBLICATIONS:** Information on technology used by NASA that may be of particular interest in commercial and other non-aerospace applications. Publications include Tech Briefs, Technology Utilization Reports and Notes, and Technology Surveys.

*Details on the availability of these publications may be obtained from:*

SCIENTIFIC AND TECHNICAL INFORMATION DIVISION

NATIONAL AERONAUTICS AND SPACE ADMINISTRATION

Washington, D.C. 20546

[redacted]